UNIVERSITY OF CALIFORNIA
SANTA CRUZ

CHARACTERIZING THE VXRAB TWO COMPONENT SIGNAL TRANSDUCTION SYSTEM

A dissertation submitted in partial satisfaction
of the requirements for the degree of

DOCTOR OF PHILOSOPHY

in

MICROBIOLOGY AND ENVIRONMENTAL TOXICOLOGY

by

Jennifer Kateri Teschler

September 2019

The Dissertation of
Jennifer K. Teschler is approved:

_____
Professor Fitnat H. Yildiz, Chair

_____
Professor Karen M. Ottemann

_____
Professor Victoria Auerbuch-Stone

_____
Professor Grant A. Hartzog

_____
Quentin Williams
Acting Vice Provost and Dean of Graduate Studies

TABLE OF CONTENTS

LIST OF FIGURES

Characterizing the VxrAB two component signal transduction system

by

Jennifer K. Teschler

ABSTRACT

Pathogenic strains of *Vibrio cholerae* cause the acute diarrheal disease cholera, which can result in hypotonic shock and death within 12 hours of the first symptoms. *V. cholerae* is found primarily in the aquatic environment but can be transmitted to a human host through the consumption of contaminated food or water. In order to survive in the aquatic environment and human host, *V. cholerae* must sense and respond to the fluctuating external conditions encountered in these varied environments. To do this, *V. cholerae* and other bacterial species utilize two-component signal transduction systems (TCSs), which employ a sensor histidine kinase (HK) to sense a cognate signal and activate its associated response regulator (RR) to initiate a cellular response.

One such TCS is the *V. cholerae* VxrAB (*Vibrio* type six regulator) TCS, which has been shown to positively regulate a number of important cellular processes, including virulence, a bacterial defense system known as the Type Six Secretion System (T6SS), and cell wall homeostasis. In this work we further characterize the VxrAB system, identifying it as a positive regulator of biofilm formation, demonstrating a role for its activation of T6SS within biofilms, and

further characterizing the role of its regulon members in virulence and cell wall homeostasis.

First, we identified VxrB as a new regulator of biofilm formation through the systematic analysis of *V. cholerae* RRs (Chapter 2). Nearly all bacteria form biofilms as a strategy for survival and persistence. Biofilms are associated with biotic and abiotic surfaces and are composed of aggregates of cells that are encased by a self-produced or acquired extracellular matrix. VxrB, regulates expression of key structural and regulatory biofilm-genes in *V. cholerae*. Additionally, *vxrB* is encoded as part of a 5-gene operon, which encodes the cognate HK *vxrA*, and three genes of unknown function. Δ*vxrA* and Δ*vxrB* are both deficient in biofilm formation, while Δ*vxrC* enhances biofilm formation in a *vxrB* dependent manner, indicating that VxrC may act as a repressor of this system. This work revealed a new function for the Vxr TCS as a regulator of biofilm formation and suggests that this regulation may act through key biofilm regulators and the modulation of cellular c-di-GMP levels.

Given that VxrB co-regulates T6SS genes and biofilm genes, I next investigated the role of the T6SS in biofilms (Chapter 3). The T6SS is a contractile nanomachine capable to injecting toxins into neighboring cells. Given the close proximity of cells to one another in a biofilm environment I demonstrated that the T6SS can actively fire and kill susceptible neighboring

cells within the biofilm. This is the first evidence of T6SS activity within *V. cholerae* biofilms and suggests that VxrB's co-regulation of biofilm formation and T6SS genes may contribute to the ability of *V. cholerae* to persist in intra- and inter-species biofilms.

Finally, though our lab previously established that VxrB-mediated virulence is partially due to its activation of the T6SS, we also demonstrated that other factors contribute to VxrB-mediated intestinal colonization. Using RNA-seq analysis we identified a number of hypothetical genes regulated by VxrB and tested their contribution to VxrB-mediated phenotypes, including virulence, T6SS activity, and cell wall homeostasis (Chapter 4). We identified two operons that contribute to intestinal colonization, VC1162-60 and VC2548-47, and one operon that contributes to cell wall homeostasis, VC2520-16, all of which appear to converge around the cell envelope and are conserved systems in numerous other bacteria. This work enhances our understanding of hypothetical proteins and provides a more in depth understanding how VxrB-related phenotypes are mediated.

This work is dedicated to the numerous people who helped me get here, but most of all my parents. Thank you for everything.

ACKNOWLEDGEMENTS

I am very grateful to my advisor, Dr. Fitnat Yildiz, who has set the bar for the kind of researcher and mentor I hope to one day be. Her dedication to science is rivaled only by her dedication to her students' success and I have benefited enormously from her encouragement and guidance. I would like to thank her for the many opportunities she provided, as well as for her unwavering support in the face of both successes and failures. In fact, I'm sure she would object to the term failure, preferring instead to see any temporary setback as an opportunity for growth and learning. I do not think I can adequately express my gratitude and appreciation, but I hope I can demonstrate it by carrying forward all that she has taught me and always striving to be a better scientist, mentor, and friend.

I would like to thank my committee members, Dr. Karen Ottemann, Dr. Victoria Auerbuch Stone, and Dr. Grant Hartzog, who provided valuable advice and support and made this work possible. I would also like to express my gratitude to the members of my qualifying exam committee, Dr. Seth Rubin, Dr. Karen Ottemann, and Dr. Victoria Auerbuch Stone, whose input and insight shaped and strengthened my project.

I was very lucky to work with incredibly talented, intelligent, and kind individuals during my time at UC Santa Cruz. I would like to thank the members of the

Yildiz Lab, past and present, for their support, collaboration, and camaraderie. I would like to especially thank Dr. Andrew T. Cheng for discovering the VxrAB system and allowing me to take over such a wonderful project. In addition, I would like to thank Dr. Jinhwan Park, Avatar Joshi, Giordan Kitts, Adiaratou Ba, Andrew Rogers, William Garvey, Dr. Fernando Pagliai, Joe Kiblen, Megan Mouw, Bao Nguyen, Dr. Nick Fong, Dr. Sinem Beyhan, Dr. Zehra Tuzun Guvener, Dr. Loni Townsley, Dr. Chris Jones, Dr. David Sanchez-Zamorano, Dr. Ana Gallego, Dr. Carmen Schwechheimer, Jenna Conner, Giselle Aguayo, Dr. Kyle Floyd, Maya Modak, Sandra Aquino, Semin Shazir, and Thuy Nguyen. I am very grateful to have had the pleasure of working together and I hope our paths cross again in the future. I would also like to thank the UCSC SASFLNH Cabin Crew, Dr. SA Smythe, Dr. Alix Johnson, and soon to be doctors Nadia Roche and Suraiya Jetha for keeping me sane and in the game. I would like to give a special mention to Nadia's son, Kai, whose dimples and enthusiasm lightens even the hardest days.

I would like to thank my parents, Dale and Carolyn Teschler, for their unconditional support and encouragement. Thank you to my sister, Katie Teschler, for her patience and optimism. Thank you to all my friends who supported me through this process. Thank you to my dogs, Lily and Cally, for always bringing a smile to my face.

Finally, thank you to my wonderful partner, Adam Alpine, for his endless support, love, and willingness to help me with my figures.

The text of this dissertation includes partial reprints of the following previously published material:

Teschler JK, Zamorano-Sánchez D, Utada AS, Warner CJA, Wong GCL, Linington RG, Yildiz FH. 2015. Living in the matrix: assembly and control of *Vibrio cholerae* biofilms. Nat. Rev. Microbiol. 13:255–68.

Yildiz FH, Conner JG, Jones CJ, Teschler JK. 2016. Staying Alive: *Vibrio cholerae*'s Cycle of Environmental Survival, Transmission, and Dissemination. Microbiol. Spectr. 4.

These publications are presented in Chapter 1.

Teschler JK, Cheng AT, Yildiz FH. 2017. The Two-Component Signal Transduction System VxrAB Positively Regulates *Vibrio cholerae* Biofilm Formation. J. Bacteriol. 199:e00139-17.

This publication is presented in Chapter 2.

CHAPTER 1: Introduction

Jennifer K. Teschler and Fitnat H. Yildiz

Background

Nearly all bacteria form biofilms as a strategy for survival and persistence. Biofilms are associated with biotic and abiotic surfaces and are composed of aggregates of cells that are encased by a self-produced or acquired extracellular matrix. This growth mode is distinct from the planktonic growth mode and confers a number of advantages to biofilm inhabitants, including protection from environmental stresses, enhanced survival and persistence, and capacity for resource capturing (1). Biofilms represent a significant threat to human health, as they have been associated with the contamination of medical devices, disease transmission, and increased severity and duration of infections (2). *Vibrio cholerae* has been studied as a model organism for understanding biofilm formation, the cycle of environmental survival, transmission, and dissemination of bacterial pathogens between hosts. The ability of *V. cholerae* to transition between the human host and the aquatic environment is essential for the explosive waterborne spread of cholera during outbreaks, as well as the persistence of *V. cholerae* in endemic areas during non-epidemic periods.

In this introduction I review the cellular processes involved in *V. cholerae* biofilm formation, the regulatory network that governs *V. cholerae* biofilm formation, and the impact of aquatic and host environmental inputs on biofilm formation. I additionally discuss our current understanding of biofilm community structure and highlight emergent properties of biofilms, introducing the Type Six Secretion System (T6SS) and its potential to shape biofilm dynamics. I introduce the two-

component signal transduction system, VxrAB, which regulates biofilm formation (discussed in Chapter 2), the T6SS, virulence, and cell wall homeostasis. The impact of the co-regulation of biofilm formation and the T6SS is not known, and results from our studies assessing the impacts of T6SS activation within biofilms are discussed in Chapter 3. Finally, the contribution of VxrB-regulated proteins of unknown function to VxrB-mediated phenotypes are discussed in Chapter 4.

Cholera

Filippo Pacini first isolated and described the Gram-negative bacterium *V. cholerae* in 1854—the same year that Dr. John Snow's "ghost maps" revealed that a tainted water supply was the source of a deadly cholera outbreak. *Vibrio cholerae* causes 3 to 5 million cases of cholera annually, resulting in 100,000-120,000 deaths (3). Infection occurs through the ingestion of contaminated water or food, primarily impacting regions that lack adequate sanitation and clean drinking water (4, 5). The disease is characterized by watery diarrhea and rapid dehydration, which, if untreated, can lead to hypotonic shock and death within 12 hours of the first symptoms (4, 5). Large outbreaks of the disease have occurred throughout the past two centuries, including several recent epidemics in Haiti, Vietnam, and Zimbabwe (6–8). Annual, seasonal outbreaks also occur in many areas of the world where cholera is endemic, including countries in Asia, Africa, and the Americas, due to the ability of toxigenic *V. cholerae* to survive in the aquatic environment year round (9, 10). The timing and severity of seasonal outbreaks

vary depending on a number of environmental factors, including rainfall, salinity, temperature, and plankton blooms (11).

V. cholerae forms biofilms during aquatic and intestinal phases of its life cycle (12–14). The role of biofilms in *V. cholerae* environmental persistence, dissemination, and transmission has been well established (Figure 1.1). This growth mode provides protection from a number of environmental stresses, including nutrient limitation, predation by unicellular eukaryotes known as protozoa, and attack by bacterial viruses known as bacteriophages (15, 16). While *V. cholerae* can form biofilms on many biotic and abiotic surfaces, several field studies demonstrated that *V. cholerae* preferentially forms biofilms on phytoplankton, zooplankton, and oceanic chitin rain (17, 18). The exoskeletons of zooplankton contain chitin, which *V. cholerae* can utilize as its sole carbon source (19, 20). Growth on chitin also induces natural competence and allows cells to acquire new genetic material (21). As physical carriers and primary sources of nutrients for *V. cholerae,* zooplankton serve as reservoirs and disease vectors of cholera (22).

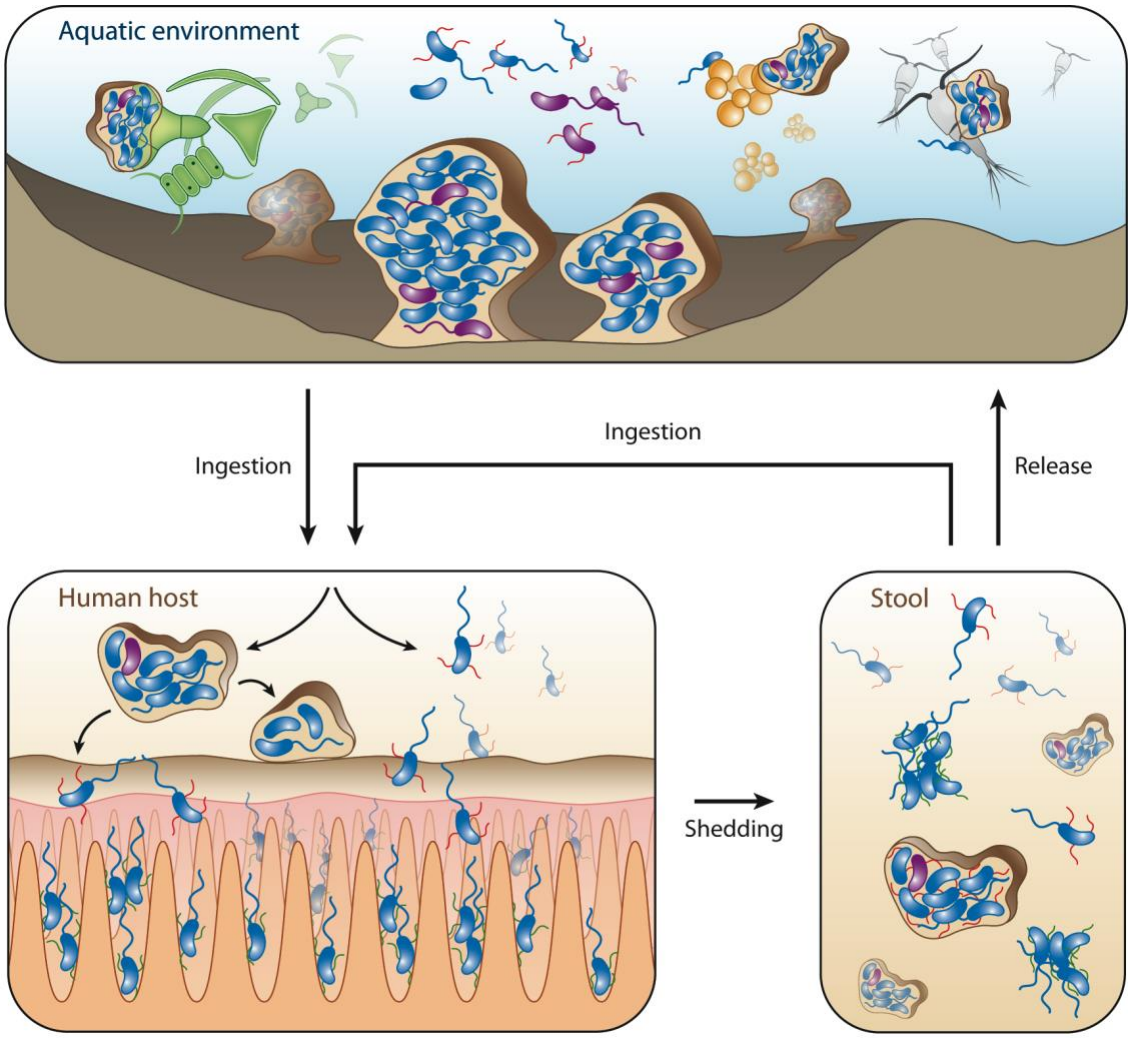

Figure 1.1. Biofilms in *V. cholerae* life cycle.

In the aquatic environment *V. cholerae* is found in its highly mobile planktonic form as well as in biofilms formed on zooplankton, phytoplankton, detritus, and other surfaces, such as sediments. Following the initial stages of attachment to abiotic and biotic surfaces, which involves the type IV pili mannose-sensitive haemagglutinin (MSHA) pili, cells produce the extracellular matrix, which is essential to achieve mature biofilms with a three-dimensional structure. Because it is unknown whether the flagellum is lost during biofilm formation, cells are depicted with or without the flagellum in biofilms. *V. cholera* can be ingested by

humans from environmental sources causing seasonal outbreaks. During intestinal colonization, *V. cholerae* produce toxin co-regulated pili (TCP). Both planktonic cells and biofilm aggregates are found in patient stool, and these cells can re-infect a new host or return to the aquatic environment.

Although *V. cholerae* is found year-round in the coastal and estuarine environments where cholera is endemic, outbreaks are seasonal and correlate with changes in environmental conditions (22). Plankton blooms, which are influenced by water temperature, hours of sunlight, sea surface height, rainfall, and salinity, are thought to be the major environmental factor impacting seasonal outbreaks (11). Simple filtration practices that remove particles larger than 20 μm were shown to significantly reduce cholera cases, suggesting that the removal of biofilm-associated and plankton-associated *V. cholerae* from the environment can reduce transmission (23).

Between epidemics, nonculturable, metabolically quiescent *V. cholerae* cells have been observed in biofilms that appear to contribute to *V. cholerae* persistence (13, 14). These quiescent cells may lose their typical curved rod shape, becoming coccoid, and are not culturable under standard lab conditions, but can return to an active state in response to signaling from active cells or interactions with a host (13, 24, 25). Biofilms containing metabolically quiescent *V. cholerae* may have significant biological relevance, as their reduced metabolic needs and slowed growth may allow them to survive harsh environmental conditions until circumstances improve. Once activated, they may act as seed cells for *V. cholerae* growth in the water supply and contribute to an outbreak (24).

V. cholerae biofilms play an established role in transmission, delivering both higher doses of bacteria and hyperinfective cells (13, 26). When *V. cholerae* is in a

hyperinfective state, the infectious dose required for infection is decreased and the risk of disease transmission is increased. However, the role of *V. cholerae* biofilm formation once inside the host is poorly understood. Both single cells and dense clumps of *V. cholerae* were observed in a rabbit ileal loop infection model, supporting an earlier finding that biofilms may form *in vivo* and subsequently be excreted in stool (13, 27). Several studies suggest that a key component of the biofilm, *Vibrio* polysaccharide (VPS), is produced during infection (28, 29). Additionally, a defect in intestinal colonization was observed in a murine model when genes contributing to VPS and the production of the matrix protein RbmA were deleted (30). Collectively, these findings imply that biofilms play a role during *V. cholerae* infection, but further study is needed to elucidate the underlying mechanisms and functions of *in vivo* biofilms. Currently, much of what we know about *V. cholerae* biofilm structure, function, and regulation comes from the study of *in vitro* biofilms.

Cellular processes governing biofilm formation

Surface attachment. *V. cholerae* biofilm formation is a multistep process that begins with near-surface motility that mechanically 'scans' the surface, followed by surface attachment, the subsequent development of microcolonies, and finally the formation of an organized, three-dimensional structure (Figure 1.2) (31).

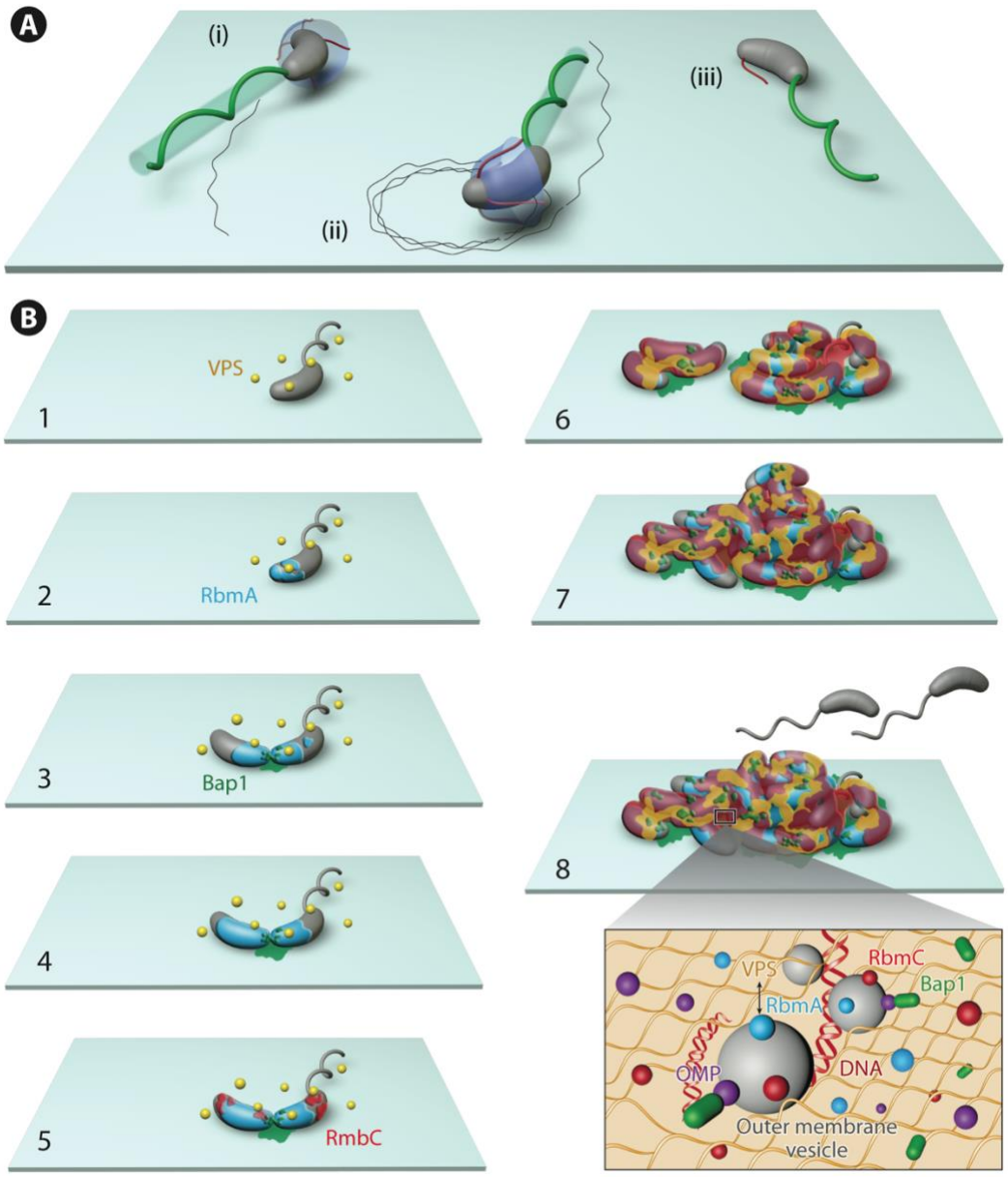

Figure 1.2. Building a *V. cholerae* biofilm.

A) Surface motility and initial attachment: Surface-skimming cells use flagella (green) to swim, but 'scan' the surface mechanically via mannose-sensitive haemagglutinin (MSHA) pili appendages (red). Surfaces with weak pili interactions lead to 'roaming' behavior (i), whereas surfaces with strong pili interactions lead to

‘orbiting’ behavior (ii), which allow cells to loiter over these regions and eventually attach (iii). Motility trajectories are depicted by the black lines on the surface and correspond to roaming (i) and orbiting behavior (ii), respectively.

B) Microcolony formation and matrix production: Early after initial attachment, *Vibrio* polysaccharide (VPS) is excreted from cell surfaces (panel 1). VPS extrusion from cells is observed throughout biofilm formation. Next, the biofilm matrix protein RbmA accumulates on the cell surface (panel 2). When cell division occurs, the daughter cell remains attached to the parental cell, confirming RbmA’s role in cell-to-cell adhesion (panel 3). As division occurs, the biofilm matrix protein Bap1 is excreted between the two cells and on the substrate near the two cells (panel 3). Bap1 gradually accumulates on nearby surfaces radially, though the concentration of Bap1 remains the highest near the parental, or founder cell (panel 4). The biofilm matrix protein RbmC is then excreted and is found on discrete sites on the cell surface (panel 5). As biofilms develop, VPS, RbmC and Bap1 form envelopes that can grow as cells divide (panels 6). The mature biofilm is a composite of organized clusters composed of cells, VPS, RbmA, Bap1, and RbmC, in addition to other matrix components, such as outer membrane vesicles (OMVs) and extracellular DNA (eDNA) (panel 8). Outer membrane proteins (OMPs) are shown as purple spheres and are known to associate with Bap1 in OMVs and contribute to increased antimicrobial peptide resistance. While dispersal, shown by the gray *V. cholerae* bacteria depicted in panel 8, is an important part of the *V. cholerae* biofilm cycle, little is known about its mechanism.

Bacteria swimming near surfaces experience hydrodynamic forces that both attract them towards the surface and cause them to swim in circular trajectories (32). *V. cholerae* is equipped with a single polar flagellum driven by a Na^+ motor (33). When *V. cholerae* cells swim near surfaces, viscous drag forces act on the flagellum as it sweeps past the surface and induces a torque on the cell body; this surface-induced torque deflects the swimming direction of cells into curved clockwise paths (34).

By using high-speed tracking of *V. cholera* grown in flow cell chambers, two types of trajectories are discerned: 'orbiting' involves with tight, repetitive, near-circular orbits with high curvatures (Radius of gyration R_{gyr} < 8 μm), while 'roaming' involves long directional persistence and small curvatures (R_{gyr} > 8 μm) (31). In both motility modes cells move in an oblique direction that deviates strongly from the major cell axis and have strong nutations along the trajectory. Moreover, the direction of motion seems to be exclusively in the clockwise direction for both motility modes (31). These motility modes are ablated in strains lacking mannose sensitive hemagglutinin pili (MSHA) type IV pili (TFP) or the flagellum, which suggests that both appendages are necessary for these characteristic behaviors (31).

Theoretical modeling was used to elucidate the origins of orbiting and roaming motility behavior. This was accomplished by considering the hydrodynamic motilities of both the cell body and the flagellum and solving for their velocities

using a force and torque balance (31). In free-swimming cells, flagellar rotation causes the cell body to counter rotate. For surface-skimming *V. cholerae*, this body rotation associated with swimming causes MSHA appendages to have periodic mechanical contact with the surface. Interactions between the MSHA pili and the glass surface are accounted for using a friction coefficient. This behavior has significant implications for the surface engagement strategy of *V. cholerae*. The consequence of this interaction is that surface-skimming cells continuously assay the surface mechanically using MSHA pili. They naturally loiter over surface regions that interact more strongly with MSHA pili, by executing orbiting motility over those regions, whereas they pass over surface regions that interact more weakly with MSHA pili via roaming motility (Figure 1.2a) (31).

Orbiting *V. cholerae* cells exhibit a distribution of intermittent pauses of various temporal durations before eventually attaching to the surface. Both the frequency and duration of these pauses decreased significantly when cells were incubated with a non-metabolizable mannose derivative to saturate MSHA pili binding (31). This suggests that MSHA pili-surface interactions are mechano-chemical in nature, and that MSHA pili binding to the surface may be an important step in the *V. cholerae* 'landing sequence.' Taken together, these observations suggest that MSHA pili-surface binding is crucial to arrest cell motion during near-surface swimming and to transition to surface attachment and microcolony formation. Consistent with this, strains lacking MSHA are defective in initial surface attachment (31, 35).

It is important to note that the initial surface attachment behavior of *V. cholerae* is unlike the case for *Pseudomonas aeruginosa*, which reversibly attach to surfaces in a vertical orientation and move along random trajectories with TFP driven 'walking motility' after initial attachment (36, 37). These cells transition to an irreversibly attached state where the cell axis is oriented parallel to the surface, and move by TFP driven 'twitching' motility, guided by a network of secreted polysaccharides and extracellular DNA (eDNA) (38, 39). This surface motility ultimately results in the formation of microcolonies. The surface-motility behavior of *V. cholerae* is drastically different—*V. cholerae* use their polar flagellum and MSHA pili synergistically to scan a surface mechanically before surface attachment. The sites of surface attachment correlate strongly with the positions of eventual microcolonies, which indicates that purely TFP driven motility plays a minor role in determining positions of *V. cholerae* microcolonies (31).

After *V. cholerae* cells attach to a surface it is unknown if the flagellum is functional, if it is lost and degraded, or if it acts as a structural component in the biofilm. However, lack of flagellum likely serves as a signal for biofilm formation, as mutations in a flagellar structural gene, *flaA*, resulted in higher production of the biofilm exopolysaccharides (40, 41). Surprisingly, mutations in the flagellar motor genes, *motB* and *motY*, eliminate the biofilm-inducing signal caused by loss of the flagellum (40, 41). This suggests that the Na^+ driven flagellar motor may act as a

mechanosensor, allowing *V. cholerae* to recognize when it encounters a surface and subsequently induce the appropriate attachment response (40, 41).

Macro-colony formation and the matrix. Following the initial stages of cell attachment, cells begin the production of an extracellular matrix. Matrix production is essential to achieve mature biofilms with three-dimensional structure and distinct morphological and phenotypic differences can be observed depending on the quantity of biofilm matrix components being produced. Compositional analysis of an intact *V. cholerae* biofilm matrix by solid state Nuclear Mass Resonance (NMR) using ^{15}N profiling and spectroscopic analysis of the extracellular matrix carbon pools demonstrated that the extracellular matrix is primarily composed of polysaccharides, phospholipids, and proteins, along with small amounts of nucleic acids (42). Additionally, the *V. cholerae* biofilm matrix seems to be sugar-rich, especially when compared to the protein-rich biofilm matrix of *Escherichia coli* (42). Defining and quantifying the major building blocks of the *V. cholerae* biofilm not only furthers our understanding of how individual components interact to support the formation of a complete biofilm matrix, but also highlights differences between species that may inform how biofilm components better facilitate pathogen survival and transmission.

Biofilm components.

***Vibrio polysaccharide*.** *Vibrio* polysaccharide (VPS) makes up 50% of the biofilm matrix by mass and is essential for the development of three-dimensional biofilm

structures (30, 43, 44). VPS is a glycoconjugate composed of a polysaccharide conjugated to an, as of yet, unidentified component. Only recently was the chemical structure of VPS revealed. Two types of VPS are produced during biofilm formation. The repeating unit of the major variant of the polysaccharide portion of VPS is [–4)-L-α-Gul*p*NAcAGly3OAc-(1-4)-β-D-Glc*p*-(1-4)-α-D-Glc*p*-(1-4)-α-D-Gal*p*-(1-]$_n$, while the minor variant replaces α-D-Glc*p* with α-D-Glc*p*NAc(44). It is still unclear if VPS remains tethered to the cell or if it is cleaved after secretion and identification of its unknown component may reveal more about how VPS is retained in the biofilm.

Genes involved in VPS production are organized into two *vps* clusters— 12 are found in *vps-1* and 6 are found in *vps-2* (30, 43). These genes are divided into six classes, with different predicted functions: Class I encodes for the nucleotide sugar precursors, VpsA and VpsB, Class II encodes the glycosyltrasferases, VpsD, VpsI, VpsK, and VpsL, Class III encodes the VPS polymerization and export proteins, VpsE, VpsH, VpsN, and VpsO, Class IV encodes the acetyltransferases, VpsC and VpsG, Class V encodes the phosphotyrosine-protein phosphatase VpsU, and Class VI encodes the hypothetical proteins, VpsF, VpsJ, VpsM, VpsP, and VpsQ.(30). Deletion of *vpsF, vpsJ,* or *vpsM* results in the complete loss of colony corrugation, an inability to form pellicles, and a reduction in biofilm and VPS production, implying that these hypothetical proteins may play a significant role in biofilm formation (30). In total, in-frame deletion of 15 of the 18 *vps* genes resulted

in strains with altered phenotypes compared to wild-type, and it is possible that under other conditions further differentiation from wild type may be observed (30).

The structure of VPS is in agreement with many of the proteins encoded by the *vps* genes, as their predicted functions match potential steps in the VPS biosynthesis pathway (30, 44). The *vps* clusters are separated by an 8.3 kb *rbm* cluster containing 6 genes, which encode for matrix proteins (43, 45, 46). The *vps-1, rbm, vps-2* clusters comprise a functional genetic module, here referred to as the *V. cholerae* biofilm-matrix cluster (VcBMC), which encodes many of the genes that generate VPS and major biofilm proteins. Two additional genes involved in UDP-glucose and UDP-galactose synthesis, *galU* and *galE*, respectively, are also necessary for biofilm production, suggesting these substrates may be essential for VPS biosynthesis (47). VPS plays an essential role in *V. cholerae* biofilm formation and is secreted from cell surfaces shortly after initial attachment. VPS extrusion from cells is observed throughout biofilm development (Figure 1.2b) (48).

Matrix proteins. Three matrix proteins, RbmA, RbmC, and Bap1, are produced and secreted from the cell at various times during biofilm formation and play different roles within the biofilm. *rbmA* (*r*ugosity and *b*iofilm structure *m*odulator A) is the 13th gene of the VcBMC and encodes a protein involved in cell-cell and cell-biofilm adhesion (46, 48, 49). RbmA accumulates on the cell surface after initial attachment and VPS production (Figure 1.2b) (48). RbmA also contributes to early elasticity and corrugation in pellicle biofilms, playing an important role in the

development of biofilm architecture and stability (50). Analysis of the crystal structure revealed that RbmA contains two fibronectin type III (FnIII) folds, commonly found in cell surface receptors and cell adhesion proteins. The FnIII folds of two RbmA monomers are connected by a linker segment and form a bilobal structure with unique surface properties (51). The dimer interface forms a wide groove, capable of accommodating large, filamentous substrates, such as VPS, and a tight groove, capable of binding negatively charged carbohydrates found on cellular surfaces. Saturation transfer difference (STD) experiments indicate that these two binding sites preferentially bind monosaccharides from VPS and lipopolysaccharide (LPS), implying that RmbA likely acts as a biofilm scaffolding protein (52). RbmA's scaffolding role was recently described in more detail, when it was shown that the exposed FnIII-2 domain directly binds VPS, while the FnIII-1 domain acts as a bistable structural switch that controls interactions with the FnIII-2 domain, resulting in an open or closed state (53). The switch between these two states influences the formation of higher-order oligomers of RbmA and VPS and impacts biofilm structure and architecture (53).

Two other major biofilm matrix proteins, Bap1 and its homolog RbmC, share 47% sequence similarity, but play nonredundant roles in biofilm formation (45). Bap1 contains four overlapping *Vibrio-Colwellia-Bradyrhizobium-Shewanella* repeat (VCBS) domains, which may play a role in cell adhesion, and four FG-GAP domains, which are thought to be important for recognition and binding of an, as of yet, unidentified ligand (45, 48, 54). During biofilm formation, Bap1 is secreted

at the cell-surface interface and gradually accumulates on nearby surfaces radially, although the concentration of Bap1 remains the highest near the parent, or founder cell. This both supports a role for Bap1 in surface adhesion and suggests that the founder cell and its earliest descendants are primarily responsible for the production of Bap1 (Figure 1.2b) (48). In rugose pellicles, Bap1 was found to be uniquely required for maintaining pellicle strength over time and scanning electron microscopy revealed that a Bap1 mutant exhibited a distinctly different pellicle microstructure. Bap1 was also shown to significantly contribute to pellicle hydrophobicity, allowing it to spread and remain at an air-water interface (50).

RbmC also has four overlapping repeat VCBS domains that form two VCBS regions, but only contains two FG-GAP domains. RbmC is larger than Bap1 and has a second C-terminal β-prism domain and two N-terminal domains of unknown function (49). The β-prism domains have been demonstrated to have lectin and carbohydrate binding activity in other proteins, but the significance of its binding properties in RbmC is still being explored (55). Glycan array studies aimed at identifying possible RbmC ligands showed that RbmC has a strong preference for complex *N*-glycans and further binding and modeling suggested that a branched pentasaccharide core ($GlcNAc_2$-Man_3) likely interacts with the β-prism domains (56). As biofilms develop and more cell division occurs, RbmC is secreted at discrete sites on the cell surface, and RbmC and Bap1 form flexible envelopes that can grow as cells divide (Figure 1.2b) (48). During biofilm formation on a solid-water interface, RbmA, RbmC, and Bap1 were unable to accumulate on the

surface of cells that did not produce VPS, and RmbC was shown to be critical for incorporation of VPS throughout the biofilm. The mature biofilm is a composite of organized clusters composed of cells, VPS, RbmA, Bap1, and RbmC (Figure 1.2b) (48).

The type II secretion system (T2SS), a multiprotein system that exports proteins from the cell by translocating folded proteins from the periplasm through the outer membrane, is responsible for the secretion of RbmA, RbmC, and Bap1 (57). T2SS mutants were unable to secrete RbmA, RbmC, and Bap1 into culture and exhibited diminished biofilm formation, although VPS excretion from the cell remained unaffected. Additionally, elimination of the T2SS in a rugose strain abolished colony corrugation and pellicle formation, further supporting the significant role of the T2SS in biofilm formation and morphology (57).

V. cholerae biofilm proteins have also been associated with outer membrane vesicles (OMVs), which can act as secretory vehicles for a number of proteins. In *V. cholerae* 90 proteins are associated with OMVs, including RbmA, RbmC, and Bap1 (58). It is unknown if the association of biofilm proteins with OMVs is a regulated cellular program or if it is the result of the random inclusion of proteins that pass through the periplasm. However, in the presence of antimicrobial peptides, Bap1 was shown to bind to the surface of OMVs via its association with the outer membrane protein OmpT. Evidence suggests that OMV-associated Bap1 then binds to antimicrobial peptides and attenuates their impact on *V. cholerae,*

thus increasing bacterial resistance to antimicrobial peptides (54). Contribution of other OMV-associated and free matrix proteins to biofilm structure and function are yet to be determined.

Detachment and dispersal.

The last stages in biofilm development are detachment and dispersal. Although dispersal is an important step in the biofilm cycle, allowing exiting cells to seek out and colonize new resources, little is known about this process in *V. cholerae*. Two extracellular nucleases, Dns and Xds, are implicated in biofilm development and dispersal (59). Dns and Xds regulate eDNA, which plays a role in evolution, nutrient delivery, and biofilm structure (59). eDNA released by cell lysis or active secretion may be taken up by competent cells during growth on chitin, where it can act as a source of organic nutrients or become incorporated in the genome. It may alternatively remain in the biofilm matrix, where it appears to act as an important structural component (59). Deletion of Dns and Xds led to promoted biofilm formation independent of *vps* production, altered biofilm structure, and impaired detachment from biofilms (59). Evidence suggests that degradation of eDNA by these nucleases impacts biofilm formation and may facilitate detachment and dispersal. Impaired *in vivo* colonization was also observed, suggesting that dispersal may be necessary for colonization of the host (59).

Additionally, *rbmB* encodes a putative polysaccharide lyase and has been hypothesized to play a role in VPS degradation and cell detachment. Strains

lacking RbmB have enhanced biofilm formation though enzymatic activity of RbmB has not been demonstrated experimentally (45). Downregulation of production of biofilm components, discussed in more detail below, likely plays a role in dispersal; however, genes involved in degradation of biofilm proteins have yet to be identified. Extracellular signals, such as the bile salt taurocholate, may also act as a signal for passive biofilm dispersal (60). Identification of the proteins crucial for detachment and dispersal is essential and would contribute to a better understanding of how and when *V. cholerae* disperses from a biofilm.

V. cholerae **biofilm regulation**

V. cholerae biofilm formation is controlled by an integrated regulatory network of transcriptional activators: VpsR, VpsT, and AphA; repressors: HapR and H-NS; alternative sigma factors: RpoN, RpoS, and RpoE; small regulatory RNAs; and signaling molecules (Figure 1.3). The regulation of biofilm matrix production is controlled by a highly connected regulatory network that integrates at least three different nucleotide second messengers and the quorum-sensing (QS) response (Figure 1.3b). Biofilm formation is an energetically costly process and commitment to the biofilm lifestyle has significant biological consequences. Thus, biofilm development must be tightly regulated and highly plastic to be responsive to a variety of environmental cues experienced by the pathogen during its life cycle.

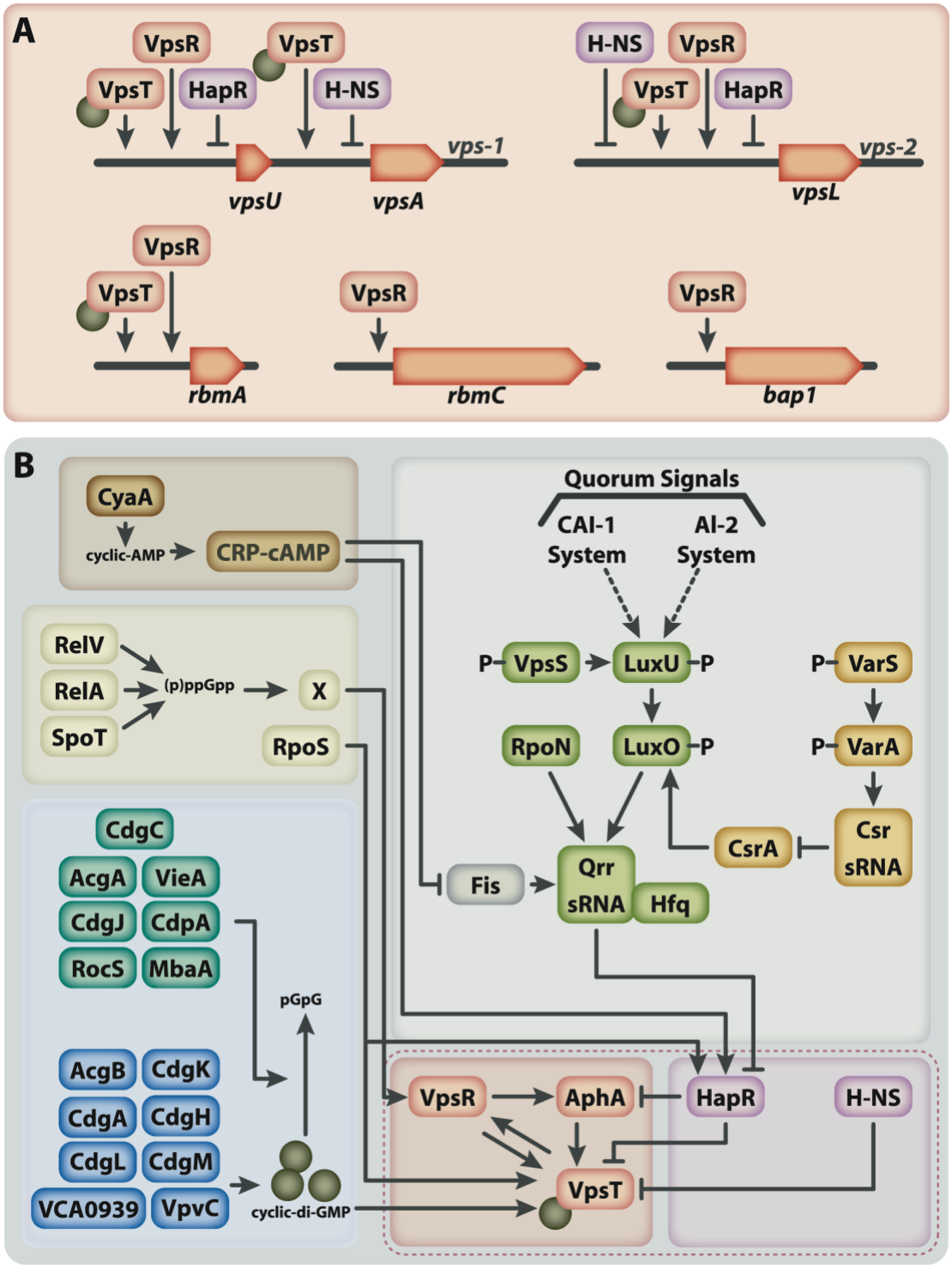

Figure 1.3. *V. cholerae* biofilm regulatory network.

A) The core regulators, VpsR, VpsT, and HapR, directly and indirectly regulate biofilm matrix genes, shown as the *vps* (*vibrio* polysaccharide) and *rbm* (rugosity

and biofilm structure modulator) clusters, found in the VcBMC, and the *bap1* (biofilm-associated extracellular matrix protein) gene, which is encoded elsewhere on the genome. The VpsR, VpsT, HapR, and H-NS recognition sequences have been identified in the regulatory region of *vps-1* and *vps-2* clusters and certain biofilm matrix genes. C-di-GMP, shown as green spheres, interaction with VpsT is essential to VpsT's ability to bind to promoter regions. It has also been shown that H-NS directly binds to the regulatory regions of *vps-1* and *vps-2* clusters. Positive regulators of biofilm are shown in orange, while negative regulators are shown in purple.

B) An extensive regulatory network governs *V. cholerae* biofilm formation. VpsR, VpsT, and AphA, the main activators of biofilm formation, and HapR and H-NS, the main repressors of biofilm formation, are shown in the core regulatory network denoted by the dashed box region. The direct regulation of VpsR, VpsT, HapR, and H-NS on biofilm matrix genes is shown in part A.

These core regulators directly and indirectly regulate one another and are modulated by a complex regulatory network thought to respond to a number of environmental and host signals.

Small nucleotide signaling subnetworks are shown in the left hand panel, and show the influence of cyclic-AMP (cAMP), (p)ppGpp, and cyclic-di-GMP on the activation and repression of major regulators. RpoS is depicted with (p)ppGpp because the stringent response regulation of *vpsT* and *vpsR* has been shown to partially occur through RpoS. Several diguanylate cyclases (DGCs) that cumulatively contribute to c-di-GMP levels are shown in dark blue, while phosphodiesterases (PDEs)

known to decrease cellular c-di-GMP are shown in teal. C-di-GMP interaction with VpsT—this is required for VpsT activation.

Quorum sensing (QS), which responds to cell density via bacterial signaling, plays a key role in the regulation of HapR and, thus, the other major biofilm regulators. HapR production is repressed at low cell density, when CAI-1 and AI-2 production is not high, shown by dashed arrows, leading to LuxO phosphorylation by the QS signal transduction pathway. The VarS/VarA system responds to an unknown environmental cue to repress biofilm production, by post-transcriptionally upregulating HapR. The integration of many regulatory pathways allows for the activation or repression of biofilm formation in response to a number of extracellular and intracellular signals that *V. cholerae* may encounter in its life cycle.

Positive regulation. VpsR, the master regulator of biofilm formation, is a member of the two-component signal transduction system (TCS) response regulator family. It harbors an N-terminal response regulator receiver domain (REC), an ATPases associated with a wide variety of cellular activities (AAA+) domain, and a C-terminal helix-turn-helix (HTH) DNA-binding domain (61). VpsR is required for biofilm formation—disruption of *vpsR* prevents expression of the *vps* and matrix protein genes and abolishes formation of biofilms. VpsR binds to the *vps* promoter regions and controls their expression directly (Fig. 3)(62). VpsR also upregulates *eps* genes that form part of the type II secretion system, matrix protein genes, and *aphA*, a major regulator of virulence, demonstrating that it may also play a role in pathogenesis (61, 63, 64). VpsR contains a conserved aspartate residue, D59, which seems to be critical for its function. Conversion of this aspartate to alanine renders VpsR inactive, while conversion to glutamate creates constitutively active VpsR, supporting the premise that phosphorylation controls DNA binding of VpsR (41). It has been shown that VpsR can bind the second messenger cyclic dimeric guanosine monophosphate (c-di-GMP), but that c-di-GMP does not alter dimerization or its DNA binding ability (65). The binding conformation of a σ70-RNA polymerase (RNAP), VpsR, and c-di-GMP complex, however, is different than σ70-RNAP alone, with VpsR, or with c-di-GMP alone and evidence suggests that c-di-GMP is required for VpsR to form specific protein-DNA architecture needed for activated *vps* transcription (66). Sensor histidine kinase(s) that play a role in activating VpsR and positively regulating *vps* gene expression and biofilm formation are not known. VpsR expression is positively regulated by VpsT and

negatively regulated by HapR, though other players are likely involved in VpsR regulation and further study is needed to fully characterize its regulation (63).

A second positive regulator of biofilm formation, VpsT, is also a response regulator. VpsT consists of an N-terminal REC domain and a C-terminal HTH domain. Unlike other REC domains, the canonical (α/β) 5-fold in VpsT is extended by an additional helix (α6) at its C-terminus (67). Disruption of *vpsT* reduces expression of *vps* and matrix protein genes and reduces biofilm forming capacity. VpsT binds to the *vps* promoter region to directly control the expression of *vps* genes (Figure 1.3a) (62, 67). VpsT must bind to c-di-GMP in order to initiate DNA binding and transcriptional regulation (67). A dimer of c-di-GMP binds to a dimer of VpsT with an infinity of 3.2 μM. The VpsT c-di-GMP binding motif has conserved sequence of: W[F/L/M][T/S]R(67). Mutations in the putative phosphorylation site that were designed to produce a constitutively inactive or active state do not alter the efficiency of VpsT, indicating that regulation of gene expression is independent of phosphorylation of VpsT (67). Transcription of *vpsT* is highly regulate and the promoter region of *vpsT* has VpsR, AphA (master virulence regulator) and HapR, recognition sites (64, 65, 68). Expression of *vpsT* is positively controlled by VpsR, AphA and the alternative sigma factor RpoS, and negatively controlled by HapR (63, 68–70).

The VpsR and VpsT regulons extensively overlap and both positively regulate the transcription of *vps* and biofilm related genes, but the magnitude of gene regulation

varies. The fact that VpsR and VpsT can modulate each other's expression could, in part, be responsible for the overlap in their regulons (63, 64). The VpsR and VpsT recognition sequences in the regulatory region of the first gene in the *vps-2* operon*, vpsL* (62). *In vitro* analysis demonstrated that VpsR and VpsT bind to non-overlapping sequences in the regulatory region of *vpsL*. VpsR binds to a proximal (R1 box) and distal region (R2 box) with respect to the transcriptional start site and VpsT binds in between these sites in the T box. As expected, mutations in the T and R boxes decreased *vpsL* expression, however, deletion of T or R2 boxes increased *vpsL* expression. Further analysis revealed that H-NS can also bind to these regions to silence transcription and VpsR and VpsT binding may work to counteract that silencing (62). *In silico* analysis designed to determine VpsR and VpsT recognition sites revealed that both VpsR and VpsT could bind to the regulatory region of the first gene in the *vps-1* cluster, *vpsU*, as well as to the regulatory regions of *rbmA* and *vpsT*. *In silico* analysis also showed that the promoter of another gene in the *vps-1* cluster, *vpsA*, harbors only the VpsT recognition sequence, while *rbmC* and *bapI* promoters harbor only the VpsR recognition sequence, thus supporting the premise that these two regulators act in concert by directly targeting all the regulatory regions in the VcBMC (Figure 1.3a) (64, 67, 69).

***Negative regulation*.** HapR is the main negative regulator of biofilm formation in *V. cholerae* and disruption of *hapR* enhances biofilm formation (71–73). HapR represses biofilm formation by directly binding to the regulatory regions of *vpsT*

and *vpsL*, the first gene in the *vps-2* operon (74). HapR has homology to TetR regulators; the N-terminus contains a HTH domain and the C-terminus contains a dimerization domain. This domain is predicted to have a binding pocket for an unidentified ligand, which is proposed to be to be amphipathic and contain anionic moieties (75).

The timing of *hapR* repression and activation modulates the formation of mature biofilm structures and dispersal from the biofilm, respectively (72, 76). HapR production is negatively controlled through the QS pathway, which has been recently reviewed (77). Briefly, membrane-bound sensor histidine kinases, LuxQ and CqsS, recognize signaling molecules AI-2 and CAI-1, respectively, and initiate a phosphorelay event that culminates at the histidine phosphotransfer protein, LuxU, and the response regulator, LuxO (Figure 1.3b) (77). At low cell density, LuxO~P, in concert with the alternative sigma factor RpoN, activates transcription of the quorum-regulated small RNAs (sRNAs), Qrr1–4, which work in conjunction with the sRNA chaperone Hfq to prevent the translation of *hapR* (Figure 1.3a) (77).

Several additional regulators have been shown to feed into QS regulation of HapR and impact biofilm formation (Figure 1.3b). The two-component system, VarS/A, upregulates *hapR* expression post-transcriptionally via a pathway that involves the regulatory sRNAs CsrB, CsrC, and CsrD (78, 79). These sRNAs bind to and titrate the RNA binding protein CsrA, interfering with the LuxO activation of Qrr1-4, thus leading to decreased levels of Qrr1-4 and enhanced HapR production (79). The

small protein Fis is a direct positive regulator of the QS responsive sRNAs, Qrr 1-4 (80). VpsS, a hybrid histidine kinase, also affects biofilm formation through the QS pathway by donating phosphate groups to the phosphotransfer protein LuxU (81). The global regulator, cAMP receptor protein (CRP), has been shown to upregulate HapR production through its positive regulation of the CAI-I autoinducer synthase and its negative regulation of Fis, thus linking this regulator to the QS pathway at two regulatory junctions (82). The *hapR* gene is also regulated independently of the QS regulatory pathway—the transcriptional regulator VqmA can directly activate *hapR* expression; and the sigma factor RpoS promotes expression of *hapR* (64, 83).

The H-NS protein is a histone-like protein that plays an important role in modulating nucleoid topology and also functions as a transcriptional regulator. It has low sequence-specificity and shows preference for AT rich regions with high curvature (84). In *V. cholerae* H-NS negatively controls expression of virulence genes (85). A strain lacking *hns* has a significantly enhanced ability to form biofilms. It has been shown that H-NS acts as a direct negative regulator of *vpsL*, *vpsA* and *vpsT* both *in vitro* and *in vivo*, although little is known about the role of H-NS in controlling other biofilm genes (84). A recent study revealed that VpsT is required at the *vpsL* regulatory region to counteract the silencing effect of H-NS, but that VpsT also regulates biofilm formation independently of H-NS (62).

Small nucleotide signaling. A key signaling molecule controlling *V. cholerae* motility and biofilm matrix production, and thus the planktonic to biofilm transition, is the nucleotide-based, second messenger c-di-GMP (Figure 1.3b) (86). C-di-GMP is synthesized by diguanylate cyclases (DGC), proteins containing a GGDEF domain, and it is degraded by phosphodiesterases (PDE), proteins containing an EAL or HD-GYP domain (87). The *V. cholerae* genome encodes 31 proteins with a GGDEF domain, 12 proteins with an EAL domain, and 9 proteins with a HD-GYP domain (88). Though an additional 10 genes encode proteins with both GGDEF and EAL domains, this does not necessarily suggest that the protein exhibits both DGC and PDE activity, as it is common for one domain to be degenerate. In *V. cholerae* c-di-GMP is sensed by receptor proteins, including PilZ and VpsT, or c-di-GMP riboswitches (67, 89, 90).

At present, little is known about the precise molecular mechanisms by which c-di-GMP affects motility and planktonic to biofilm transition in *V. cholerae*. Systematic phenotypic characterization of isogenic mutants with in-frame deletions of the predicted c-di-GMP-related genes (except HD-GYP genes) of *V. cholerae* revealed that four DGCs (CdgH, CdgK, CdgL, and CdgD) inhibit motility and two PDEs (CdgJ and RocS) promote motility (Figure 1.3b) (91). Regulation of abundance or activity of these c-di-GMP signaling proteins is predicted to be critical for the motile to sessile transition. Increases in cellular c-di-GMP can repress transcription of flagellar genes, or act post-transcriptionally to regulate swimming velocity and alter flagellar rotational switching by interacting with a yet

to be identified c-di-GMP receptor or through interaction with flagellar motor proteins (87). Transcriptional profiling experiments revealed that high concentrations of c-di-GMP promote transcription of *msh*, the operon encoding the MSHA pilus, *vps*, and other biofilm genes, and repress transcription of flagellar genes (92). FlrA, the activator of flagellar genes, and VpsT, the activator of biofilm genes, function as repressors of flagellar genes in their c-di-GMP bound state (67, 93). MshE, the ATPase responsible for polymerizing and depolymerizing the MSHA pili discussed in the 'surface attachment' section of this chapter, is a c-di-GMP receptor whose ATPase activity is enhanced upon c-di-GMP binding (94–96). Increased c-di-GMP production results in enhanced pili production, which in turn impacts near surface motility and attachment. The role of MshE as a c-di-GMP receptor provides a possible mechanism for the connection between c-di-GMP levels and the impact on motility and biofilm formation via its regulation of MSHA pilus production (96).

High cellular levels of c-di-GMP stimulate enhanced transcription of genes involved in biofilm formation (92). VpsT, a key c-di-GMP receptor, induces expression of biofilm genes in its c-di-GMP bound state (67). Analysis of *vpsL* expression and biofilm formation in strains containing in-frame deletions of genes encoding proteins with GGDEF, EAL, or GGDEF and EAL domains revealed that strains lacking the DGCs CdgA, CdgH, CdgK, CdgL, and CdgM show a decrease in expression of *vpsL* and biofilm formation (88, 97). Furthermore, while c-di-GMP levels decreased to 86%-54% when compared to wild-type in each single DGC

deletion strain, in the Δ5DGC strain c-di-GMP levels decreased to 17% (97). These results show that multiple DGCs are involved in maintaining cellular c-di-GMP levels and contribute additively to *vps* expression and biofilm formation. Conversely, mutants lacking PDEs (CdgJ, CdgC, RocS, MbaA, VieA) have enhanced biofilm formation compared with wild-type (86, 91, 97, 98).

Cellular c-di-GMP levels could be maintained by transcriptional or post-transcriptional regulation of c-di-GMP signaling proteins and we are only beginning to understand how the vast repertoire of *V. cholerae* DGCs and PDEs is regulated. VpsR, VpsT, and HapR all appear to play a role in the regulation of these genes. Transcriptome studies indicate that VpsR and VpsT influence the expression of ten c-di-GMP genes, though it is interesting to note that they do not universally upregulate DGCs and downregulate PDEs, and instead appear to upregulate key DGCs that enhance biofilm formation while repressing key PDEs that decrease biofilm formation (63, 64). The promoter regions of genes encoding proteins predicted to be involved in c-di-GMP signaling, including *cdgA, cdgC, cdgD*, and *VCA0165*, have predicted VpsR binding domains, indicating they may be directly regulated by VpsR (99). HapR was shown to influence the expression of 14 DGCs and PDEs and was demonstrated to directly bind to the promoter region of *cdgA, cdgG, VCA0080, VC2370*, and *VC1851* and *VC1086* genes. Again, while HapR upregulated PDEs shown to decrease biofilm formation and downregulated DGCs shown to increase biofilm formation, this trend was not universal (63, 74). Some DGCs and PDEs appear to be regulated by QS independently of HapR, through

LuxO and Qrr1-4 (100). Additionally, environmental signals, such as polyamines and bile components, have been shown to modulate abundance and activity of c-di-GMP signaling enzymes (63, 74, 101, 102).

The second messenger cyclic *adenosine-monophosphate (cAMP) is involved in a variety of cellular responses and acts as a repressor of V. cholerae* biofilm formation (Figure 1.3b) (103). When glucose is limited, cAMP is synthesized by the adenylyl cyclase, CyaA, and binds CRP to initiate the carbon catabolite repression response. The cAMP-CRP complex downregulates expression of *rbmA*, *rbmC*, *bap1, vpsR,* and other *vps* genes (104). A number of DGC and PDE genes controlling c-di-GMP levels are also regulated by cAMP-CRP, including its downregulation of *rocS, cdgA, cdgH,* and *cgdI* (104). Interestingly, all of these genes contain the GGDEF domain required for DGC activity, but RocS and CdgI also contain EAL domains and are thought to act as PDEs rather than DGCs. This further highlights the complexity of the regulatory network governing c-di-GMP synthesis and degradation and its influence on biofilm formation. cAMP-CRP also upregulates HapR and the biosynthesis of the autoinducer CAI-I, as mentioned above (82, 104). Regulation of biofilm formation by cAMP-CRP provides a link between nutritional status and biofilm formation.

The *V. cholerae* stringent response is triggered by nutritional stress and results in the synthesis of the two small molecules guanosine 3’-diphosphate 5’-triphosphate and guanosine 3’,5’-bis(diphosphate), collectively called (p)ppGpp, by RelA, SpoT,

and RelV (70, 105, 106). Mutants deficient in the stringent response were shown to have decreased, although not completely deficient, biofilm formation (70). All three (p)ppGpp synthases—RelA, SpoT, and RelV—are necessary for *vpsR* transcription, but only RelA is necessary for *vpsT* transcription. While the regulation of *vpsT* expression through the stringent response is strongly dependent on RpoS, the regulation of *vpsR* likely involves additional factors that have yet to be identified (Figure 1.3b) (70).

***sRNA regulation of V. cholerae biofilms*.** The significance of small, non-coding RNAs (sRNAs) in the regulation of cellular processes is becoming increasingly recognized (Figure 1.3b). Besides sRNAs controlling HapR levels, two additional sRNAs were shown to regulate biofilm formation in *V. cholerae*. VrrA, the expression of which is controlled by the sigma factor RpoE, negatively regulates the expression of the biofilm matrix protein RbmC by directly pairing with the 5' end of its mRNA transcript, thereby inhibiting the translation of RbmC mRNA and downregulating biofilm formation (107, 108). This is the first link between biofilm formation and RpoE and the first example of a sRNA bypassing the master regulators of biofilm formation to directly regulate a biofilm matrix component (107). Furthermore, the sRNA RyhB, which is negatively regulated by iron and Fur, is involved in biofilm formation. A *ryhB* mutant exhibits a defect in biofilm formation when grown in low-iron medium, but this defect can be rescued by the addition of excess iron or succinate. The molecular basis by which RyhB controls biofilm remains to be determined (109). The regulatory RNA, VqmA, represses biofilm

formation via repression of *vpsT* transcript (110). The role of sRNAs in biofilm formation is relatively unexplored but adds a different level of regulation to the elaborate regulatory network that controls biofilm development.

Regulation of biofilm formation in response to changing environmental conditions in the aquatic environment and the human host.

Estuaries, which act as environmental reservoirs for *V. cholerae*, undergo significant nutrient, temperature, salinity, and osmolarity fluctuations that can impact biofilm formation and *vps* expression (111–113). Additionally, signals encountered during passage through a human host can impact biofilm formation, including bile and the organic compound indole (114, 115). Nutritional status appears to play a key role in biofilm formation and the highly conserved bacterial phosphoenolpyruvate phosphotransferase system (PTS) was recently linked to the regulation of *V. cholerae* biofilm formation. Four independent PTS pathways have been identified in activation or repression of *V. cholerae* biofilm formation and are mainly responsible for the positive regulation of biofilm in response to PTS sugars (116, 117). In contrast, the parallel nitrogen-specific PTS pathway appears to repress biofilm formation in LB, but not in minimal media (116). The involvement of PTS in biofilm formation suggests that the PTS may play a role in determining environmental suitability for biofilm growth and provides a clear link between *V. cholerae*'s nutrition status and ability to form biofilms.

In addition to PTS substrates, a number of other environmental signals can influence *V. cholerae* biofilm formation. Small organic cations known as

polyamines are produced by both eukaryotic and bacterial cells and are known to influence biofilm formation in *V. cholerae* (118–120). Increased environmental concentrations of the polyamine norspermidine increases biofilm formation and leads to NspS-mediated activation of *vpsL* transcription (120). Spermidine, which has a similar structure to norspermidine, represses biofilm formation and it has been hypothesized that excess exogenous spermidine may inhibit NspS interaction with norspermidine (119). Calcium (Ca^{+2}) levels can vary in the aquatic environment and extracellular Ca^{+2} has been demonstrated to inhibit *vps* transcription and lead to the dissolution of biofilms (121, 122). Indole, which is produced by bacteria found in the human gut, is thought to activate expression of *vps* genes (114). Additional signals and their impacts on biofilm formation are discussed in the subsequent sections. Though the mechanisms by which many of these signals are sensed have yet to be determined, elucidation of signal sensing and response is essential to our understanding of *V. cholerae* survival and could lead to the development of targeted treatments that interrupt these pathways.

Nutrient Acquisition in the Aquatic Environment.

V. cholerae is prototrophic and acquires nutrients from its environment. Procuring essential nutrients can be challenging in the aquatic environment, where seasonally variable conditions and inter- and intra-species competition limit access and availability. *V. cholerae* employs a number of tightly regulated nutrient acquisition strategies to enable its survival and persistence in the aquatic

environment; some of these strategies are also utilized when similar conditions are met in the host.

Chitin utilization. Chitin, an abundant insoluble polymer found in the exoskeleton of zooplankton and other marine crustaceans, provides a significant source of carbon and nitrogen for *V. cholerae* in the aquatic environment (12, 17, 19, 123). Composed of β-1,4-linked *N*-acetylglucosamine (GlcNAc) residues, chitin not only serves as a nutrient source, but also acts as a signaling molecule, a substrate for biofilm growth, and a mode of dissemination for *V. cholerae* (19). *V. cholerae* utilizes chemotaxis to swim toward chitin subunits, followed by attachment to chitin via a mechanism involving the MSHA pilus and the chitin-binding protein GbpA (19, 124). In response to chitin attachment, *V. cholerae* initiates a chitin catabolic response, which allows cells to degrade and catabolize chitin residues, and simultaneously induces natural competency, which allows cells to acquire new genetic material (21). Competent bacteria and eDNA are in close proximity in biofilms, therefore the bacteria can readily take up DNA and expand the genome to better cope with the stresses of the environmental lifestyle. Additionally, biofilm formation on chitinous zooplankton allows *V. cholerae* to disseminate to new waterways via passive locomotion or by mechanical transfer (125–127). Thus, *V. cholerae* growth on chitin supports survival, evolution, and transmission.

Two extracellular chitinases, ChiA-1 and ChiA-2, are activated during growth on chitin and degrade insoluble chitin polymers into shorter GlcNAc oligomers, which

are then transported into the cell via an ABC transporter (19, 20). The *V. cholerae* response to chitin is mediated by a two-component signal transduction system. In a typical two-component system (TCS) signal transduction cascade, the membrane-bound histidine kinase senses an environmental signal and autophosphorylates. The phosphate is then transferred to its cognate response regulator (RR), which alters the conformation of its output domain and initiates changes in gene expression or enzymatic activities. The sensor kinase ChiS initiates the chitin signaling cascade, though it does not appear to utilize the canonical TCS signaling described above. Instead, a high-affinity chitin binding protein (CBP) interacts with ChiS in the periplasm to keep it in the inactive state. In the presence of chitin, chitin subunits enter the periplasm through chitoporins and bind to CBP. The binding of chitin subunits to CBP allows it to dissociate from ChiS and activates the ChiS signaling cascade; it is unknown if this activation is initiated by autophosphorylation or an alternative mechanism (20). ChiS regulates the expression of 41 chitin-induced genes, including the GlcNAc catabolic operon, two extracellular chitinases, a chitoporin, and a type IV pilus involved in natural competency (19, 128). Recent work implies ChiS likely has two independent targets: a catabolic regulon and a competence regulon. ChiS activation of the catabolic regulon is mediated by a hypothetical canonical response regulator, ChiR, which remains to be identified and is required for transcription of the chitin catabolic genes in the *chb* operon (19, 128). Active ChiS also activates the transmembrane regulator, TfoS, which is responsible for regulating natural competency. TfoS subsequently promotes the transcription of the competence-

inducing sRNA, *tfoR* (128, 129). Transcription of *tfoR* is essential for the translation of *tfoX* mRNA*,* a positive regulator of natural competence and chitin metabolism genes in *V. cholerae* (130). TfoX and HapR activate expression of the regulator QstR, which is required for the expression of a subset of competence genes (131). Both activation of catabolism and competence appear to be independent of the ChiS conserved phosphorelay residues, indicating that ChiS activates chitin catabolism and natural competency through an atypical and, as of yet, unidentified mechanism.

Provision of competing carbon sources can downregulate the chitin utilization program via carbon catabolite repression (CCR) (125). CCR allows *V. cholerae* to preferentially utilize easily-metabolized carbon sources by repressing less desirable pathways, and glucose and other PTS sugars were shown to repress chitin utilization and natural competency. The PTS interferes with the accumulation of cAMP, which is required to work with its binding partner CRP, to initiate efficient colonization of the chitin surface, chitin degradation and utilization, and the induction of natural competency. Thus, PTS sugars inhibit the chitin utilization program via its repression of cAMP synthesis (125). Intriguingly, cAMP-CRP has been shown to repress biofilm formation, a phenotype associated with growth on chitin. This highlights the intricate and complex regulatory network that governs these phenotypes and further investigation is needed to understand how biofilm formation evades repression via cAMP-CRP when growing on chitin.

The chitin utilization program alleviates starvation due to the lack of nutrients in the water column, promotes the formation of biofilms, and initiates natural competency in *V. cholerae*. Additionally, components of this system may play roles in survival and pathogenesis during infection. Similarities between chitin and intestinal mucins allow the *N*-acetylglucosamine binding protein (GbpA) to aid in both attachment to chitin and in intestinal colonization of the host (132, 133). The extracellular chitinase ChiA2 was found to promote survival and pathogenesis in the host by allowing *V. cholerae* to utilize mucin as a nutrient source. ChiA2 was shown to de-glycoslate mucin, resulting in the release of GlcNAc and its oligomers, which can then be utilized for growth and survival in the host (134). This link between environmental and host nutrient acquisition is important in the evolution of *V. cholerae* to become a suxccessful environmental pathogen, allowing it to readily navigate two different systems using similar tools.

Nutrient storage granules. In addition to chitin utilization, *V. cholerae* copes with carbon limitation in the environment by using intracellular glycogen stores that are synthesized and accumulated when carbon sources are highly available. Glycogen, a polysaccharide made of glucose monomers with α-1,4 linkages and α-1,6 branches, serves as a common form of energy storage for many organisms. *V. cholerae* glycogen accumulation is regulated by nitrogen and carbon availability. When nitrogen is in excess, glycogen is continually synthesized and degraded at basal levels. When nitrogen is limited, enzymes involved in glycogen synthesis are upregulated and glycogen accumulation within the cell is stimulated (135). During

the first step of glycogen synthesis in *V. cholerae*, the ADP-glucose pyrophosphorylase enzymes GlgC1 and GlgC2 generate ADP-glucose from ATP and glucose-1-phosphate. Subsequently, the enzymes GlgA and GlgB build glycogen by forming α-1,4 and α-1,6 linkages, respectively, between ADP-glucose monomers (135). Depending on nitrogen and carbon availability, *V. cholerae* initiates glycogen breakdown via three enzymes: the glycogen debranching protein GlgX, the maltodextrin phosphorylase GlgP, and the 4-α-glucanotransferase MalQ (135, 136). The global transcriptional regulator CsrA (*c*arbon *s*torage *r*egulator) has been shown to negatively control the *glg* genes in *E. coli* and is thought to play a similar role in *V. cholerae* (136, 137). In *V. cholerae,* CsrA is post-transcriptionally regulated by the TCS VarSA, which represses CsrA translation via the activation of three sRNAs in response to an unknown environmental signal. A mutant lacking the HK gene *varS* had significantly less glycogen storage than wild type, indicating that this system and CsrA are involved in glycogen storage in *V. cholerae* (78, 136). Activation of VarSA and repression of CsrA are also known to inhibit biofilm formation via activation of HapR and may link carbon storage and nutritional status to QS and biofilm formation (78).

Glycogen storage and utilization promote *V. cholerae* dissemination and environmental survival in multiple ways. It is known that *V. cholerae* cells in rice water stool contain glycogen storage granules, indicating that the organism stores glycogen in preparation for dissemination from the nutrient-rich host into nutrient-poor environments like stool or pond water (135). These glycogen stores have

been shown to prolong *V. cholerae* survival in rice water stool, pond water, and the infant rabbit host (135, 136). Interestingly, a mutant unable to degrade glycogen survived as long as wild type in two of three rice water stool samples, while mutants defective in glycogen storage had reduced survival compared to wild type in all samples. This demonstrated that the presence of glycogen plays a protective role against environmental stresses, regardless of its ability to be metabolized, and can prolong survival after *V. cholerae* is shed in stool. However, in carbon-poor environments, the ability to degrade and utilize glycogen stores appears to be essential for survival, as mutants unable to degrade glycogen were dramatically attenuated in survival when compared to wild type under these conditions (135).

Glycogen-rich *V. cholerae* were also shown to be more virulent in an infant mouse model of transmission. Mutants lacking the ability to synthesize or degrade glycogen were attenuated for transmission in infant mice following incubation in pond water, indicating that the abilities to store and use glycogen are critical for *V. cholerae* to infect new hosts. Passage through pond water prior to infection was intended to mimic the environment *V. cholerae* encounters when it is shed in stool before it encounters a new host. This passage was necessary to observe the attenuated phenotype and supports the hypothesis that glycogen storage is important for transmission from host to host (135). Glycogen storage and metabolism appear to play significant roles in *V. cholerae* transmission, dissemination, and environmental survival.

Inorganic phosphate availability. *V. cholerae* must cope with the limited availability of inorganic phosphate (Pi), an essential nutrient, during its residence in the aquatic environment. In *V. cholerae,* PhoBR activates the Pho regulon, which includes genes involved in phosphate homeostasis, biofilm formation, motility, and virulence (138, 139). PhoBR is composed of the histidine kinase, PhoR, which phosphorylates its response regulator, PhoB, in response to low extracellular Pi levels. Once phosphorylated, PhoB regulates the expression of the genes that make up the Pho regulon through direct binding to DNA sequences known as Pho boxes. When Pi levels are sufficient, the phosphate-specific transport system (Pst) is inactive and represses activation of PhoBR through an unknown mechanism; this repression is lifted when Pi levels are low and the Pst becomes activated. Induction of PhoBR activity results in significant production of PstS, the periplasmic component of the Pst (140). Phosphorylated PhoB (P~PhoB) stimulates production of the alkaline phosphatase PhoA, which provides the cell with exogenous Pi, and two PhoH-family ATPases, which have unknown roles in mediating Pi limitation. P~PhoB also inhibits production of the outer membrane pore forming proteins OmpU and OmpT, while stimulating production of the phosphate-specific porin, PhoE (140, 141). Pi limitation induces genes that are part of the general stress regulon, which is controlled by the alternative sigma factor RpoS, and likely contributes to the ability of *V. cholerae* to survive low Pi conditions (140).

PhoBR also plays a role during infection and dissemination, suggesting that *V. cholerae* may experience Pi limitation in the host. *phoB* mutants had diminished survival in low-phosphate medium and infant mouse and rabbit intestines, as well as in pond water after passage through a host (138, 141). The response regulator PhoB is also required for *V. cholerae* survival in pond water following dissemination from the host (138). *In vivo* Pi supplementation only partially restored the colonization defect of a *phoB* mutant, indicating that this response regulator may respond to other signals in the small intestine. Additionally, PhoBR is a negative regulator of the major virulence activator *tcpP* and appears to play a temporal role in infection, as both strains lacking PhoBR and strains with constitutively activated PhoBR resulted in attenuated colonization in an infant mouse model (138). During late stage infection, PhoB is known to regulate genes involved in c-di-GMP metabolism that positively regulate motility, supporting a model in which phosphate limitation in the host prepares *V. cholerae* for dissemination by activating PhoB and motility (139). Together, these studies indicate that PhoBR is important for *V. cholerae* during much of its life cycle.

V. cholerae synthesizes large amounts of inorganic polyphosphate (poly-P), composed of long chains of linked Pi, in response to surplus extracellular phosphate (Figure 1.2). Loss of *ppk*, which encodes for the polyphosphate kinase required for poly-P synthesis, did not impact *V. cholerae* motility, biofilm formation, starvation survival, virulence or colonization of the suckling mouse intestine. However, sensitivity to other environmental stressors was enhanced, including

sensitivity to acid stress, osmotic stress, and oxidative stress in Pi-limited medium (142). Molecular mechanisms by which *ppk* provides protection from these stresses are yet to be determined.

Response to Physiological and Biological Stressors in the Aquatic Environment.

Physiological conditions such as salinity and temperature can change drastically in *V. cholerae*'s aquatic habitats and can alter the growth patterns and population dynamics of the organism. Biological stressors can also impact *V. cholerae* survival and abundance, including inter- and intra-species competition and predation by protozoa and bacteriophages. *V. cholerae* has evolved mechanisms for adapting to these physiological and biological stressors, which allow it to survive in aquatic reservoirs when conditions are unfavorable.

Adaptations to changes in salinity. In the coastal and estuarine habitats of *V. cholerae*, fluctuations in salinity and osmolarity are common and vary seasonally. Additionally, *V. cholerae* must adapt to salinity shifts upon host entry and exit. While the optimal salinity for *V. cholerae* growth is equivalent to 200 mM NaCl, a concentration commonly observed in estuarine habitats, it has adapted to tolerate a wide range of salinities and osmolarities. In response to osmotic stress, *V. cholerae* synthesizes ectoine and imports glycine betaine; these molecules are compatible solutes, or small, highly soluble molecules that balance extracellular osmotic pressure. Ectoine is synthesized via gene products from a four-gene

operon composed of a putative aspartokinase gene and *ectABC* (143). Expression of *ectABC* genes is regulated by osmolarity (112). Because *V. cholerae* lacks the genes needed for glycine betaine synthesis, it imports glycine betaine produced by other organisms via the transporter OpuD (111).

V. cholerae also responds to changes in osmolarity by regulating biofilm formation. Biofilm formation is highest in medium with osmolarity equal to that of 100 mM NaCl, which falls within the range typically found in estuaries, and lessens with increased or decreased osmolarity (112). Low osmolarity induces expression of the transcriptional regulator gene *oscR*, which represses biofilm genes (112). In contrast, the transcriptional regulator CosR activates biofilm genes and represses motility genes in response to high ionic strength. Additionally, CosR represses compatible solute biosynthesis and transporter genes at optimal ionic strength (~200 mM), independently of its function as a regulator of biofilm formation (113). These regulators link changes in external conditions with the production of biofilms, demonstrating both the significance of this growth mode in environmental survival and the complex regulatory networks that govern it.

Adaptations to changes in temperature. Temperature fluctuations due to seasonal changes are known to correlate with other factors that influence *V. cholerae* growth and survival, including shifts in plankton concentration, nutrient availability, and salinity, making it a suitable marker for indirect detection of *V. cholerae* occurrence via remote sensing (144). Ecological studies have

demonstrated that high water temperature, typically above 15°C, is a good predictor for the presence of *V. cholerae* (22, 145, 146). Temperature can also act as a signal for the transition between environment and host. When shifted to low temperatures relative to the host temperature of 37°C, *V. cholerae* has been shown to initiate biofilm formation via the activation of 6 DGCs that collectively increase c-di-GMP levels. Increased biofilm formation was observed at 15°C and 25°C when compared to growth at 37°C, with the greatest biofilm formation observed at the lowest temperature of 15°C (147). This indicates that biofilm formation may be initiated once *V. cholerae* transitions from the human host into the aquatic environment and may be upregulated when seasonal downshifts in temperature occur. In contrast, another study showed that attachment to chitin and biofilm formation was increased from 15°C and 25°C in *V. cholerae* N16961, as was *gbpA* and *mshA* expression. *In situ* analysis of zooplankton and water samples over an annual cycle demonstrated a higher percentage of plankton-associated *V. cholerae* at temperatures above 22°C, which could potentially enhance vector transmission to the host (148). Additionally, translation of a major *V. cholerae* virulence regulator, ToxT, appears to be activated via an RNA thermometer when the organism is shifted to 37°C, the internal temperature of its human host (149). These findings collective demonstrate that temperature plays an important, and complex, role in *V. cholerae* regulation of environmental survival, transmission, and infection.

V. cholerae utilizes several survival mechanisms in response to suboptimal temperatures. Two cold shock proteins, CspA and CspV, are induced when *V. cholerae* experiences low temperatures, and appear to play roles in cold adaptation. However, the mechanism of adaptation and regulons of these cold shock proteins have not been extensively explored (150). CspA and CspV are hypothesized to play roles in induction of a nonculturable state in response to 4°C temperatures. The nonculturable state, which is induced in response to cold stress or nutritional starvation, allows *V. cholerae* to survive unfavorable environmental conditions and is described in greater detail at the end of this section (151). CspV was also shown to positively regulate biofilm formation and T6SS activity in a temperature dependent manner (152). This process indicates that *V. cholerae* can respond to the broad range of temperatures it encounters during its life cycle and initiate the appropriate responses, either activating protective measures to improve environmental survival during seasonal temperature drops or inducing virulence factors that enhance intestinal colonization once it transitions from the aquatic environment into the human host.

Protozoan Grazing. In aquatic environments, *V. cholerae* is preyed upon by a variety of bacterivorous predators, including ciliated and flagellated protozoa. In response to this biological stress, the bacterium has evolved mechanisms to shield itself from grazing and to actively kill predators. The T6SS, which is described in the more detail in the next section, can be mobilized to kill predatory protozoa and was, in fact, initially discovered for its ability to attack and kill the model host

amoeba *Dictyostelium discoideum* (153). This defense mechanism requires direct contact with predator cells, as the T6SS structure must puncture the cell membrane to deliver the VasX and TseL toxins (154, 155).

Predator grazing also stimulates VPS production, leading to enhanced biofilm formation and a switch from smooth to rugose morphology associated with higher VPS production. VPS provides a physical barrier that partially protects *V. cholerae* from grazing (156). Additionally, *V. cholerae* biofilms grown on chitin appear to have higher antiprotozoal activity than those grown on abiotic surfaces and were shown to significantly reduce numbers of the surface-feeding flagellate *Rhynchomonas nasuta*, which is sensitive to ammonium produced by *V. cholerae* as a byproduct of chitin metabolism. The loss of QS in biofilms grown on chitin results in lower ammonium production and reduced toxicity to *R. nasuta* (157). Non-chitin biofilms have also been demonstrated to promote predator killing via the production of QS-dependent anti-protozoal factors and reduce predatory numbers at higher rates than planktonic cultures (15). While these anti-protozoal factors have not yet been identified, the HapR-regulated secreted protease PrtV is thought to be a candidate and was shown to be responsible for *V. cholerae* killing of *Cafeteria roenbergensis* and *Tetrahymena pyriformis* (158). The fact that both VPS and HapR contribute to grazing resistance is intriguing, as HapR downregulates *vps* expression. The role of HapR/QS in grazing resistance appears to be greater than that of VPS, because *hapR* mutants are less resistant to grazing than *vps* mutants (156). However, *hapR* mutants exhibit some grazing resistance

in field and microcosm experiments, likely due to the increased biofilm formation phenotypes associated with *hapR* mutations. This physical protection from predators likely accounts for the enhanced grazing resistance of *hapR* mutants compared to wild type, and demonstrates that *V. cholerae* uses multiple, independent mechanisms for evading predation (64, 159, 160). Pyomelanin production, and thus reactive oxygen species (ROS) production, was additionally shown to increase the grazing resistance of *V. cholerae* biofilms, suggesting that ROS production is a defensive mechanism used against predation (161).

Type VI secretion system. *V. cholerae* utilizes the T6SS, to translocate effector proteins into a diverse group of target cells, including other bacteria, phagocytic amoebas, and human macrophages. This secretion system contributes to environmental survival and persistence by providing a defense against other bacteria and eukaryotic predators, and appears to play a role in host survival by interrupting host phagocytosis (153, 162–164). The T6SS is ubiquitous among gram-negative bacteria and is composed of a dynamic, contractile phage tail-like structure anchored to a membrane associated, cell-envelope spanning assembly. T6SS delivers effector proteins in a contact-dependent manner, which occurs via assembly of the phage tail-like structure, composed of a baseplate, tube, and sheath, onto the membrane complex. This is followed by the contraction of the sheath-like structure, resulting in the propulsion of the inner tube towards the target cell and the delivery the effector protein. The contracted sheath is then disassembled and sheath components are recycled (165).

The T6SS delivery tube is composed of repeating units of the hemolysin coregulated protein (Hcp) and a trimeric tip is composed of the valine–glycine repeat proteins G (VgrG1-3). Some VgrGs carry C-terminal extensions that are enzymatically active and can impact the target cell, including *V. cholerae*'s VgrG-1, which cross links actin in eukaryotic cells, and VgrG-3, which carries a C-terminal domain with peptidoglycan degrading activity that kills other bacterial cells (163, 166). The T6SS can be used to deliver VgrG-associated effectors or independent effectors, such as the *V. cholerae* T6SS toxins VasX and TseL, which disrupt both prokaryotic and eukaryotic cell membranes (154, 155, 167). Most T6SS effectors have corresponding antagonistic immunity proteins that inactivate the effector and prevent self-killing (155). Three main *V. cholerae* effectors, VgrG-3, VasX, and TseL, are known to be inactivated by the immunity genes *tsiV3*, *tsiV2*, and *tsiV1*, respectively, which are encoded directly downstream of their corresponding effectors (167, 168).

The T6SS plays an important role in inter- and intra-species competition (153, 164). Strains of *V. cholerae* that constitutively express the T6SS are not only highly virulent towards other bacteria, but they are also more virulent against other *V. cholerae* strains that constitutively express the T6SS (164, 169). While all *V. cholerae* strains sequenced to date harbor T6SS genes, the effectors and immunity proteins within these conserved genes exhibit diversity between strains. Compatible strains do not kill one another because they harbor the same immunity

proteins, but incompatible strains that carry different effector modules are subject to intraspecies killing (168). Some strains that do not constitutively express the T6SS carry the immunity proteins necessary for protection against the strains that constitutively express the T6SS; however, different strains that constitutively express the T6SS were shown to enhance killing of one another, likely due to heterologous effector-immunity sets (169).

Three genomic loci encode for the *V. cholerae* T6SS. The major, or large, cluster encodes for the structural components of the T6SS, while two auxiliary clusters encode Hcp proteins (153). All three clusters harbor effector and immunity proteins (168). Though our understanding of the regulation of these genes is incomplete, several regulators of the T6SS have been identified, including VasH, RpoN, HapR, LuxO, cAMP-CRP, FliA, TsrA, TfoX, TfoY, LonA, QstR, and OscR (Figure 1.4) (153, 170–178). VasH is an RpoN-dependent transcriptional regulator encoded within the T6SS large cluster that upregulates the expression of the *hcp* and *vasX* genes by binding to the promoter regions of the large T6SS cluster and the satellite cluster starting with *hcp-1* (153, 154). VasH is predicted to activate the alternative sigma factor RpoN, which positively regulates the *hcp* operons and *vrgG3*, but has no effect on the main T6SS cluster (171, 173, 179). QS also plays a role in T6SS regulation. T6SS genes are positively regulated by HapR and negatively regulated by phosphorylated LuxO and QS sRNAs, which inhibit HapR translation and base pair to the large T6SS to inhibit transcription (172–174). The regulatory complex cAMP-CRP, which is required for the biosynthesis of the cholera autoinducer (CAI-

1) to activate QS, positively controls expression of *hcp* and elimination of cAMP-CRP was shown to ablate production of Hcp (173). Additional negative regulators of T6SS genes have been identified, including the protease LonA (178). Deletion of flagellar regulatory genes results in the upregulation of T6SS genes, including the alternative sigma factor responsible for activating late stage flagellin genes, FliA (176, 180). The global transcriptional regulator TsrA has some structural similarity to H-NS and appears to play a similar silencing role to repress T6SS genes (172).

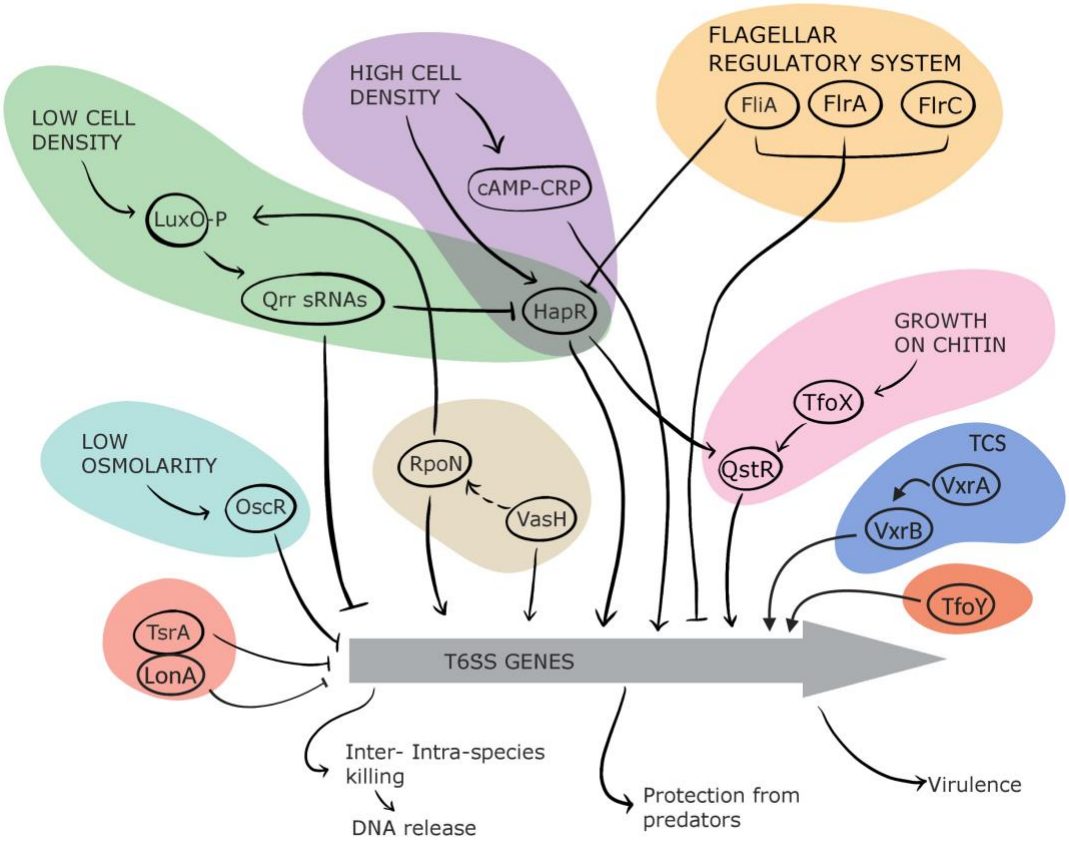

Figure 1.4. Regulation of *V. cholerae* Type Six Secretion System (T6SS).

The *V. cholerae* T6SS plays an important role in the life cycle of this pathogen, enhancing inter- and intra-species competition, protection from predators, and virulence. In strains where this system is not constitutively active, the T6SS is regulated in response to a number of environmental signals. The TCS VxrAB is a positive regulator of the T6SS. Though it is unknown what signal TsrA responds to, this global regulator represses the T6SS and the master virulence regulator ToxT, while activating HapA expression, which is involved in mucin degradation. The protease LonA also represses T6SS-killing. Low osmolarity results in activation of the osmoregulator, OscR, which represses the T6SS. Quorum

sensing (QS) also regulates the T6SS in response to cell density. At low cell density, LuxO is phosphorylated and activates the expression of quorum regulatory small RNAs (Qrr sRNAs), which repress the T6SS through both direct binding to the promoter regions of T6SS genes and through their inhibition of the positive regulator of T6SS, HapR. At high cell density, both HapR and the cAMP-CRP complex activate T6SS. HapR also actives QstR, as does TfoX, which upregulates T6SS in response to growth on chitin. The TfoX homolog, TfoY, positively regulates the T6SS when c-di-GMP levels are low. Flagellar regulatory genes are known to repress the T6SS through an unknown mechanism. Additionally, VasH, which is encoded by the T6SS pathogenicity island, is known to activate T6SS genes, potentially through its interaction with the alternative sigma factor RpoN, which appears to co-regulate T6SS genes in cAMP-CRP dependent manner. Intriguingly, RpoN is also known to active Qrr sRNAs, which repress the T6SS.

Environmental signals stimulating expression of T6SS genes have been identified. A recent study revealed that expression of the T6SS is positively controlled by two major regulators of competency, TfoX and QstR, which are activated in response to growth on chitin (175). Growth on chitin supports the formation of biofilms and allows predatory cells close access to neighboring bacteria within the densely packed microbial community. Upregulation of the T6SS by natural competency regulatory circuitry results in the killing of nonimmune neighboring cells during growth on chitin. DNA is released from the lysed target cell, which is then taken up by the predatory cell via the competency machinery. In addition to its role in competition, this study demonstrated that the T6SS can enhance DNA uptake, potentially leading to increased evolution via horizontal gene transfer when the new DNA is incorporated into the genome (175). A TfoX homolog, TfoY, was shown to regulate the T6SS independently of QS. In response to low c-di-GMP levels, TfoY activates T6SS-dependent and -independent toxins, as well as motility, as part of what is predicted to be a defensive escape mechanism (177).

T6SS expression is enhanced under high osmolarity and low temperature conditions, which mimic estuarine conditions, suggesting that this system may be important in defense against predation and intraspecies competition in the aquatic environment. Genetic evidence suggests that the osmoregulator, OscR, represses the T6SS under low osmolarity at 37°C, though the mechanism of regulation has not been determined (181). It is hypothesized that expression of the T6SS in O1 strains is regulated in a pathoadaptive manner by osmolarity and temperature

shifts; however, the T6SS also appears to play a role in the human host and likely responds to additional signals. The immunity gene *tsiV3* was shown to contribute to colonization of infant rabbit intestines when co-colonized with bacterial cells carrying a functional T6SS, indicating that *in vivo* species competition may contribute to virulence (182). Additionally, the effector VgrR-1 is known to increase inflammation and colonization in an infant mouse model (183). Our lab also demonstrated that key structural components of the T6SS are important for efficient host colonization, supporting earlier findings that other T6SS genes contribute to virulence (184). Thus, the T6SS contributes to both environmental and host survival, though further characterization of this important system is needed to fully determine its role in *V. cholerae* ecology.

Community structure

Biofilm formation is a complex and multi-step process governed by numerous environmental and cellular inputs. In the natural environment these dynamics are expected to be even more complex, as biofilms are frequently composed of multiple species and strains that may cooperate or compete for resources (185). Physiological heterogeneity develops in both mono-species and mixed species biofilms, contributing to the emergence of oxygen, nutrient, and pH gradients within the biofilm (186, 187). Our understanding of social interactions within biofilms is still evolving, however, metabolic activity, cell-to-cell signaling, and even cell shape appear to further influence the balance between cooperation and competition within the biofilm (188–190).

Cooperative behavior within the biofilm includes the secretion of adhesins, digestive enzymes, and chelators, which provides advantages to the biofilm-living cells compared to their free-living counterparts (19, 30, 49, 191–194). This can lead to the so-called “public-goods” dilemma, in which ‘cheaters,’ or non-producers, benefit from secreted compounds without contributing (192, 193, 195). This is partially combatted by clonal clustering, which limits these resources to kin producing cells and excludes non-producers, however, spatial mixing due to dispersal or physical disturbance can force interactions that disrupt this segregation (193, 196). When these encounters occur, competition strategies are often employed, including rapid growth, resource sequestration, and toxin/antibiotic secretion to actively kill neighboring cells (197–200).

Currently, little information about *V. cholerae* T6SS activity within biofilms is available. Recent work demonstrated that *vibrio*polysaccharide (*vps*) can protect *V. cholerae* against exogenous T6SS attack without preventing *V. cholerae* from utilizing its own T6SS (201). The *V. cholerae* T6SS has also been shown to contribute to horizontal gene transfer on chitin, indicating that cell lysis and extracellular DNA exchange may be an important consequence of T6SS activity (175). Finally, *V. cholerae* uses the T6SS to compete with the gut microbiota and colonize the small intestine (184, 202–204). The ability of the T6SS to lyse neighboring cells may additionally contribute to biofilm structure and architecture, as extracellular DNA is known to be an important component of the biofilm matrix

(59). Results from experiments designed to analyze the impact of the T6SS in biofilms is discussed in Chapter 3.

References

1. **Flemming H-C**, **Wingender J**, **Szewzyk U**, **Steinberg P**, **Rice SA**, **Kjelleberg S**. 2016. Biofilms: an emergent form of bacterial life. Nat. Rev. Microbiol. **14**:563–575.
2. **Donlan RM**. 2002. Biofilms: microbial life on surfaces. Emerg. Infect. Dis. **8**:881–90.
3. **Ali M**, **Lopez AL**, **You YA**, **Kim YE**, **Sah B**, **Maskery B**, **Clemens J**. 2012. The global burden of cholera. Bull. World Health Organ. **90**:209-218A.
4. **Kaper JB**, **Morris JG**, **Levine MM**. 1995. Cholera. Clin. Microbiol. Rev. **8**:48–86.
5. **Charles RC**, **Ryan ET**. 2011. Cholera in the 21st century. Curr. Opin. Infect. Dis. **24**:472–7.
6. **Chin C-S**, **Sorenson J**, **Harris JB**, **Robins WP**, **Charles RC**, **Jean-Charles RR**, **Bullard J**, **Webster DR**, **Kasarskis A**, **Peluso P**, **Paxinos EE**, **Yamaichi Y**, **Calderwood SB**, **Mekalanos JJ**, **Schadt EE**, **Waldor MK**. 2011. The origin of the Haitian cholera outbreak strain. N. Engl. J. Med. **364**:33–42.
7. **Nguyen BM**, **Lee JH**, **Cuong NT**, **Choi SY**, **Hien NT**, **Anh DD**, **Lee HR**, **Ansaruzzaman M**, **Endtz HP**, **Chun J**, **Lopez AL**, **Czerkinsky C**, **Clemens JD**, **Kim DW**. 2009. Cholera outbreaks caused by an altered *Vibrio cholerae* O1 El Tor biotype strain producing classical cholera toxin B in Vietnam in 2007 to 2008. J. Clin. Microbiol. **47**:1568–71.
8. **Mason PR**. 2009. Zimbabwe experiences the worst epidemic of cholera in

Africa. J. Infect. Dev. Ctries. **3**:148–151.

9. **Alam M**, **Sultana M**, **Nair GB**, **Sack RB**, **Sack DA**, **Siddique AK**, **Ali A**, **Huq A**, **Colwell RR**. 2006. Toxigenic *Vibrio cholerae* in the aquatic environment of Mathbaria, Bangladesh. Appl. Environ. Microbiol. **72**:2849–55.

10. **Faruque SM**, **Albert MJ**, **Mekalanos JJ**. 1998. Epidemiology, genetics, and ecology of toxigenic *Vibrio cholerae*. Microbiol. Mol. Biol. Rev. **62**:1301–14.

11. **Huq A**, **Sack RB**, **Nizam A**, **Longini IM**, **Nair GB**, **Ali A**, **Morris JG**, **Khan MNH**, **Siddique AK**, **Yunus M**, **Albert MJ**, **Sack DA**, **Colwell RR**. 2005. Critical factors influencing the occurrence of *Vibrio cholerae* in the environment of Bangladesh. Appl. Environ. Microbiol. **71**:4645–54.

12. **Islam MS**, **Jahid MIK**, **Rahman MM**, **Rahman MZ**, **Islam MS**, **Kabir MS**, **Sack DA**, **Schoolnik GK**. 2007. Biofilm acts as a microenvironment for plankton-associated *Vibrio cholerae* in the aquatic environment of Bangladesh. Microbiol. Immunol. **51**:369–79.

13. **Faruque SM**, **Biswas K**, **Udden SMN**, **Ahmad QS**, **Sack DA**, **Nair GB**, **Mekalanos JJ**. 2006. Transmissibility of cholera: *in vivo*-formed biofilms and their relationship to infectivity and persistence in the environment. Proc. Natl. Acad. Sci. U. S. A. **103**:6350–5.

14. **Alam M**, **Sultana M**, **Nair GB**, **Siddique AK**, **Hasan NA**, **Sack RB**, **Sack DA**, **Ahmed KU**, **Sadique A**, **Watanabe H**, **Grim CJ**, **Huq A**, **Colwell RR**. 2007. Viable but nonculturable *Vibrio cholerae* O1 in biofilms in the aquatic

environment and their role in cholera transmission. Proc. Natl. Acad. Sci. U. S. A. **104**:17801–6.

15. **Matz C**, **McDougald D**, **Moreno AM**, **Yung PY**, **Yildiz FH**, **Kjelleberg S**. 2005. Biofilm formation and phenotypic variation enhance predation-driven persistence of *Vibrio cholerae*. Proc. Natl. Acad. Sci. U. S. A. **102**:16819–24.
16. **Beyhan S**, **Yildiz FH**. 2007. Smooth to rugose phase variation in *Vibrio cholerae* can be mediated by a single nucleotide change that targets c-di-GMP signalling pathway. Mol. Microbiol. **63**:995–1007.
17. **Tamplin ML**, **Gauzens AL**, **Huq A**, **Sack DA**, **Colwell RR**. 1990. Attachment of *Vibrio cholerae* serogroup O1 to zooplankton and phytoplankton of Bangladesh waters. Appl. Environ. Microbiol. **56**:1977–80.
18. **Rawlings TK**, **Ruiz GM**, **Colwell RR**. 2007. Association of *Vibrio cholerae* O1 El Tor and O139 Bengal with the Copepods Acartia tonsa and Eurytemora affinis. Appl. Environ. Microbiol. **73**:7926–33.
19. **Meibom KL**, **Li XB**, **Nielsen AT**, **Wu C-Y**, **Roseman S**, **Schoolnik GK**. 2004. The *Vibrio cholerae* chitin utilization program. Proc. Natl. Acad. Sci. U. S. A. **101**:2524–9.
20. **Li X**, **Roseman S**. 2004. The chitinolytic cascade in *Vibrios* is regulated by chitin oligosaccharides and a two-component chitin catabolic sensor/kinase. Proc. Natl. Acad. Sci. U. S. A. **101**:627–31.
21. **Meibom KL**, **Blokesch M**, **Dolganov NA**, **Wu C-Y**, **Schoolnik GK**. 2005. Chitin induces natural competence in *Vibrio cholerae*. Science **310**:1824–7.

22. **Lipp EK**, **Huq A**, **Colwell RR**. 2002. Effects of global climate on infectious disease: the cholera model. Clin. Microbiol. Rev. **15**:757–70.

23. **Colwell RR**, **Huq A**, **Islam MS**, **Aziz KMA**, **Yunus M**, **Khan NH**, **Mahmud A**, **Sack RB**, **Nair GB**, **Chakraborty J**, **Sack DA**, **Russek-Cohen E**. 2003. Reduction of cholera in Bangladeshi villages by simple filtration. Proc. Natl. Acad. Sci. U. S. A. **100**:1051–5.

24. **Bari SMN**, **Roky MK**, **Mohiuddin M**, **Kamruzzaman M**, **Mekalanos JJ**, **Faruque SM**. 2013. Quorum-sensing autoinducers resuscitate dormant *Vibrio cholerae* in environmental water samples. Proc. Natl. Acad. Sci. U. S. A. **110**:9926–31.

25. **Colwell RR**, **Brayton P**, **Herrington D**, **Tall B**, **Huq A**, **Levine MM**. 1996. Viable but non-culturable *Vibrio cholerae* O1 revert to a cultivable state in the human intestine. World J. Microbiol. Biotechnol. **12**:28–31.

26. **Tamayo R**, **Patimalla B**, **Camilli A**. 2010. Growth in a biofilm induces a hyperinfectious phenotype in *Vibrio cholerae*. Infect. Immun. **78**:3560–9.

27. **Nielsen AT**, **Dolganov NA**, **Rasmussen T**, **Otto G**, **Miller MC**, **Felt SA**, **Torreilles S**, **Schoolnik GK**. 2010. A bistable switch and anatomical site control *Vibrio cholerae* virulence gene expression in the intestine. PLoS Pathog. **6**:e1001102.

28. **Hang L**, **John M**, **Asaduzzaman M**, **Bridges EA**, **Vanderspurt C**, **Kirn TJ**, **Taylor RK**, **Hillman JD**, **Progulske-Fox A**, **Handfield M**, **Ryan ET**, **Calderwood SB**. 2003. Use of in vivo-induced antigen technology (IVIAT) to identify genes uniquely expressed during human infection with *Vibrio*

cholerae. Proc. Natl. Acad. Sci. U. S. A. **100**:8508–13.

29. **Lombardo M-J**, **Michalski J**, **Martinez-Wilson H**, **Morin C**, **Hilton T**, **Osorio CG**, **Nataro JP**, **Tacket CO**, **Camilli A**, **Kaper JB**. 2007. An in vivo expression technology screen for *Vibrio cholerae* genes expressed in human volunteers. Proc. Natl. Acad. Sci. U. S. A. **104**:18229–34.
30. **Fong JCN**, **Syed KA**, **Klose KE**, **Yildiz FH**. 2010. Role of Vibrio polysaccharide (vps) genes in VPS production, biofilm formation and *Vibrio cholerae* pathogenesis. Microbiology **156**:2757–69.
31. **Utada AS**, **Bennett RR**, **Fong JCN**, **Gibiansky ML**, **Yildiz FH**, **Golestanian R**, **Wong GCL**. 2014. *Vibrio cholerae* use pili and flagella synergistically to effect motility switching and conditional surface attachment. Nat. Commun. **5**:4913.
32. **Berke A**, **Turner L**, **Berg H**, **Lauga E**. 2008. Hydrodynamic attraction of swimming microorganisms by surfaces. Phys. Rev. Lett. **101**:038102.
33. **Kojima S**, **Yamamoto K**, **Kawagishi I**, **Homma M**. 1999. The polar flagellar motor of *Vibrio cholerae* is driven by an Na+ motive force. J. Bacteriol. **181**:1927–30.
34. **Lauga E**, **DiLuzio WR**, **Whitesides GM**, **Stone HA**. 2006. Swimming in circles: motion of bacteria near solid boundaries. Biophys. J. **90**:400–12.
35. **Watnick PI**, **Kolter R**. 1999. Steps in the development of a *Vibrio cholerae* El Tor biofilm. Mol. Microbiol. **34**:586–95.
36. **Gibiansky ML**, **Conrad JC**, **Jin F**, **Gordon VD**, **Motto DA**, **Mathewson MA**, **Stopka WG**, **Zelasko DC**, **Shrout JD**, **Wong GCL**. 2010. Bacteria

use type IV pili to walk upright and detach from surfaces. Science **330**:197.

37. **O'Toole GA**, **Kolter R**. 1998. Flagellar and twitching motility are necessary for *Pseudomonas aeruginosa* biofilm development. Mol. Microbiol. **30**:295–304.

38. **Zhao K**, **Tseng BS**, **Beckerman B**, **Jin F**, **Gibiansky ML**, **Harrison JJ**, **Luijten E**, **Parsek MR**, **Wong GCL**. 2013. Psl trails guide exploration and microcolony formation in *Pseudomonas aeruginosa* biofilms. Nature **497**:388–91.

39. **Gloag ES**, **Turnbull L**, **Huang A**, **Vallotton P**, **Wang H**, **Nolan LM**, **Mililli L**, **Hunt C**, **Lu J**, **Osvath SR**, **Monahan LG**, **Cavaliere R**, **Charles IG**, **Wand MP**, **Gee ML**, **Prabhakar R**, **Whitchurch CB**. 2013. Self-organization of bacterial biofilms is facilitated by extracellular DNA. Proc. Natl. Acad. Sci. U. S. A. **110**:11541–6.

40. **Watnick PI**, **Lauriano CM**, **Klose KE**, **Croal L**, **Kolter R**. 2001. The absence of a flagellum leads to altered colony morphology, biofilm development and virulence in *Vibrio cholerae* O139. Mol. Microbiol. **39**:223–235.

41. **Lauriano CM**, **Ghosh C**, **Correa NE**, **Klose KE**. 2004. The sodium-driven flagellar motor controls exopolysaccharide expression in *Vibrio cholerae*. J. Bacteriol. **186**:4864–74.

42. **Reichhardt C**, **Fong JCN**, **Yildiz F**, **Cegelski L**. 2015. Characterization of the *Vibrio cholerae* extracellular matrix: a top-down solid-state NMR approach. Biochim. Biophys. Acta **1848**:378–83.

43. **Yildiz FH**, **Schoolnik GK**. 1999. *Vibrio cholerae* O1 El Tor: identification of a gene cluster required for the rugose colony type, exopolysaccharide production, chlorine resistance, and biofilm formation. Proc. Natl. Acad. Sci. U. S. A. **96**:4028–33.

44. **Yildiz F**, **Fong J**, **Sadovskaya I**, **Grard T**, **Vinogradov E**. 2014. Structural characterization of the extracellular polysaccharide from *Vibrio cholerae* O1 El-Tor. PLoS One **9**:e86751.

45. **Fong JCN**, **Yildiz FH**. 2007. The *rbmBCDEF* gene cluster modulates development of rugose colony morphology and biofilm formation in *Vibrio cholerae*. J. Bacteriol. **189**:2319–30.

46. **Fong JCN**, **Karplus K**, **Schoolnik GK**, **Yildiz FH**. 2006. Identification and characterization of RbmA, a novel protein required for the development of rugose colony morphology and biofilm structure in *Vibrio cholerae*. J. Bacteriol. **188**:1049–59.

47. **Nesper J**, **Lauriano CM**, **Klose KE**, **Kapfhammer D**, **Kraiss A**, **Reidl J**. 2001. Characterization of *Vibrio cholerae* O1 El tor *galU* and *galE* mutants: influence on lipopolysaccharide structure, colonization, and biofilm formation. Infect. Immun. **69**:435–45.

48. **Berk V**, **Fong JCN**, **Dempsey GT**, **Develioglu ON**, **Zhuang X**, **Liphardt J**, **Yildiz FH**, **Chu S**. 2012. Molecular architecture and assembly principles of *Vibrio cholerae* biofilms. Science **337**:236–9.

49. **Absalon C**, **Van Dellen K**, **Watnick PI**. 2011. A communal bacterial adhesin anchors biofilm and bystander cells to surfaces. PLoS Pathog.

7:e1002210.

50. **Hollenbeck EC**, **Fong JCN**, **Lim JY**, **Yildiz FH**, **Fuller, Gerald G. and Cegelski L**. 2014. Molecular determinants of mechanical properties of *V. cholerae* biofilms at the air-liquid interface. Biophys. J. **Accepted**.
51. **Giglio KM**, **Fong JC**, **Yildiz FH**, **Sondermann H**. 2013. Structural basis for biofilm formation via the *Vibrio cholerae* matrix protein RbmA. J. Bacteriol. **195**:3277–86.
52. **Maestre-Reyna M**, **Wu W-J**, **Wang AH-J**. 2013. Structural insights into RbmA, a biofilm scaffolding protein of *V. cholerae*. PLoS One **8**:e82458.
53. **Fong JC**, **Rogers A**, **Michael AK**, **Parsley NC**, **Cornell W-C**, **Lin Y-C**, **Singh PK**, **Hartmann R**, **Drescher K**, **Vinogradov E**, **Dietrich LE**, **Partch CL**, **Yildiz FH**. 2017. Structural dynamics of RbmA governs plasticity of *Vibrio cholerae* biofilms. Elife **6**.
54. **Duperthuy M**, **Sjöström AE**, **Sabharwal D**, **Damghani F**, **Uhlin BE**, **Wai SN**. 2013. Role of the *Vibrio cholerae* matrix protein Bap1 in cross-resistance to antimicrobial peptides. PLoS Pathog. **9**:e1003620.
55. **Levan SR**, **Olson R**. 2012. Determination of the carbohydrate-binding specificity of lectin-like domains in *Vibrio cholerae* cytolysin. Biophys. J. **102**:461a-462a.
56. **De S**, **Kaus K**, **Sinclair S**, **Case BC**, **Olson R**. 2018. Structural basis of mammalian glycan targeting by *Vibrio cholerae* cytolysin and biofilm proteins. PLOS Pathog. **14**:e1006841.
57. **Johnson TL**, **Fong JC**, **Rule C**, **Rogers A**, **Yildiz FH**, **Sandkvist M**. 2014.

The Type II secretion system delivers matrix proteins for biofilm formation by *Vibrio cholerae*. J. Bacteriol. **196**:4245–52.

58. **Altindis E**, **Fu Y**, **Mekalanos JJ**. 2014. Proteomic analysis of *Vibrio cholerae* outer membrane vesicles. Proc. Natl. Acad. Sci. U. S. A. **111**:E1548-56.

59. **Seper A**, **Fengler VHI**, **Roier S**, **Wolinski H**, **Kohlwein SD**, **Bishop AL**, **Camilli A**, **Reidl J**, **Schild S**. 2011. Extracellular nucleases and extracellular DNA play important roles in *Vibrio cholerae* biofilm formation. Mol. Microbiol. **82**:1015–37.

60. **Hay AJ**, **Zhu J**. 2015. Host intestinal signal-promoted biofilm dispersal induces *Vibrio cholerae* colonization. Infect. Immun. **83**:317–23.

61. **Yildiz FH**, **Dolganov NA**, **Schoolnik GK**. 2001. VpsR, a member of the response regulators of the two-component regulatory systems, is required for expression of *vps* biosynthesis genes and EPS(ETr)-associated phenotypes in *Vibrio cholerae* O1 El Tor. J. Bacteriol. **183**:1716–26.

62. **Zamorano-Sánchez D**, **Fong JCN**, **Kilic S**, **Erill I**, **Yildiz FH**. 2015. Identification and characterization of VpsR and VpsT binding sites in *Vibrio cholerae*. J. Bacteriol. **Accepted**.

63. **Beyhan S**, **Bilecen K**, **Salama SR**, **Casper-Lindley C**, **Yildiz FH**. 2007. Regulation of rugosity and biofilm formation in *Vibrio cholerae*: comparison of VpsT and VpsR regulons and epistasis analysis of *vpsT*, *vpsR*, and *hapR*. J. Bacteriol. **189**:388–402.

64. **Yildiz FH**, **Liu XS**, **Heydorn A**, **Schoolnik GK**. 2004. Molecular analysis of

rugosity in a *Vibrio cholerae* O1 El Tor phase variant. Mol. Microbiol. **53**:497–515.

65. **Srivastava D**, **Harris RC**, **Waters CM**. 2011. Integration of cyclic di-GMP and quorum sensing in the control of *vpsT* and *aphA* in *Vibrio cholerae*. J. Bacteriol. **193**:6331–41.

66. **Hsieh M-L**, **Hinton DM**, **Waters CM**. 2018. VpsR and cyclic di-GMP together drive transcription initiation to activate biofilm formation in *Vibrio cholerae*. Nucleic Acids Res. **46**:8876–8887.

67. **Krasteva P V**, **Fong JCN**, **Shikuma NJ**, **Beyhan S**, **Navarro MVAS**, **Yildiz FH**, **Sondermann H**. 2010. *Vibrio cholerae* VpsT regulates matrix production and motility by directly sensing cyclic di-GMP. Science **327**:866–8.

68. **Yang M**, **Frey EM**, **Liu Z**, **Bishar R**, **Zhu J**. 2010. The virulence transcriptional activator AphA enhances biofilm formation by *Vibrio cholerae* by activating expression of the biofilm regulator VpsT. Infect. Immun. **78**:697–703.

69. **Casper-Lindley C**, **Yildiz FH**. 2004. VpsT Is a transcriptional regulator required for expression of *vps* biosynthesis genes and the development of rugose colonial morphology in *Vibrio cholerae* O1 El Tor. J. Bacteriol. **186**:1574–1578.

70. **He H**, **Cooper JN**, **Mishra A**, **Raskin DM**. 2012. Stringent response regulation of biofilm formation in *Vibrio cholerae*. J. Bacteriol. **194**:2962–72.

71. **Zhu J**, **Mekalanos JJ**. 2003. Quorum sensing-dependent biofilms enhance

colonization in *Vibrio cholerae*. Dev. Cell **5**:647–656.

72. **Hammer BK**, **Bassler BL**. 2003. Quorum sensing controls biofilm formation in *Vibrio cholerae*. Mol. Microbiol. **50**:101–4.

73. **Jobling MG**, **Holmes RK**. 1997. Characterization of *hapR* , a positive regulator of the *Vibrio cholerae* HA/protease gene hap , and its identification as a functional homologue of the *Vibrio harveyi luxR* gene. Mol. Microbiol. **26**:1023–1034.

74. **Waters CM**, **Lu W**, **Rabinowitz JD**, **Bassler BL**. 2008. Quorum sensing controls biofilm formation in *Vibrio cholerae* through modulation of cyclic di-GMP levels and repression of vpsT. J. Bacteriol. **190**:2527–36.

75. **De Silva RS**, **Kovacikova G**, **Lin W**, **Taylor RK**, **Skorupski K**, **Kull FJ**. 2007. Crystal structure of the *Vibrio cholerae* quorum-sensing regulatory protein HapR. J. Bacteriol. **189**:5683–91.

76. **Liu Z**, **Stirling FR**, **Zhu J**. 2007. Temporal quorum-sensing induction regulates *Vibrio cholerae* biofilm architecture. Infect. Immun. **75**:122–6.

77. **Ng W-L**, **Bassler BL**. 2009. Bacterial quorum-sensing network architectures. Annu. Rev. Genet. **43**:197–222.

78. **Tsou AM**, **Liu Z**, **Cai T**, **Zhu J**. 2011. The VarS/VarA two-component system modulates the activity of the *Vibrio cholerae* quorum-sensing transcriptional regulator HapR. Microbiology **157**:1620–8.

79. **Lenz DH**, **Miller MB**, **Zhu J**, **Kulkarni R V**, **Bassler BL**. 2005. CsrA and three redundant small RNAs regulate quorum sensing in *Vibrio cholerae*. Mol. Microbiol. **58**:1186–202.

80. **Lenz DH**, **Bassler BL**. 2007. The small nucleoid protein Fis is involved in *Vibrio cholerae* quorum sensing. Mol. Microbiol. **63**:859–71.

81. **Shikuma NJ**, **Fong JCN**, **Odell LS**, **Perchuk BS**, **Laub MT**, **Yildiz FH**. 2009. Overexpression of VpsS, a hybrid sensor kinase, enhances biofilm formation in *Vibrio cholerae*. J. Bacteriol. **191**:5147–58.

82. **Liang W**, **Pascual-Montano A**, **Silva AJ**, **Benitez JA**. 2007. The cyclic AMP receptor protein modulates quorum sensing, motility and multiple genes that affect intestinal colonization in *Vibrio cholerae*. Microbiology **153**:2964–75.

83. **Liu Z**, **Hsiao A**, **Joelsson A**, **Zhu J**. 2006. The transcriptional regulator VqmA increases expression of the quorum-sensing activator HapR in *Vibrio cholerae*. J. Bacteriol. **188**:2446–53.

84. **Wang H**, **Ayala JC**, **Silva AJ**, **Benitez JA**. 2012. The histone-like nucleoid structuring protein (H-NS) is a repressor of *Vibrio cholerae* exopolysaccharide biosynthesis (*vps*) genes. Appl. Environ. Microbiol. **78**:2482–8.

85. **Stonehouse EA**, **Hulbert RR**, **Nye MB**, **Skorupski K**, **Taylor RK**. 2011. H-NS binding and repression of the *ctx* promoter in *Vibrio cholerae*. J. Bacteriol. **193**:979–88.

86. **Tischler AD**, **Camilli A**. 2004. Cyclic diguanylate (c-di-GMP) regulates *Vibrio cholerae* biofilm formation. Mol. Microbiol. **53**:857–69.

87. **Römling U**, **Galperin MY**, **Gomelsky M**. 2013. Cyclic di-GMP: the first 25 years of a universal bacterial second messenger. Microbiol. Mol. Biol. Rev.

77:1–52.

88. **Beyhan S**, **Odell LS**, **Yildiz FH**. 2008. Identification and characterization of cyclic diguanylate signaling systems controlling rugosity in *Vibrio cholerae*. J. Bacteriol. **190**:7392–405.

89. **Pratt JT**, **Tamayo R**, **Tischler AD**, **Camilli A**. 2007. PilZ domain proteins bind cyclic diguanylate and regulate diverse processes in *Vibrio cholerae*. J. Biol. Chem. **282**:12860–70.

90. **Sudarsan N**, **Lee ER**, **Weinberg Z**, **Moy RH**, **Kim JN**, **Link KH**, **Breaker RR**. 2008. Riboswitches in eubacteria sense the second messenger cyclic di-GMP. Science **321**:411–3.

91. **Liu X**, **Beyhan S**, **Lim B**, **Linington RG**, **Yildiz FH**. 2010. Identification and characterization of a phosphodiesterase that inversely regulates motility and biofilm formation in *Vibrio cholerae*. J. Bacteriol. **192**:4541–52.

92. **Beyhan S**, **Tischler AD**, **Camilli A**, **Yildiz FH**. 2006. Transcriptome and phenotypic responses of *Vibrio cholerae* to increased cyclic di-GMP level. J. Bacteriol. **188**:3600–13.

93. **Srivastava D**, **Hsieh M-L**, **Khataokar A**, **Neiditch MB**, **Waters CM**. 2013. Cyclic di-GMP inhibits *Vibrio cholerae* motility by repressing induction of transcription and inducing extracellular polysaccharide production. Mol. Microbiol. **90**:1262–76.

94. **Roelofs KG**, **Jones CJ**, **Helman SR**, **Shang X**, **Orr MW**, **Goodson JR**, **Galperin MY**, **Yildiz FH**, **Lee VT**. 2015. Systematic identification of cyclic-di-GMP binding proteins in *Vibrio cholerae* reveals a novel class of cyclic-

di-GMP-binding ATPases associated with Type II Secretion Systems. PLOS Pathog. **11**:e1005232.

95. **Wang Y-C**, **Chin K-H**, **Tu Z-L**, **He J**, **Jones CJ**, **Sanchez DZ**, **Yildiz FH**, **Galperin MY**, **Chou S-H**. 2016. Nucleotide binding by the widespread high-affinity cyclic di-GMP receptor MshEN domain. Nat. Commun. **7**:12481.

96. **Jones CJ**, **Utada A**, **Davis KR**, **Thongsomboon W**, **Zamorano Sanchez D**, **Banakar V**, **Cegelski L**, **Wong GCL**, **Yildiz FH**. 2015. C-di-GMP regulates motile to sessile transition by modulating MshA pili biogenesis and near-surface motility behavior in *Vibrio cholerae*. PLOS Pathog. **11**:e1005068.

97. **Shikuma NJ**, **Fong JCN**, **Yildiz FH**. 2012. Cellular levels and binding of c-di-GMP control subcellular localization and activity of the *Vibrio cholerae* transcriptional regulator VpsT. PLoS Pathog. **8**:e1002719.

98. **Lim B**, **Beyhan S**, **Yildiz FH**. 2007. Regulation of *Vibrio* polysaccharide synthesis and virulence factor production by CdgC, a GGDEF-EAL domain protein, in *Vibrio cholerae*. J. Bacteriol. **189**:717–29.

99. **Beyhan S**, **Yildiz FH**. 2010. Cyclic Di-GMP Signaling in *Vibrio cholerae*, p. 253–269. *In* Wolfe, AJ, Visick, KL (eds.), The Second Messenger Cyclic Di-GMP. ASM Press, Maywood, Illinois.

100. **Hammer BK**, **Bassler BL**. 2007. Regulatory small RNAs circumvent the conventional quorum sensing pathway in pandemic *Vibrio cholerae*. Proc. Natl. Acad. Sci. U. S. A. **104**:11145–9.

101. **Koestler BJ**, **Waters CM**. 2014. Bile acids and bicarbonate inversely regulate intracellular cyclic-di-GMP in *Vibrio cholerae*. Infect. Immun. **82**:3002–3014.

102. **Cockerell SR**, **Rutkovsky AC**, **Zayner JP**, **Cooper RE**, **Porter LR**, **Pendergraft SS**, **Parker ZM**, **McGinnis MW**, **Karatan E**. 2014. *Vibrio cholerae* NspS, a homologue of ABC-type periplasmic solute binding proteins, facilitates transduction of polyamine signals independent of their transport. Microbiology **160**:832–43.

103. **Liang W**, **Silva AJ**, **Benitez JA**. 2007. The cyclic AMP receptor protein modulates colonial morphology in *Vibrio cholerae*. Appl. Environ. Microbiol. **73**:7482–7.

104. **Fong JCN**, **Yildiz FH**. 2008. Interplay between cyclic AMP-cyclic AMP receptor protein and cyclic-di-GMP signaling in *Vibrio cholerae* biofilm formation. J. Bacteriol. **190**:6646–59.

105. **Das B**, **Pal RR**, **Bag S**, **Bhadra RK**. 2009. Stringent response in *Vibrio cholerae*: genetic analysis of *spoT* gene function and identification of a novel (p)ppGpp synthetase gene. Mol. Microbiol. **72**:380–98.

106. **Raskin DM**, **Judson N**, **Mekalanos JJ**. 2007. Regulation of the stringent response is the essential function of the conserved bacterial G protein CgtA in *Vibrio cholerae*. Proc. Natl. Acad. Sci. U. S. A. **104**:4636–41.

107. **Song T**, **Sabharwal D**, **Gurung JM**, **Cheng AT**, **Sjöström AE**, **Yildiz FH**, **Uhlin BE**, **Wai SN**. 2014. *Vibrio cholerae* utilizes direct sRNA regulation in expression of a biofilm matrix protein. PLoS One **9**:e101280.

108. **Song T**, **Mika F**, **Lindmark B**, **Liu Z**, **Schild S**, **Bishop A**, **Zhu J**, **Camilli A**, **Johansson J**, **Vogel J**, **Wai SN**. 2008. A new *Vibrio cholerae* sRNA modulates colonization and affects release of outer membrane vesicles. Mol. Microbiol. **70**:100–11.

109. **Mey AR**, **Craig SA**, **Payne SM**. 2005. Characterization of *Vibrio cholerae* RyhB: the RyhB regulon and role of *ryhB* in biofilm formation. Infect. Immun. **73**:5706–19.

110. **Papenfort K**, **Förstner KU**, **Cong J-P**, **Sharma CM**, **Bassler BL**. 2015. Differential RNA-seq of *Vibrio cholerae* identifies the VqmR small RNA as a regulator of biofilm formation. Proc. Natl. Acad. Sci. U. S. A. **112**:E766-75.

111. **Kapfhammer D**, **Karatan E**, **Pflughoeft KJ**, **Watnick PI**. 2005. Role for glycine betaine transport in *Vibrio cholerae* osmoadaptation and biofilm formation within microbial communities. Appl. Environ. Microbiol. **71**:3840–7.

112. **Shikuma NJ**, **Yildiz FH**. 2009. Identification and characterization of OscR, a transcriptional regulator involved in osmolarity adaptation in *Vibrio cholerae*. J. Bacteriol. **191**:4082–96.

113. **Shikuma NJ**, **Davis KR**, **Fong JNC**, **Yildiz FH**. 2013. The transcriptional regulator, CosR, controls compatible solute biosynthesis and transport, motility and biofilm formation in *Vibrio cholerae*. Environ. Microbiol. **15**:1387–99.

114. **Mueller RS**, **Beyhan S**, **Saini SG**, **Yildiz FH**, **Bartlett DH**. 2009. Indole acts as an extracellular cue regulating gene expression in *Vibrio cholerae*.

J. Bacteriol. **191**:3504–16.

115. **Hung DT**, **Zhu J**, **Sturtevant D**, **Mekalanos JJ**. 2006. Bile acids stimulate biofilm formation in *Vibrio cholerae*. Mol. Microbiol. **59**:193–201.

116. **Houot L**, **Chang S**, **Pickering BS**, **Absalon C**, **Watnick PI**. 2010. The phosphoenolpyruvate phosphotransferase system regulates *Vibrio cholerae* biofilm formation through multiple independent pathways. J. Bacteriol. **192**:3055–67.

117. **Ymele-Leki P**, **Houot L**, **Watnick PI**. 2013. Mannitol and the mannitol-specific enzyme IIB subunit activate *Vibrio cholerae* biofilm formation. Appl. Environ. Microbiol. **79**:4675–83.

118. **Igarashi K**, **Kashiwagi K**. 2000. Polyamines: mysterious modulators of cellular functions. Biochem. Biophys. Res. Commun. **271**:559–64.

119. **McGinnis MW**, **Parker ZM**, **Walter NE**, **Rutkovsky AC**, **Cartaya-Marin C**, **Karatan E**. 2009. Spermidine regulates *Vibrio cholerae* biofilm formation via transport and signaling pathways. FEMS Microbiol. Lett. **299**:166–74.

120. **Karatan E**, **Duncan TR**, **Watnick PI**. 2005. NspS, a predicted polyamine sensor, mediates activation of *Vibrio cholerae* biofilm formation by norspermidine. J. Bacteriol. **187**:7434–43.

121. **Kierek K**, **Watnick PI**. 2003. Environmental determinants of *Vibrio cholerae* biofilm development. Appl. Environ. Microbiol. **69**:5079–5088.

122. **Bilecen K**, **Yildiz FH**. 2010. Identification of a calcium-controlled negative regulatory system affecting *Vibrio cholerae* biofilm formation. Environ. Microbiol. **11**:2015–2029.

123. **Huq A**, **Small EB**, **West PA**, **Huq MI**, **Rahman R**, **Colwell RR**. 1983. Ecological relationships between *Vibrio cholerae* and planktonic crustacean copepods. Appl. Environ. Microbiol. **45**:275–83.

124. **Kirn TJ**, **Jude BA**, **Taylor RK**. 2005. A colonization factor links *Vibrio cholerae* environmental survival and human infection. Nature **438**:863–6.

125. **Blokesch M**. 2012. Chitin colonization, chitin degradation and chitin-induced natural competence of *Vibrio cholerae* are subject to catabolite repression. Environ. Microbiol. **14**:1898–912.

126. **Broza M**, **Gancz H**, **Halpern M**, **Kashi Y**. 2005. Adult non-biting midges: possible windborne carriers of *Vibrio cholerae* non-O1 non-O139. Environ. Microbiol. **7**:576–85.

127. **Nahar S**, **Sultana M**, **Naser MN**, **Nair GB**, **Watanabe H**, **Ohnishi M**, **Yamamoto S**, **Endtz H**, **Cravioto A**, **Sack RB**, **Hasan NA**, **Sadique A**, **Huq A**, **Colwell RR**, **Alam M**. 2011. Role of shrimp chitin in the ecology of toxigenic *Vibrio cholerae* and cholera transmission. Front. Microbiol. **2**:260.

128. **Yamamoto S**, **Mitobe J**, **Ishikawa T**, **Wai SN**, **Ohnishi M**, **Watanabe H**, **Izumiya H**. 2014. Regulation of natural competence by the orphan two-component system sensor kinase ChiS involves a non-canonical transmembrane regulator in *Vibrio cholerae*. Mol. Microbiol. **91**:326–47.

129. **Dalia AB**, **Lazinski DW**, **Camilli A**. 2014. Identification of a membrane-bound transcriptional regulator that links chitin and natural competence in *Vibrio cholerae*. MBio **5**:e01028-13-e01028-13.

130. **Yamamoto S**, **Izumiya H**, **Mitobe J**, **Morita M**, **Arakawa E**, **Ohnishi M**,

Watanabe H. 2011. Identification of a chitin-induced small RNA that regulates translation of the *tfoX* gene, encoding a positive regulator of natural competence in *Vibrio cholerae*. J. Bacteriol. **193**:1953–65.

131. **Lo Scrudato M**, **Blokesch M**. 2013. A transcriptional regulator linking quorum sensing and chitin induction to render *Vibrio cholerae* naturally transformable. Nucleic Acids Res. **41**:3644–58.
132. **Wong E**, **Vaaje-Kolstad G**, **Ghosh A**, **Hurtado-Guerrero R**, **Konarev P V**, **Ibrahim AFM**, **Svergun DI**, **Eijsink VGH**, **Chatterjee NS**, **van Aalten DMF**. 2012. The *Vibrio cholerae* colonization factor GbpA possesses a modular structure that governs binding to different host surfaces. PLoS Pathog. **8**:e1002373.
133. **Bhowmick R**, **Ghosal A**, **Das B**, **Koley H**, **Saha DR**, **Ganguly S**, **Nandy RK**, **Bhadra RK**, **Chatterjee NS**. 2008. Intestinal adherence of *Vibrio cholerae* involves a coordinated interaction between colonization factor GbpA and mucin. Infect. Immun. **76**:4968–77.
134. **Mondal M**, **Nag D**, **Koley H**, **Saha DR**, **Chatterjee NS**. 2014. The *Vibrio cholerae* extracellular chitinase ChiA2 is important for survival and pathogenesis in the host intestine. PLoS One **9**:e103119.
135. **Bourassa L**, **Camilli A**. 2009. Glycogen contributes to the environmental persistence and transmission of *Vibrio cholerae*. Mol. Microbiol. **72**:124–138.
136. **Kamp HD**, **Patimalla-Dipali B**, **Lazinski DW**, **Wallace-Gadsden F**, **Camilli A**. 2013. Gene fitness landscapes of *Vibrio cholerae* at important

stages of its life cycle. PLoS Pathog. **9**:e1003800.

137. **Baker CS**, **Morozov I**, **Suzuki K**, **Romeo T**, **Babitzke P**. 2002. CsrA regulates glycogen biosynthesis by preventing translation of *glgC* in *Escherichia coli.* Mol. Microbiol. **44**:1599–610.

138. **Pratt JT**, **Ismail AM**, **Camilli A**. 2010. PhoB regulates both environmental and virulence gene expression in *Vibrio cholerae*. Mol. Microbiol. **77**:1595–605.

139. **Pratt JT**, **McDonough E**, **Camilli A**. 2009. PhoB regulates motility, biofilms, and cyclic di-GMP in *Vibrio cholerae*. J. Bacteriol. **191**:6632–42.

140. **von Krüger WMA**, **Lery LMS**, **Soares MR**, **de Neves-Manta FS**, **Batista e Silva CM**, **Neves-Ferreira AGDC**, **Perales J**, **Bisch PM**. 2006. The phosphate-starvation response in *Vibrio cholerae* O1 and *phoB* mutant under proteomic analysis: disclosing functions involved in adaptation, survival and virulence. Proteomics **6**:1495–511.

141. **von Kruger WMA**, **Humphreys S**, **Ketley JM**. 1999. A role for the PhoBR regulatory system homologue in the *Vibrio cholerae* phosphate-limitation response and intestinal colonization. Microbiology **145**:2463–2475.

142. **Jahid IK**, **Silva AJ**, **Benitez JA**. 2006. Polyphosphate stores enhance the ability of *Vibrio cholerae* to overcome environmental stresses in a low-phosphate environment. Appl. Environ. Microbiol. **72**:7043–9.

143. **Pflughoeft KJ**, **Kierek K**, **Paula I**, **Watnick PI**. 2003. Role of ectoine in *Vibrio cholerae* osmoadaptation. Appl. Environ. Microbiol. **69**.

144. **Lobitz B**, **Beck L**, **Huq A**, **Wood B**, **Fuchs G**, **Faruque ASG**, **Colwell R**.

2000. Climate and infectious disease: Use of remote sensing for detection of *Vibrio cholerae* by indirect measurement. Proc. Natl. Acad. Sci. **97**:1438–1443.

145. **Lama JR**, **Seas CR**, **León-Barúa R**, **Gotuzzo E**, **Sack RB**. 2004. Environmental temperature, cholera, and acute diarrhoea in adults in Lima, Peru. J. Health. Popul. Nutr. **22**:399–403.

146. **Louis VR**, **Russek-Cohen E**, **Choopun N**, **Rivera ING**, **Gangle B**, **Jiang SC**, **Rubin A**, **Patz JA**, **Huq A**, **Colwell RR**. 2003. Predictability of *Vibrio cholerae* in Chesapeake Bay. Appl. Environ. Microbiol. **69**:2773–2785.

147. **Townsley L**, **Yildiz FH**. 2015. Temperature affects c-di-GMP signaling and biofilm formation in *Vibrio cholerae*. Environ. Microbiol. **In review**.

148. **Stauder M**, **Vezzulli L**, **Pezzati E**, **Repetto B**, **Pruzzo C**. 2010. Temperature affects *Vibrio cholerae* O1 El Tor persistence in the aquatic environment via an enhanced expression of GbpA and MSHA adhesins. Environ. Microbiol. Rep. **2**:140–4.

149. **Weber GG**, **Kortmann J**, **Narberhaus F**, **Klose KE**. 2014. RNA thermometer controls temperature-dependent virulence factor expression in *Vibrio cholerae*. Proc. Natl. Acad. Sci. U. S. A. **111**:14241–6.

150. **Datta PP**, **Bhadra RK**. 2003. Cold shock response and major cold shock proteins of *Vibrio cholerae*. Appl. Environ. Microbiol. **69**:6361–6369.

151. **Asakura H**, **Ishiwa A**, **Arakawa E**, **Makino S**, **Okada Y**, **Yamamoto S**, **Igimi S**. 2007. Gene expression profile of *Vibrio cholerae* in the cold stress-induced viable but non-culturable state. Environ. Microbiol. **9**:869–

79.

152. **Townsley L**, **Sison Mangus MP**, **Mehic S**, **Yildiz FH**. 2016. Response of *Vibrio cholerae* to low-temperature shifts: CspV Regulation of Type VI secretion, biofilm formation, and association with zooplankton. Appl. Environ. Microbiol. **82**:4441–52.

153. **Pukatzki S**, **Ma AT**, **Sturtevant D**, **Krastins B**, **Sarracino D**, **Nelson WC**, **Heidelberg JF**, **Mekalanos JJ**. 2006. Identification of a conserved bacterial protein secretion system in *Vibrio cholerae* using the *Dictyostelium* host model system. Proc. Natl. Acad. Sci. U. S. A. **103**:1528–33.

154. **Miyata ST**, **Kitaoka M**, **Brooks TM**, **McAuley SB**, **Pukatzki S**. 2011. *Vibrio cholerae* requires the type VI secretion system virulence factor VasX to kill *Dictyostelium discoideum*. Infect. Immun. **79**:2941–9.

155. **Dong TG**, **Ho BT**, **Yoder-Himes DR**, **Mekalanos JJ**. 2013. Identification of T6SS-dependent effector and immunity proteins by Tn-seq in *Vibrio cholerae*. Proc. Natl. Acad. Sci. U. S. A. **110**:2623–8.

156. **Sun S**, **Kjelleberg S**, **McDougald D**. 2013. Relative contributions of *Vibrio* polysaccharide and quorum sensing to the resistance of *Vibrio cholerae* to predation by heterotrophic protists. PLoS One **8**:e56338.

157. **Sun S**, **Tay QXM**, **Kjelleberg S**, **Rice SA**, **McDougald D**. 2015. Quorum sensing-regulated chitin metabolism provides grazing resistance to *Vibrio cholerae* biofilms. ISME J.

158. **Vaitkevicius K**, **Lindmark B**, **Ou G**, **Song T**, **Toma C**, **Iwanaga M**, **Zhu J**,

Tuck S, **Wai SN**, **Andersson A**, **Hammarstro M**. 2006. A *Vibrio cholerae* protease needed for killing of *Caenorhabditis elegans* has a role in protection from natural predator grazing.

159. **Erken M**, **Weitere M**, **Kjelleberg S**, **McDougald D**. 2011. *In situ* grazing resistance of *Vibrio cholerae* in the marine environment. FEMS Microbiol. Ecol. **76**:504–12.
160. **Lutz C**, **Erken M**, **Noorian P**, **Sun S**, **McDougald D**. 2013. Environmental reservoirs and mechanisms of persistence of *Vibrio cholerae*. Front. Microbiol. **4**:375.
161. **Noorian P**, **Hu J**, **Chen Z**, **Kjelleberg S**, **Wilkins MR**, **Sun S**, **McDougald D**. 2017. Pyomelanin produced by *Vibrio cholerae* confers resistance to predation by *Acanthamoeba castellanii*. FEMS Microbiol. Ecol. **93**.
162. **Zheng J**, **Ho B**, **Mekalanos JJ**. 2011. Genetic analysis of anti-amoebae and anti-bacterial activities of the type VI secretion system in *Vibrio cholerae*. PLoS One **6**:e23876.
163. **Pukatzki S**, **Ma AT**, **Revel AT**, **Sturtevant D**, **Mekalanos JJ**. 2007. Type VI secretion system translocates a phage tail spike-like protein into target cells where it cross-links actin. Proc. Natl. Acad. Sci. U. S. A. **104**:15508–13.
164. **MacIntyre DL**, **Miyata ST**, **Kitaoka M**, **Pukatzki S**. 2010. The *Vibrio cholerae* type VI secretion system displays antimicrobial properties. Proc. Natl. Acad. Sci. U. S. A. **107**:19520–4.
165. **Basler M**, **Pilhofer M**, **Henderson GP**, **Jensen GJ**, **Mekalanos JJ**. 2012.

Type VI secretion requires a dynamic contractile phage tail-like structure. Nature **483**:182–6.

166. **Brooks TM**, **Unterweger D**, **Bachmann V**, **Kostiuk B**, **Pukatzki S**. 2013. Lytic activity of the *Vibrio cholerae* type VI secretion toxin VgrG-3 is inhibited by the antitoxin TsaB. J. Biol. Chem. **288**:7618–25.

167. **Miyata ST**, **Unterweger D**, **Rudko SP**, **Pukatzki S**. 2013. Dual expression profile of type VI secretion system immunity genes protects pandemic *Vibrio cholerae*. PLoS Pathog. **9**:e1003752.

168. **Unterweger D**, **Miyata ST**, **Bachmann V**, **Brooks TM**, **Mullins T**, **Kostiuk B**, **Provenzano D**, **Pukatzki S**. 2014. The *Vibrio cholerae* type VI secretion system employs diverse effector modules for intraspecific competition. Nat. Commun. **5**:3549.

169. **Unterweger D**, **Kitaoka M**, **Miyata ST**, **Bachmann V**, **Brooks TM**, **Moloney J**, **Sosa O**, **Silva D**, **Duran-Gonzalez J**, **Provenzano D**, **Pukatzki S**. 2012. Constitutive type VI secretion system expression gives *Vibrio cholerae* intra- and interspecific competitive advantages. PLoS One **7**:e48320.

170. **Kitaoka M**, **Miyata ST**, **Brooks TM**, **Unterweger D**, **Pukatzki S**. 2011. VasH is a transcriptional regulator of the type VI secretion system functional in endemic and pandemic *Vibrio cholerae*. J. Bacteriol. **193**:6471–82.

171. **Dong TG**, **Mekalanos JJ**. 2012. Characterization of the RpoN regulon reveals differential regulation of T6SS and new flagellar operons in *Vibrio*

cholerae O37 strain V52. Nucleic Acids Res. **40**:7766–75.

172. **Zheng J**, **Shin OS**, **Cameron DE**, **Mekalanos JJ**. 2010. Quorum sensing and a global regulator TsrA control expression of type VI secretion and virulence in *Vibrio cholerae*. Proc. Natl. Acad. Sci. U. S. A. **107**:21128–33.

173. **Ishikawa T**, **Rompikuntal PK**, **Lindmark B**, **Milton DL**, **Wai SN**. 2009. Quorum sensing regulation of the two *hcp* alleles in *Vibrio cholerae* O1 strains. PLoS One **4**:e6734.

174. **Shao Y**, **Bassler BL**. 2014. Quorum regulatory small RNAs repress type VI secretion in *Vibrio cholerae*. Mol. Microbiol.

175. **Borgeaud S**, **Metzger LC**, **Scrignari T**, **Blokesch M**. 2015. The type VI secretion system of *Vibrio cholerae* fosters horizontal gene transfer. Science (80-.). **347**:63–67.

176. **Syed KA**, **Beyhan S**, **Correa N**, **Queen J**, **Liu J**, **Peng F**, **Satchell KJF**, **Yildiz F**, **Klose KE**. 2009. The *Vibrio cholerae* flagellar regulatory hierarchy controls expression of virulence factors. J. Bacteriol. **191**:6555–70.

177. **Metzger LC**, **Stutzmann S**, **Scrignari T**, **Henst C Van Der**, **Blokesch M**. 2016. Independent regulation of Type VI Secretion in *Vibrio cholerae* by TfoX and TfoY report independent regulation of Type VI Secretion in *Vibrio cholerae* by TfoX and TfoY 1–8.

178. **Rogers A**, **Townsley L**, **Gallego-hernandez AL**, **Beyhan S**, **Kwuan L**, **Yildiz FH**. 2016. The LonA protease regulates biofilm formation, motility, virulence, and the Type VI Secretion System in *Vibrio cholerae* **198**:973–

985.

179. **Bernard CS**, **Brunet YR**, **Gavioli M**, **Lloubès R**, **Cascales E**. 2011. Regulation of type VI secretion gene clusters by sigma54 and cognate enhancer binding proteins. J. Bacteriol. **193**:2158–67.

180. **Liu Z**, **Miyashiro T**, **Tsou A**, **Hsiao A**, **Goulian M**, **Zhu J**. 2008. Mucosal penetration primes *Vibrio cholerae* for host colonization by repressing quorum sensing. Proc. Natl. Acad. Sci. U. S. A. **105**:9769–74.

181. **Ishikawa T**, **Sabharwal D**, **Bröms J**, **Milton DL**, **Sjöstedt A**, **Uhlin BE**, **Wai SN**. 2012. Pathoadaptive conditional regulation of the type VI secretion system in *Vibrio cholerae* O1 strains. Infect. Immun. **80**:575–84.

182. **Fu Y**, **Waldor MK**, **Mekalanos JJ**. 2013. Tn-Seq analysis of *Vibrio cholerae* intestinal colonization reveals a role for T6SS-mediated antibacterial activity in the host. Cell Host Microbe **14**:652–63.

183. **Ma AT**, **Mekalanos JJ**. 2010. *In vivo* actin cross-linking induced by *Vibrio cholerae* type VI secretion system is associated with intestinal inflammation. Proc. Natl. Acad. Sci. U. S. A. **107**:4365–70.

184. **Cheng AT**, **Ottemann KM**, **Yildiz FH**. 2015. *Vibrio cholerae* response regulator VxrB controls colonization and regulates the Type VI secretion system. PLoS Pathog. **11**:e1004933.

185. **Nadell CD**, **Xavier JB**, **Foster KR**. 2009. The sociobiology of biofilms. FEMS Microbiol. Rev. **33**:206–224.

186. **Chang Y-W**, **Fragkopoulos AA**, **Marquez SM**, **Kim HD**, **Angelini TE**, **Fernández-Nieves A**. 2015. Biofilm formation in geometries with different

surface curvature and oxygen availability. New J. Phys. **17**:033017.

187. **Boles BR**, **Thoendel M**, **Singh PK**. 2004. Self-generated diversity produces “insurance effects” in biofilm communities. Proc. Natl. Acad. Sci. **101**:16630–16635.

188. **Parsek MR**, **Greenberg EP**. 2005. Sociomicrobiology: the connections between quorum sensing and biofilms. Trends Microbiol. **13**:27–33.

189. **Zelezniak A**, **Andrejev S**, **Ponomarova O**, **Mende DR**, **Bork P**, **Patil KR**. 2015. Metabolic dependencies drive species co-occurrence in diverse microbial communities. Proc. Natl. Acad. Sci. **112**:6449–6454.

190. **Smith WPJ**, **Davit Y**, **Osborne JM**, **Kim W**, **Foster KR**, **Pitt-Francis JM**. 2017. Cell morphology drives spatial patterning in microbial communities. Proc. Natl. Acad. Sci. U. S. A. **114**:E280–E286.

191. **Griffin AS**, **West SA**, **Buckling A**. 2004. Cooperation and competition in pathogenic bacteria. Nature **430**:1024–1027.

192. **Drescher K**, **Nadell CD**, **Stone HA**, **Wingreen NS**, **Bassler BL**. 2014. Solutions to the public goods dilemma in bacterial biofilms. Curr. Biol. **24**:50–5.

193. **Nadell CD**, **Drescher K**, **Foster KR**. 2016. Spatial structure, cooperation and competition in biofilms. Nat. Rev. Microbiol. **14**:589–600.

194. **Lee KWK**, **Periasamy S**, **Mukherjee M**, **Xie C**, **Kjelleberg S**, **Rice SA**. 2014. Biofilm development and enhanced stress resistance of a model, mixed-species community biofilm. ISME J. **8**:894–907.

195. **Czárán T**, **Hoekstra RF**. 2009. Microbial communication, cooperation and

cheating: quorum sensing drives the evolution of cooperation in bacteria. PLoS One **4**:e6655.

196. **Nadell CD**, **Foster KR**, **Xavier JB**. 2010. Emergence of spatial structure in cell groups and the evolution of cooperation. PLoS Comput. Biol. **6**:e1000716.
197. **Schluter J**, **Nadell CD**, **Bassler BL**, **Foster KR**. 2015. Adhesion as a weapon in microbial competition. ISME J. **9**:139–149.
198. **Xavier JB**, **Foster KR**. 2007. Cooperation and conflict in microbial biofilms. Proc. Natl. Acad. Sci. U. S. A. **104**:876–81.
199. **Pfeiffer T**, **Schuster S**, **Bonhoeffer S**. 2001. Cooperation and competition in the evolution of ATP-producing pathways. Science (80-.). **292**:504–507.
200. **Foster KR**, **Bell T**. 2012. Competition, not cooperation, dominates interactions among culturable microbial species. Curr. Biol. **22**:1845–50.
201. **Toska J**, **Ho BT**, **Mekalanos JJ**. 2018. Exopolysaccharide protects *Vibrio cholerae* from exogenous attacks by the type 6 secretion system. Proc. Natl. Acad. Sci. U. S. A. **115**:7997–8002.
202. **Fu Y**, **Ho BT**, **Mekalanos JJ**. 2018. Tracking *Vibrio cholerae* cell-cell interactions during infection reveals bacterial population dynamics within intestinal microenvironments. Cell Host Microbe **23**:274-281.e2.
203. **Zhao W**, **Caro F**, **Robins W**, **Mekalanos JJ**. 2018. Antagonism toward the intestinal microbiota and its effect on *Vibrio cholerae* virulence. Science **359**:210–213.
204. **Logan SL**, **Thomas J**, **Yan J**, **Baker RP**, **Shields DS**, **Xavier JB**,

Hammer BK, **Parthasarathy R**. 2018. The *Vibrio cholerae* type VI secretion system can modulate host intestinal mechanics to displace gut bacterial symbionts. Proc. Natl. Acad. Sci. U. S. A. **115**:E3779–E3787.

CHAPTER 2: The two-component signal transduction system VxrAB positively regulates *Vibrio cholerae* biofilm formation

Jennifer K. Teschler, Andrew T. Cheng, and Fitnat H. Yildiz

ABSTRACT

Two-component signal transduction systems (TCSs), typically composed of a sensor histidine kinase (HK) and a response regulator (RR), are the primary mechanism by which pathogenic bacteria sense and respond to extracellular signals. The pathogenic bacterium *Vibrio cholerae* is no exception and encodes for 52 RR genes. Using in frame deletion mutants of each RR gene, we performed a systematic analysis of their role in *V. cholerae* biofilm formation. We determined that 7 RRs impacted expression of an essential biofilm gene and found that the recently characterized RR, VxrB, regulates expression of key structural and regulatory biofilm-genes in *V. cholerae*. *vxrB* is encoded as part of a 5-gene operon, which encodes the cognate HK *vxrA*, and three genes of unknown function. Δ*vxrA* and Δ*vxrB* are both deficient in biofilm formation, while Δ*vxrC* enhances biofilm formation. Overexpression of VxrB led to a decrease in motility. We also observed a small but reproducible effect of the absence of VxrB on the levels of c-di-GMP. Our work reveals a new function for the Vxr TCS as a regulator of biofilm formation and suggests that this regulation may act through key biofilm regulators and the modulation of cellular c-di-GMP levels.

Introduction

Vibrio cholerae is the causative agent of the gastrointestinal disease cholera, responsible for approximately 3 to 5 million cases of severe diarrhea and 120,000 deaths annually (1, 2). A resident of aquatic reservoirs, *V. cholerae* can be found as free-swimming planktonic cells or in matrix-protected cellular aggregates, known as biofilms (2–4). Evidence suggests that biofilms form during the aquatic and intestinal phases of the *V. cholerae* life cycle and play an important role in environmental survival, as well as in the intestinal and transmission stages of infection (5–9). *V. cholerae* biofilm formation requires the production and secretion of an extracellular matrix composed of matrix proteins, nucleic acids, and *Vibrio* polysaccharide (VPS), a glycoconjugate that is essential for the formation of three-dimensional biofilm structures (10–16). A complex regulatory network governs this process, tightly controlling *V. cholerae* biofilm production. While important biofilm regulators and their genetic interactions have been examined, there is still relatively little known about how environmental signals are integrated into the biofilm regulatory network (8, 17–19).

Like most pathogenic bacteria, *V. cholerae* utilizes two-component signal transduction systems (TCSs) as a means for sensing and responding to different environment stimuli, such as nutrient availability, pH, oxygen, osmolarity, quorum sensing signals, and numerous host factors (19–23). *V. cholerae* is predicted to encode 43 HK and 49 RR, according to the reference genome of O1 EL Tor N16961 strain (http://www.ncbi.nlm.nih.gov/Complete_Genomes/RRcensus.html

and http://www.p2cs.org). An additional 3 RRs (VpsT, VpsR, and VC0396) were identified based on analysis of the genome for REC domains, thus it is predicted that *V. cholerae* O1 EL Tor N16961 genome encodes for 53 putative RRs. Only 9 RRs have been previously shown to impact biofilm formation. VpsR, VpsT, and LuxO are activators of biofilm formation, while PhoB, VarA, VieA, and CarR are repressors of biofilm formation (22, 24–32). VC1348 and VCA0210 are RRs that contain HD-GYP domains with predicted c-di-GMP phosphodiesterase activity. Overexpression of these RRs led to a significant decrease in biofilm formation (33). To date, there is no systematic analysis reporting on the contribution of each TCS to biofilm formation in *Vibrio cholerae*.

Here we report our results for the analysis of *vpsL* expression, as a representative biofilm gene, in strains with in frame deletions of each RR. We found that VxrB, a RR recently characterized for its role in intestinal colonization, regulation of the Type 6 secretion system (T6SS), and recovery from beta lactam exposure (34), was also a positive regulator of biofilm formation.

Materials and Methods

Strains and growth conditions. Strains used in this study are listed in Table 2.1. *V. cholerae* and *Escherichia coli* strains were grown aerobically in Luria-Bertani (LB) broth (1% tryptone, 0.5% Yeast Extract, 1% NaCl), pH 7.5, at 30°C and 37°C, respectively. LB agar contained granulated agar (Difco) at 1.5% (w/v). Media additives were used when necessary at the following concentrations: rifampicin (100 µg/mL), ampicillin (100 µg/mL), and chloramphenicol (20 µg/mL for *E. coli* and 5 µg/mL or 2.5 µg/mL for *V. cholerae*).

Strain and plasmid construction. Plasmids were constructed using standard cloning methods or the Gibson Assembly recombinant DNA technique (New England Biolabs, Ipswich, MA). Gene deletions were carried out using allelic exchange of the native ORF with the truncated ORF, as previously described (35). Complementation of Δ*vxrB* was carried out using a Tn7-based system, as previously described (34). Briefly, triparental matings with donor *E. coli* S17λpir carrying pGP704-Tn7 with gene of interest, helper *E. coli* S17λpir harboring pUX-BF13, and *V. cholerae* deletion strains were carried out by mixing all three strains, and incubating mating mixtures on LB agar plates for 18 hours at 30°C. Transconjugants were selected on thiosulfate-citrate-bile salts-sucrose (TCBS) (BD Difco, Franklin Lakes, NJ) agar medium containing gentamicin 15µg/mL) at 30°C. Insertion of the complementation construct to the Tn7 site was verified by PCR. *V. cholerae* wild-type and mutant strains were tagged with the green fluorescent protein gene *(gfp*) according to a previously described procedure (14).

The *gfp* tagged *V. cholerae* strains were verified by PCR and used in biofilm analysis. Transcriptional fusions were constructed by cloning the upstream regulatory regions of selected genes into the pBBR-*lux* plasmid, as previously described (36).

Luminescence assays from planktonically grown cells. Overnight cultures *of V. cholerae* cells were diluted 1:500 in appropriate medium containing chloramphenicol (5 µg/ml). Cells were then grown aerobically at 30°C to OD_{600} of 0.3-0.4 and then luminescence of cells was measured using a Perkin Elmer Victor3 Multi-label Counter (PerkinElmer, Waltham, MA). Lux expression is reported as counts min^{-1} ml^{-1}/OD_{600}, shown as relative light units (RLU). Assays were repeated with three biological replicates. Three technical replicates were measured for all assays. Statistical analysis was performed using one-way analysis of variance (ANOVA) and Bonferroni's multiple comparison test.

Luminescence assays from biofilm grown cells. Flow cells were inoculated by diluting overnight grown cultures *of V. cholerae* cells harboring P_{vpsL}-*lux* 1:200 and injecting cells into an Ibidi m-Slide VI0.4 (Ibidi 80601; Ibidi LLC, Verona, WI). After inoculation the bacteria were allowed to adhere at room temperature for 1 h with no flow. Then, flow of 2% (vol/vol) LB (0.2 g/liter tryptone, 0.1 g/liter yeast extract, 1% NaCl) containing chloramphenicol (2.5 µg/ml) was initiated at a rate of 7.5 ml/h and continued for up to 24 h at 25°C. After 24 hours, biofilms were harvested in 1 ml phosphate-buffered saline (PBS) for luminescence reading. Luminescence of

cells were read using a Perkin Elmer Victor3 Multi-label Counter (PerkinElmer, Waltham, MA) and is reported as counts min^{-1} ml^{-1}/ µg protein concentration, as calculated by BCA assay (Thermo Fisher, Waltham, MA) using bovine serum albumin (BSA) as standards. Lux expression is reported as relative light units (RLU). Assays were repeated with two biological replicates and three technical replicates were measured for all assays. Statistical analysis was performed using ANOVA and Bonferroni's multiple comparison test.

Biofilm assays. Flow cells were inoculated by diluting overnight-grown cultures of gfp-tagged *V. cholerae* strains 1:200 (OD_{600} of 0.02) and injecting cells into an Ibidi m-Slide VI0.4 (Ibidi 80601; Ibidi LLC, Verona, WI). After inoculation the bacteria were allowed to adhere at room temperature for 1 h with no flow. Then, flow of 2% (vol/vol) LB (0.2 g/liter tryptone, 0.1 g/liter yeast extract, 1% NaCl) was initiated at a rate of 7.5 ml/h and continued for up to 72 h. Confocal laser scanning microscopy (CLSM) images of the biofilms were captured with an LSM 5 PASCAL system (Zeiss) using an excitation wavelength of 488 nm and an emission wavelength of 543 nm. Three-dimensional images of the biofilms were reconstructed using Imaris software (Bitplane) and quantified using COMSTAT 2(37). Statistical analysis of COMSTAT data was performed using ANOVA and Bonferroni's multiple comparison test.

Motility assays. Soft agar motility plates were made using LB medium with 0.3% (wt/vol) agar supplemented with 100 µg/ml ampicillin or 100 µg/ml ampicillin and

0.1mM IPTG. The plates were inoculated by stabbing the agar from an overnight colony of the strains to be tested. The plates were then incubated at 30°C. Diameters of the migration zones were measured after 16 h. Statistical analysis was performed using ANOVA and Bonferroni's multiple comparison test.

Determination of intracellular c-di-GMP levels. c-di-GMP extraction was performed as previously described (35). Briefly, *V. cholerae* wild-type, Δ*vxrB* Δ*vxrB,* Δ*vxrC*, and Δ*vxrB*Tn*7*::*vxrB*-complemented strains were grown in LB broth to an OD_{600} of 0.4 before 40 ml of culture was harvested at 4000 *g* for 30 min. Cell pellets were allowed to dry briefly then re-suspended in 1 ml extraction solution (40% acetonitrile, 40% methanol, 0.1% formic acid, 19.9% HPLC grade water), and incubated on ice for 15 min. Samples were then centrifuged at 16,000 *g* for 5 min and 800 µl of supernatant was dried under vacuum and then lyophilized. Samples were re-suspended in 50 µl of 184 mM NaCl and analyzed by liquid chromatography-tandem mass spectrometry (LC-MS/MS) on a Thermo-Electron Finnigan LTQ mass spectrometer coupled to a surveyor HPLC. The amount of c-di-GMP in samples was calculated with a standard curve generated from pure c-di-GMP suspended in 184 mM NaCl (BioLog Life Science Institute, Bremen, Germany). The concentrations used for standard curve generation were 50 nM, 100 nM, 500 nM, 2 µM, 3.5 µM, 5 µM, 7.5 µM, and 10 µM. The assay is linear from 50 nM to 10 µM, with an R^2 of 0.999. The c-di-GMP levels were normalized to total protein per ml of culture.

To determine protein concentration, 4 ml from each culture was harvested, the supernatant was removed, and cells were lysed in 1 ml of 2% sodium dodecyl sulfate (SDS). Total protein in the samples was determined with a bicinchoninic acid (BCA) assay (Thermo Fisher, Waltham, MA) using bovine serum albumin (BSA) as the standard. Each c-di-GMP quantification experiment was performed with four biological replicates. Statistical analysis was performed using ANOVA and Bonferroni's multiple comparison test.

Table 2.1. Bacterial strains and plasmids used in this study.

Strain or plasmid	Relevant genotype	Source
E. coli strains		
CC118λ*pir*	Δ(*ara-leu*) *araD* Δ*lacX74 galE galK phoA20 thi-1 rpsE rpoB argE*(*Am*) *recA1* λ*pir*	(38)
S17-1λ*pir*	Tp^r Sm^r *recA thi pro* r_K^- m_K^+ RP4::2-Tc::MuKm Tn*7* λ*pir*	(39)
V. cholerae strains		
FY_VC_0001	*Vibrio cholerae* O1 El Tor A1552, wild type, Rif^r	(40)
FY_VC_0237	FY_VC_0001 mTn7-gfp, Rif^r, Gm^r	(41)
FY_VC_2272	ΔVC0665 (*vpsR*)	(24)
FY_VC_9332	ΔVCA0565 (*vxrA*)	(34)
FY_VC_8758	ΔVCA0566 (*vxrB*)	(34)
FY_VC_0099	ΔVCA0952 (*vpsT*)	(27)
FY_VC_9369	ΔVCA0567 (*vxrC*)	(34)
FY_VC_9417	ΔVCA0568 (*vxrD*)	(34)
FY_VC_9394	ΔVCA0569 (*vxrE*)	(34)
FY_VC_9469	SΔ*vxrB*-Tn7::*vxrB*	(34)
FY_VC_9952	Δ*vxrB*Δ*hcp1*Δ*hcp2*	(34)
FY_VC_9569	ΔVC1415ΔVCA0017 (Δ*hcp1*Δ*hcp2*)	(34)
FY_VC_9390	Δ*vxrA* mTn7-*gfp*, Rif^r, Gm^r	This study
FY_VC_8764	Δ*vxrB* mTn7-*gfp*, Rif^r, Gm^r	This study
FY_VC_9392	Δ*vxrC* mTn7-*gfp*, Rif^r, Gm^r	This study
FY_VC_9437	Δ*vxrD* mTn7-*gfp*, Rif^r, Gm^r	This study
FY_VC_9439	Δ*vxrE* mTn7-*gfp*, Rif^r, Gm^r	This study
FY_VC_9234	Δ*vpsR*Δ*vxrB*, Rif^r	This study
FY_VC_9237	Δ*vpsT*Δ*vxrB*, Rif^r	This study
FY_VC_11356	FY_VC_0001 mTn7-pTAC*vpsR*, Rif^r, Gm^r	This study
FY_VC_11357	Δ*vxrA* mTn7-pTAC*vpsR*, Rif^r, Gm^r	This study
FY_VC_11358	Δ*vxrB* mTn7-pTAC*vpsR*, Rif^r, Gm^r	This study
FY_VC_11355	Δ*vxrB*Δ*vxrC*	This study
Plasmids		
pGP704*sacB*28	pGP704 derivative, *mob*/*oriT sacB*, Ap^r	(27)

pUX-BF13	oriR6K helper plasmid, mob/oriT, provides the Tn7 transposition function in trans, Ap^r	(42)
pMCM11	pGP704::mTn*7*-*gfp*, Gm^r Ap^r	M. Miller and G. Schoolnik
pBBR*lux*	*luxCDABE*-based promoter fusion vector, Cm^r	(43)
pFY-0950	pBBR*lux vpsL* promoter, Cm^r	(44)
pFY-0989	pBBR*lux vpsR* promoter, Cm^r	This study
pFY-0988	pBBR*lux vpsT* promoter, Cm^r	This study
pBAD/myc His-B	Arabinose-inducible expression vector with C-terminal myc epitope and six-His tags	
pFY-2074	pBAD-*vxrB*-noTag, Amp^r	This study
pFY-3071	pBAD-$vxrB^{D78A}$-noTag, Amp^r	This study
pFY-3073	pBAD-$vxrB^{D78E}$-noTag, Amp^r	This study

Results

The VxrB RR is a newly identified positive regulator of *vps* expression in *V. cholerae*. To assess the role of *V. cholerae* TCSs in biofilm formation, we utilized an in-frame deletion mutant library of 41 response regulators (RR). In this study the 11 RR that were predicted to be involved in chemotaxis (CheY, CheV, and CheB proteins) and VC2368 (which we were unable to generate in-frame deletion) were not included (45, 46). VPS is required for biofilm formation and *vps* transcription is a useful readout of potential biofilm forming capacity, therefore, we analyzed expression of *vpsL*, the first gene in the *vps*-II cluster, which, along with the *vps*-I cluster genes, encodes for components that are required for VPS production and biofilm formation. We used a transcriptional fusion of the regulatory region of *vpsL* and the luciferase transcriptional reporter *luxCADBE* (P_{vpsL}-*lux*). Our results revealed 7 RR null mutants with significant changes in *vpsL* expression compared to wild-type (Figure 2.1). Consistent with previous studies, we observed a 122-fold decrease in *vpsL* expression in Δ*vpsR* (VC0665), an 81-fold decrease in *vpsL* expression in Δ*luxO* (VC1021), an 11-fold decrease in *vpsL* expression in Δ*vpsT* (VCA0952), and a 4-fold increase in *vpsL* expression in Δ*carR* (VC1320) (24, 27, 28). A 3-fold increase in *vpsL* expression was observed in Δ*ntrC* (VC2749), indicating that this RR may be a repressor of biofilm formation. Additionally, we observed a 47-fold decrease in *vpsL* expression in a Δ*varA* (VC1213) mutant. Furthermore, we found that Δ*vxrB* (VCA0566) had an 11-fold decrease in *vpsL* expression, indicating that this RR may be a positive regulator of biofilm formation (Figure 2.1). Since VxrB has not been previously reported to be

a regulator of biofilm, we focused this work on characterizing how this TCS influences biofilm formation.

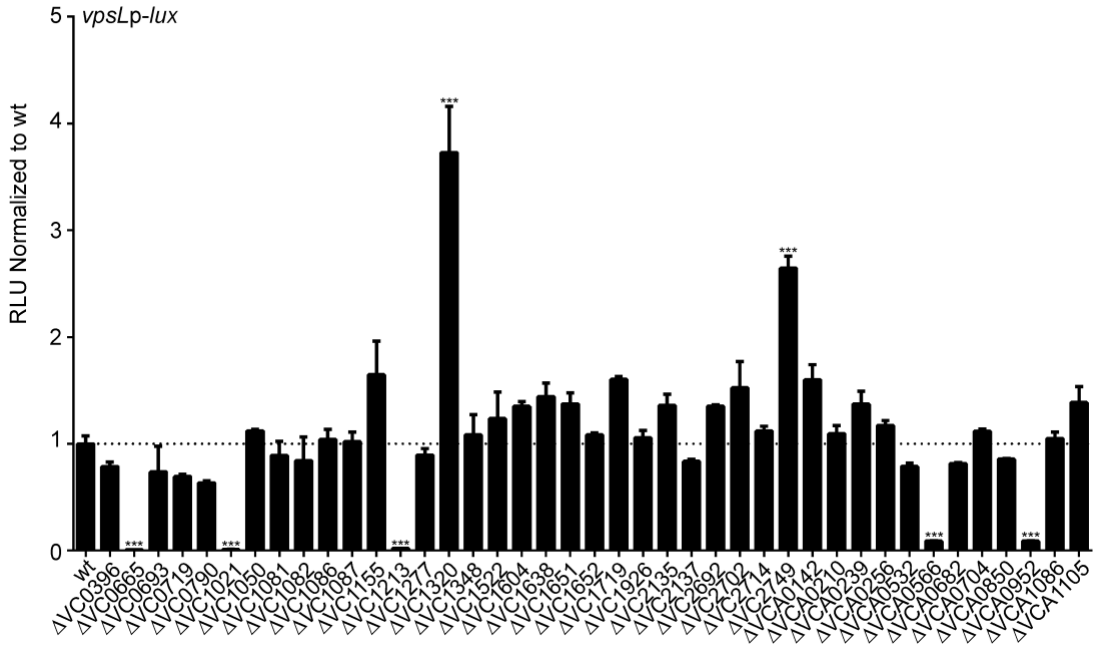

Figure 2.1. Analysis of biofilm gene expression in wild type and response regulator (RR) deletion mutants.

A transcriptional reporter harboring regulatory region of *vpsL* upstream of a promoterless *lux*-reporter (P_{vpsL}-*lux*) was used to analyze the expression of biofilm genes in 41 ΔRR mutants, including ΔVC0396 (*qstR*), ΔVC0665 (*vpsR*), ΔVC0693, ΔVC0719 (*phoB*), ΔVC0790, ΔVC1021 (*luxO*), ΔVC1050, ΔVC1081, ΔVC1082, ΔVC1086, ΔVC1087, ΔVC1155, ΔVC1213 (*varA*), ΔVC1277, ΔVC1320 (*carR*), ΔVC1348, ΔVC1522, ΔVC1604, ΔVC1638, ΔVC1651 (*vieB*), ΔVC1652 (*vieA*), ΔVC1719 (*torR*), ΔVC1926 (*dct-D1*), ΔVC2135 (*flrC*), ΔVC2137 (*flrA*), ΔVC2692 (*cpxR*), ΔVC2702 (*cbrR*), ΔVC2714 (*ompR*), ΔVC2749 (*ntrC*), ΔVCA0142 (*dct-D2*), ΔVCA0210, ΔVCA0239, ΔVCA0256, ΔVCA0532, ΔVCA0566 (*vxrB*), ΔVCA0682 (*uhpA*), ΔVCA0704 (*pgtA*), ΔVCA0850, ΔVCA0952 (*vpsT*), ΔVCA1086, and ΔVCA1105 (names included in parentheticals where relevant).

Cultures of wild-type and ΔRR mutants were grown to exponential phase (OD_{600} of ~0.3) and luminescence was measured. The graph represents the average and standard deviation of relative light units (RLU) obtained from at least three technical replicates from two biological replicates, normalized to wild type levels. RLU is reported in luminescence counts min^{-1} ml^{-1}/OD_{600}. These values were then normalized to wild-type RLU and data is shown as fold changes above or below a wild-type value of 1. Data was analyzed using one-way analysis of variance (ANOVA) and Bonferroni's multiple comparison test. Statistical significant values are represented as ***, $p< 0.001$.

VxrB, along with its cognate sensor histidine kinase (HK), VxrA, has been recently characterized to regulate the type VI secretion system (T6SS), virulence, and cell wall homeostasis in response to antibiotic treatment (in this paper the authors refer to VxrAB as WigKR, but in this work we continue to refer to this TCS as VxrAB), however, this is the first report of its role in regulation of biofilm-gene expression (34, 47). To further characterize the role of the VxrAB TCS in *vpsL* regulation, we analyzed *vpsL* expression in Δ*vxrA*. We observed that, similarly to the Δ*vxrB*, deletion, a Δ*vxrA* mutant downregulates expression of *vpsL* by 3-fold. A Δ*vxrB* strain harboring *vxrB,* under the control of its own promoter (P_{vxrA}), in the Tn7 site was complemented for *vpsL* expression (Figure 2.2A). These results demonstrate that the VxrAB TCS positively regulates *vpsL* gene expression.

VxrB acts upstream of the major biofilm regulators, VpsR and VpsT. The two major positive regulators of *vps* genes are VpsR and VpsT. To determine if VxrB affects the regulators of *vps* gene expression, we measured the expression of each regulator in Δ*vxrB* using the transcriptional fusions P_{vpsR}-*lux* and P_{vpsT}-*lux*. Expression of *vpsL, vpsR*, and *vpsT* were decreased by 4-fold, 2.5-fold, and 3-fold, respectively, in Δ*vxrB* compared to wild-type, suggesting that VxrB could regulate *vpsL* expression by activating the expression of *vpsR* and *vpsT* (Figure 2.2B). A Δ*vxrB* strain harboring *vxrB,* under the control of its own promoter (P_{vxrA}), in the Tn7 site was complemented for *vpsR* and *vpsT* expression (Figure 2.2B).

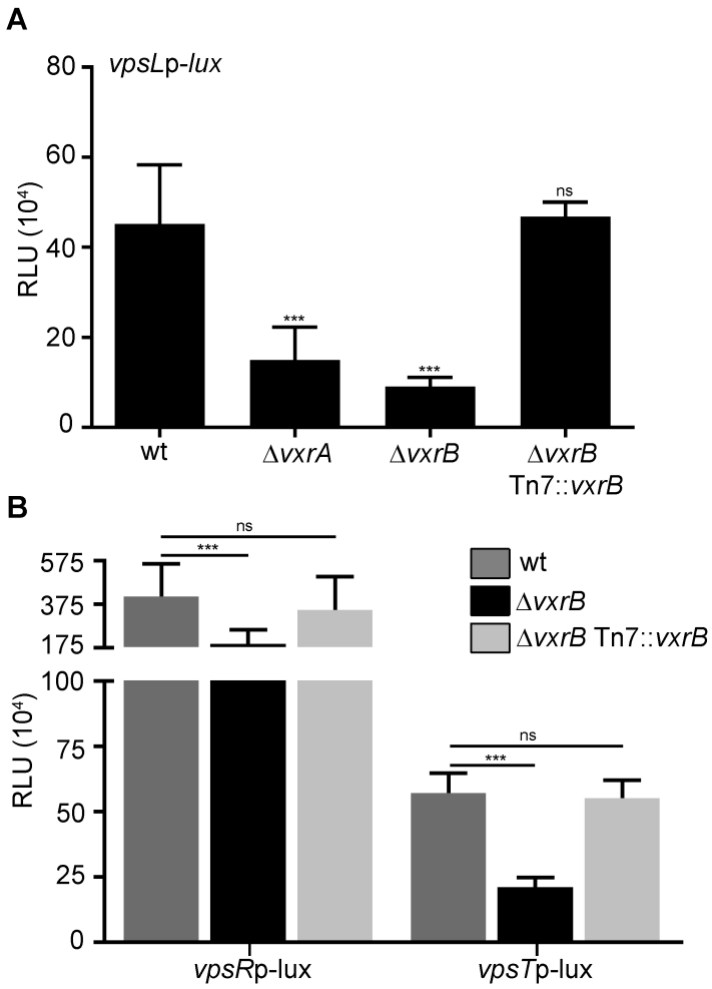

Figure 2.2. Analysis of biofilm gene expression in wild type, Δ*vxrA*, and *ΔvxrB* mutants.

(A) Cultures of wild type, Δ*vxrA*, Δ*vxrB*, and Δ*vxrB*-Tn7*vxrB* containing P_{vpsL}-*lux* were grown to exponential phase (OD_{600} of ~0.3) and luminescence was measured. The graph represents the average and standard deviation of RLU obtained from three technical replicates from three biological replicates. RLU is reported in luminescence counts min^{-1} ml^{-1}/OD_{600}. Data was analyzed using one-way analysis of variance (ANOVA) and Bonferroni's multiple comparison test. Statistical significant values are represented as *** $p< 0.001$, ns, differences were

not significant. (B) Cultures of wild type and Δ*vxrB* strains containing P_{vpsR}-*lux* or P_{vpsT}-*lux* were grown to exponential phase (OD_{600} of ~0.3) and luminescence was measured. The graph represents the average and standard deviation of RLU obtained from three technical replicates from three biological replicates. RLU is reported in luminescence counts min^{-1} ml^{-1}/OD_{600}. Data was analyzed using two-tailed student's t-test. Statistical significant values are represented as *, $p<0.005$, **, $p< 0.001$, ***, $p<0.0001$.

We performed an epsitasis analysis with *vpsR*, *vpsT* and *vxrB*. Our results revealed that deletion of *vxrB* in Δ*vpsR* or Δ*vpsT* had no significant effect on *vpsL* expression when compared to the single mutants (Δ*vpsR* and Δ*vpsT*) (Figure 2.3A). This data suggests that VpsR and VpsT function downstream of VxrB on *vpsL* expression. Given that VpsR is at the bottom of the *vps* regulatory cascade, we reasoned that VxrB-dependent regulation of *vpsL* might be ultimately due to increase expression of *vpsR*. To test this, we expressed *vpsR* (inserted in the Tn7 site) from an Isopropyl β-D-1-thiogalactopyranoside (IPTG) inducible promoter, and analyzed *vpsL* expression in WT, Δ*vxrA*, and Δ*vxrB*. We observed that *vspL* expression was increased by 11-fold when *vpsR* was overexpressed in wild-type. Overexpression of *vpsR* in Δ*vxrA* or Δ*vxrB,* also resulted in increased *vpsL* expression, although ~5 fold less than in wild-type. Taken together, these results suggest that VxrB can regulate *vpsL* expression independently of VpsR.

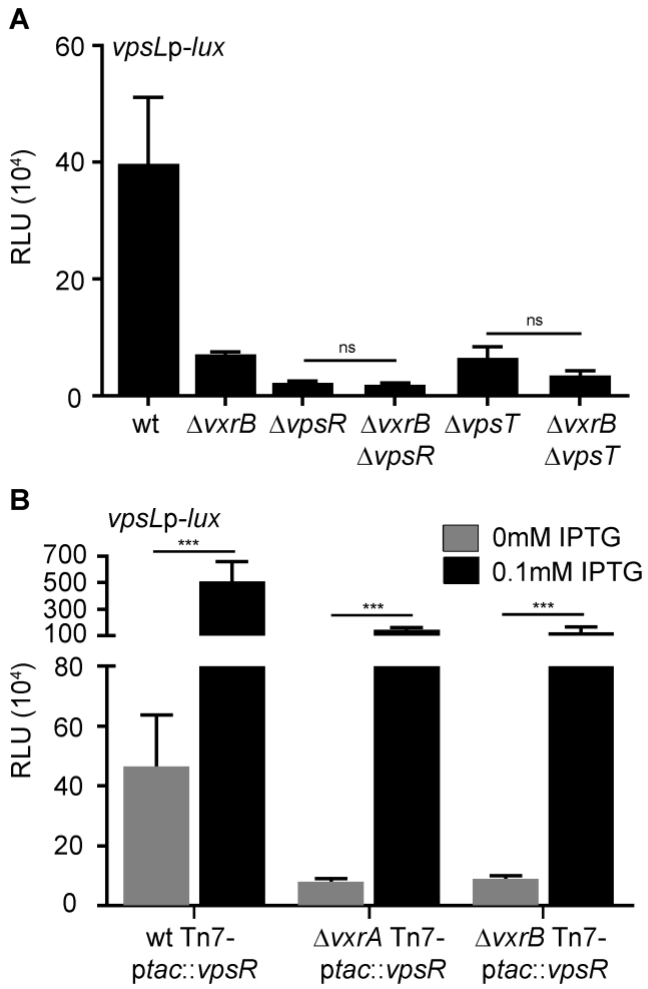

Figure 2.3. Epistasis analysis of regulators of *vps* gene expression.

(A) Cultures of wild type, Δ*vxrB*, Δ*vpsR*, Δ*vxrB*Δ*vpsR*, Δ*vpsT*, and Δ*vxrB*Δ*vpsT* strains containing P_{vpsL}-*lux* were grown to exponential phase (OD_{600} of ~0.3) and luminescence was measured. The graph represents the average and standard deviation of RLU obtained from three technical replicates from three biological replicates. RLU is reported in luminescence counts min^{-1} ml^{-1}/OD_{600}. Data was analyzed using one-way analysis of variance (ANOVA) and Bonferroni's multiple comparison test. Statistical significant values are represented as ns, differences were not significant. (B) Cultures of wild type, Δ*vxrA*, and Δ*vxrB* strains containing

P_{vpsL}-*lux* and an IPTG-inducible copy of VpsR in the Tn-7 site were grown to exponential phase (OD_{600} of ~0.3) and luminescence was measured. The graph represents the average and standard deviation of RLU obtained from three technical replicates from three biological replicates. RLU is reported in luminescence counts min^{-1} ml^{-1}/OD_{600}. Data was analyzed using two-tailed student's t-test. Statistical significant values are represented as ***, $p<0.0001$.

Members of the *vxr* operon affect *vps* expression and biofilm formation. The VxrAB TCS is encoded as part of a 5-gene operon, composed of the HK *vxrA*, the RR *vxrB*, and three genes of unknown function, *vxrC*, *vxrD*, and *vxrE* (Figure 2.4A). We previously demonstrated that the *vxrABCDE* genes are co-transcribed (34). To characterize the role of *vxr* genes in biofilm formation, we analyzed *vpsL* expression in mutants lacking *vxr* operon genes (Figure 2.4B). For this study, we analyzed P_{vpsL}-*lux* in biofilm grown cells. As demonstrated above, Δ*vxrA* and Δ*vxrB* both had decreased *vpsL* expression compared to wild-type. The Δ*vxrC* mutant showed a 1.5 fold increase in *vpsL* expression compared to wild-type, while Δ*vxrD* and Δ*vxrE* showed a 3-fold and 4-fold decrease in *vpsL* expression, respectively.

We analyzed biofilm formation of isogenic strains expressing GFP from the chromosome. These experiments were done in flow cells and the biofilms were imaged using confocal scanning-laser microscopy at 24, 48, and 72 hours post inoculation (Figure 2.4C). We used the quantitative analysis software COMSTAT (37) to calculate biomass, average and maximum thickness, substratum coverage, and roughness of the biofilms at 72 hours, when the differences in biofilm formation were most defined. Δ*vxrA* and Δ*vxrB* formed visibly thinner biofilms compared to wild-type, with a 1.5 to 1.6-fold decrease in biomass, average and maximum thickness compared to wild-type (Table 2.2). In contrast, Δ*vxrC* showed significantly increased biofilm formation compared to wild-type, biomass and average thickness were both increased by 1.4-fold, while maximum thickness increased by 1.3-fold (Table 2.2). Δ*vxrD* and Δ*vxrE* formed biofilms similar to wild-

type (Figure 2.4B-C, Table 2.2). Since Δ*vxrA*, Δ*vxrB*, and Δ*vxrC* formed biofilms that were significantly different from wild-type, we generated Δ*vxrA*, Δ*vxrB*, and Δ*vxrC* strains harboring *vxrA, vxrB*, and *vxrC*, respectively, under the control of their own promoter (P_{vxrA}), in the Tn7 site and found that in these strains *vpsL* expression was similar to wild-type (Figure 2.4D). We next analyzed the genetic interaction between *vxrC* and *vxrB* with respect to regulation of biofilm formation. Δ*vxrB* and Δ*vxrC* showed decreased and increased *vpsL* expression respectively, compared to wild-type. Δ*vxrB*Δ*vxrC* phenocopied Δ*vxrB* *vpsL* expression levels, indicating that the Δ*vxrB* mutation is epistatic to Δ*vxrC* (Figure 2.4E). All together, our results show that VxrA and VxrB both positively regulate *vpsL* expression and biofilm formation, while VxrC may act as a repressor of biofilm formation. The role of VxrD and VxrE in regulating biofilm formation is unclear, as Δ*vxrD* and Δ*vxrE* both showed decreased *vpsL* expression, but formed biofilms similar to wild type.

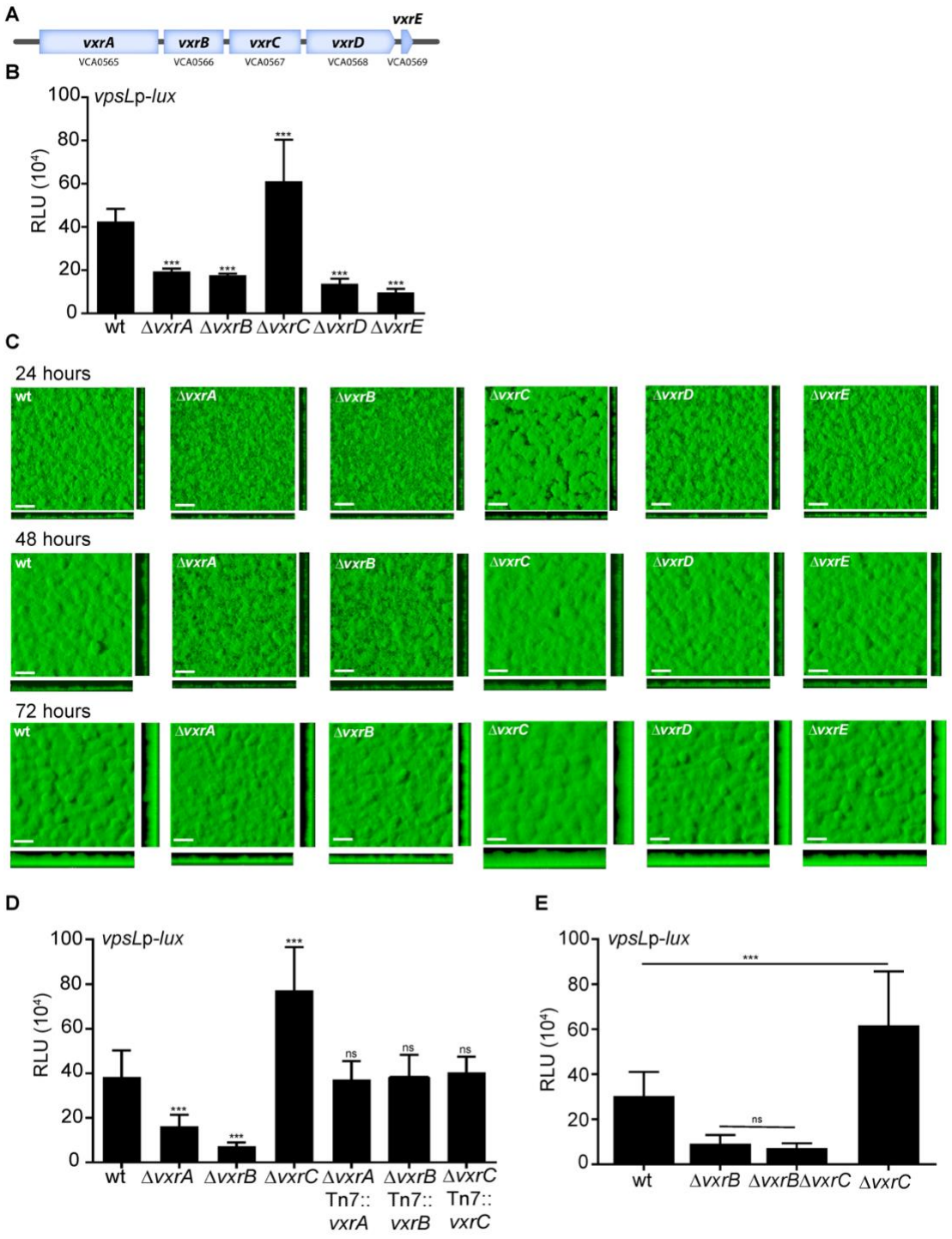

Figure 2.4. Analysis of biofilm gene expression and biofilm formation in *vxr* operon mutants.

(A) The 5 gene *vxr* operon structure, encoding for the TCS *vxrAB* and three genes of unknown function, *vxrCDE*. (B) Biofilms of wild type and Δ*vxrA*, Δ*vxrB*, Δ*vxrC*, Δ*vxrD*, Δ*vxrE* strains containing P_{vpsL}-*lux* were grown in flow cells for 24 hours and luminescence was measured from harvested biofilm cells. The graph represents the average and standard deviation of RLU obtained from three technical replicates from three independent biological samples. RLU is reported in luminescence counts min^{-1} ml^{-1}/□g total protein. Data was analyzed using one-way analysis of variance (ANOVA) and Bonferroni's multiple comparison test. Statistical significant values are represented as *** p< 0.001. (C) Top and orthogonal views of biofilms formed in flow cells by wild type, Δ*vxrA*, Δ*vxrB*, Δ*vxrC*, Δ*vxrD*, Δ*vxrE* after 72 hours post inoculation. The scale bar represents 30 μm. (D) Cultures of wild type, Δ*vxrA,* Δ*vxrB*, Δ*vxrC*, Δ*vxrA*-Tn7*vxrA,* Δ*vxrB*-Tn7*vxrB*, Δ*vxrC*-Tn7*vxrC* strains with a containing P_{vpsL}-*lux* were grown to exponential phase (OD_{600} of ~0.3) and luminescence was measured. The graph represents the average and standard deviation of RLU obtained from three technical replicates from three independent biological replicates. RLU is reported in luminescence counts min^{-1} ml^{-1}/OD_{600}. Data was analyzed using one-way analysis of variance (ANOVA) and Bonferroni's multiple comparison test. Statistical significant values are represented as *** p< 0.001, ns, differences were not significant. (E) Cultures of wild type, Δ*vxrB*, Δ*vxrC*, and Δ*vxrB*Δ*vxrC* strains containing P_{vpsL}-*lux* were grown to exponential phase (OD_{600} of ~0.3) and luminescence was measured. The graph represents the average and standard deviation of RLU obtained from three technical replicates from three independent biological replicates. RLU is reported

in luminescence counts min^{-1} ml^{-1}/OD_{600}. Data was analyzed using one-way analysis of variance (ANOVA) and Bonferroni's multiple comparison test. Statistical significant values are represented as *** $p< 0.001$, ns, differences were not significant.

TABLE 2.2

COMSTAT analysis of biofilms of wild type, Δ*vxrA*, Δ*vxrB, ΔvxrC, ΔvxrD, ΔvxrE*[a]

Time postinoculation and strain	Biomass ($\mu m^3/\mu m^2$)	Mean thickness (SD) (μm)		Substrate coverage[b]	Roughness Coefficient
		Average	Maximum		
24 h					
Wild type	7.77 (0.70)	8.53 (0.99)	14.00 (1.30)	0.90 (0.05)	0.23 (0.04)
Δ*vxrA* mutant	6.00 (0.79)**	6.38 (1.03)^{ns}	12.67 (1.74)^{ns}	0.87 (0.09)^{ns}	0.28 (0.07)^{ns}
Δ*vxrB* mutant	5.94 (0.73)**	6.25 (0.86)*	13.41 (1.30)^{ns}	0.92 (0.05)^{ns}	0.30 (0.08)^{ns}
Δ*vxrC* mutant	8.73 (0.63)^{ns}	9.43 (2.23)^{ns}	14.44 (2.14)^{ns}	0.91 (0.07)^{ns}	0.23 (0.02)^{ns}
Δ*vxrD* mutant	6.66 (0.84)^{ns}	6.40 (0.94)^{ns}	11.79 (1.55)^{ns}	0.87 (0.19)^{ns}	0.33 (0.16)^{ns}
Δ*vxrE* mutant	7.087 (0.85)^{ns}	7.88 (1.68)^{ns}	13.26 (1.48)^{ns}	0.87 (0.08)^{ns}	0.25 (0.06)^{ns}
48 h					
Wild type	10.94 (0.27)	12.12 (0.88)	22.84 (2.20)	0.91 (0.10)	0.14 (0.03)
Δ*vxrA* mutant	7.49 (1.02)***	8.31 (1.38)**	17.39 (2.89)^{ns}	0.87 (0.21)^{ns}	0.18 (0.05)^{ns}
Δ*vxrB* mutant	8.35 (1.16)**	9.59 (1.59)*	20.18 (3.18)^{ns}	0.91 (0.13)^{ns}	0.20 (0.06)^{ns}
Δ*vxrC* mutant	12.79 (2.35)^{ns}	13.86 (2.94)^{ns}	28.73 (7.43)^{ns}	0.98 (0.03)^{ns}	0.13 (0.04)^{ns}
Δ*vxrD* mutant	11.06 (1.03)^{ns}	12.49 (0.83)^{ns}	22.10 (4.15)^{ns}	0.93 (0.05)^{ns}	0.15 (0.03)^{ns}
Δ*vxrE* mutant	9.76 (1.30)^{ns}	10.99 (0.59)^{ns}	21.66 (3.78)^{ns}	0.96 (0.06)^{ns}	0.17 (0.03)^{ns}
72 h					
Wild type	19.42 (1.49)	20.29 (1.25)	31.09 (2.20)	1.00 (0.00)	0.14 (0.03)
Δ*vxrA* mutant	11.58 (2.31)***	12.36 (2.18)***	21.22 (3.31)**	0.91 (0.07)*	0.19 (0.06)^{ns}
Δ*vxrB* mutant	12.79 (2.08)**	14.61 (1.82)**	24.75 (2.44)^{ns}	0.91 (0.07)*	0.21 (0.07)*
Δ*vxrC* mutant	26.34 (3.52)***	27.82 (3.29)***	40.07 (5.86)**	0.98 (0.04)^{ns}	0.11 (0.03)^{ns}
Δ*vxrD* mutant	18.95 (3.30)^{ns}	19.61 (3.74)^{ns}	30.35 (6.51)^{ns}	0.98 (0.04)^{ns}	0.13 (0.03)^{ns}
Δ*vxrE* mutant	19.69 (3.15)^{ns}	20.75 (4.13)^{ns}	31.09 (4.79)^{ns}	0.96 (0.07)^{ns}	0.13 (0.03)^{ns}

[a]Total biomass, average and maximum thickness, substrate coverage, and roughness coefficient were calculated using COMSTAT. The values are the means (standard deviations) of data from at least six z-series image stacks. Significance was determined by ANOVA. Dunnett's multiple comparision test identified samples that differ signficantly from biofilms formed by the wild-type strain. ns, not significant, *, p≤0.05, **, p≤0.001, ***, p≤0.0001.

[b]A value of 0 indicates no coverage (equivalent to 0%), while a value of 1 indicates full coverage (equivalent to 100%).

Overexpression of wild type VxrB negatively impacts motility. Biofilm formation and motility are inversely regulated in *V. cholerae*. We therefore analyzed the role of VxrB in the regulation of motility. We measured swimming motility of Δ*vxrB* by performing a motility assay on soft agar plates. We observed no difference in the average migration zone diameter between Δ*vxrB* and wild-type (Figure 2.5A). To determine the effect that *vxrB* overexpression could have on motility, we cloned this gene in an expression plasmid under the control of an arabinose inducible promoter (pBAD-*vxrB*). In the absence of arabinose, the migration zone of wild-type harboring the empty plasmid, and wild-type containing pBAD-*vxrB* was similar (Figure 5B). In the presence of 0.2% arabinose, wild-type containing pBAD-*vxrB* showed a ~50% decrease in migration compared to wild-type with empty plasmid (Figure 5B-C). These results suggest that overexpression of VxrB can impact motility.

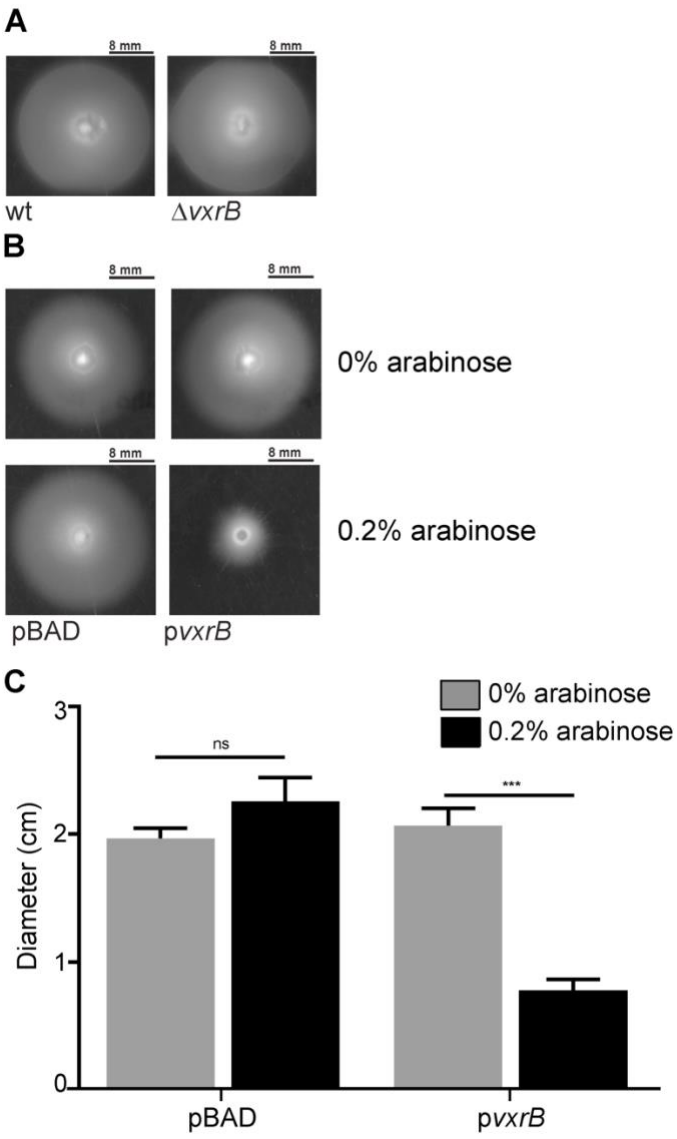

Figure 2.5. Analysis of swimming motility in Δ*vxrB* and VxrB overexpression strains.

(A) Migration zones of wild-type and Δ*vxrB* after 16 h of growth on 0.3% agar plates. (B) Migration zones of wild-type expressing empty vector and p*vxrB*, after 16 h of growth on 0.3% agar plates containing 0% or 0.2% arabinose. (C) Strains were grown on LB agar plates containing 0.3% agar at 30°C for 16 h before migration zones were measured. The error bars indicate the standard deviations

of the results from 6 biological replicates. Data was analyzed using two tailed student's t-test. Statistical significant values are represented as ***, $p<0.0001$.

VxrB increases levels of the second messenger signaling molecule c-di-GMP. Given VxrB's role as a positive regulator of biofilm and a negative regulator of motility, we asked if VxrB could be affecting cellular c-di-GMP levels, as this second messenger signaling molecule inversely regulates biofilm and motility. We measured intracellular c-di-GMP levels in wild type, Δ*vxrA,* Δ*vxrB*, and Δ*vxrC* strains and found that Δ*vxrB*, and Δ*vxrC* strains had a small, but statistically significant, decrease in levels of c-di-GMP compared to wild-type, while the Δ*vxrA* strain had c-di-GMP levels similar to wild-type (Figure 2.6). Thus, cellular c-di-GMP levels are altered in the Δ*vxrB* and Δ*vxrC* strain.

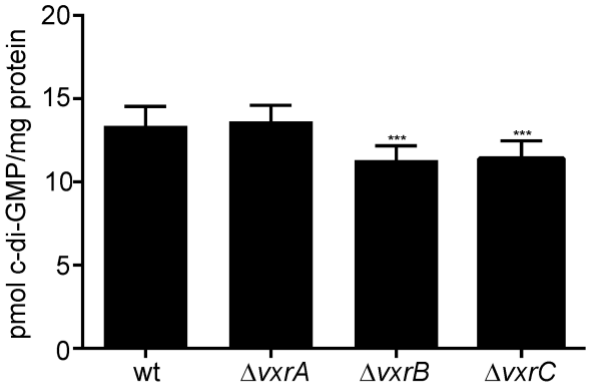

Figure 2.6. Analysis of c-di-GMP levels in wild-type, Δ*vxrA,* Δ*vxrB,* and Δ*vxrC* mutants.

Strains were grown aerobically to an OD_{600} of ~0.3 before c-di-GMP was extracted from whole-cell protein and quantified by high-performance liquid chromatography–tandem mass spectrometry (HPLC-MS/MS). The error bars indicate the standard deviations of the results from 8 biological replicates. Data was analyzed using one-way analysis of variance (ANOVA) and Bonferroni's multiple comparison test. Statistical significant values are represented as ***, $p < 0.001$.

The T6SS does not impact *vpsL* expression and biofilm formation. Our previous work indicated that VxrB positively regulates the T6SS (34). As biofilms provide an environment where cell-to-cell contact is frequent and where high activity of the T6SS might be expected, we next analyzed the role of the T6SS in biofilm formation and determined if VxrB's influence on biofilm formation could act partially through regulation of, or activation by, the T6SS.

A strain lacking *hcp1* and *hcp2*, (Δ*hcp1*Δ*hcp2*), the genes required to produce the major T6SS structural component, Hcp, was used to assess the role of the T6SS in biofilm formation (48). We also evaluated *vpsL* expression in cells grown to exponential phase in wild-type, Δ*vxrB*, Δ*hcp1*Δ*hcp2*, and Δ*vxrB*Δ*hcp1*Δ*hcp2* strains (Figure 2.7A). As expected, Δ*vxrB* demonstrated decreased *vpsL* expression, as did the Δ*vxrB*Δ*hcp1*Δ*hcp2*. The Δ*hcp1*Δ*hcp2* strain showed no significant difference in *vpsL* expression compared to wild-type. Biofilm formation was also examined by growing strains expressing GFP in flow cells and imaging using confocal scanning-laser microscopy at 72 hours post inoculation (Figure 2.7B). The Δ*vxrB* and Δ*vxrB*Δ*hcp1*Δ*hcp2* strains showed decreased biofilm formation, while the Δ*hcp1*Δ*hcp2* strain showed no significant difference in biofilm formation compared to wild-type. These observations were supported by COMSTAT analysis, which was used to analyze biomass, average and maximum thickness, substratum coverage, and roughness of biofilms (Table 2.3). Together, these findings indicate that the T6SS does not contribute to regulation of biofilm formation by VxrB under the conditions we analyzed.

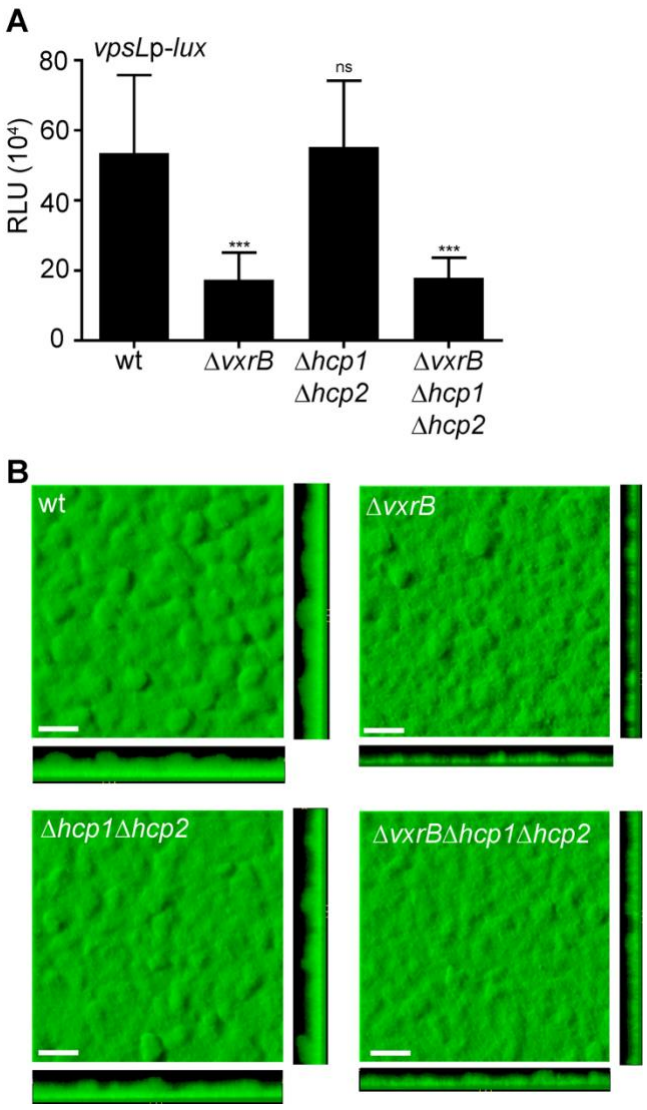

Figure 2.7. Analysis of the impact of the Type Six Secretion genes on biofilm gene expression and biofilm formation.

(A) Cultures of wild type, Δ*vxrB*, Δ*hcp1*Δ*hcp2*, and Δ*vxrB*Δ*hcp1*Δ*hcp2* strains containing P_{vpsL}-*lux* were grown to exponential phase (OD_{600} of ~0.3) and luminescence was measured. The graph represents the average and standard deviation of RLU obtained from three technical replicates from three independent biological samples. RLU is reported in luminescence counts min^{-1} ml^{-1}/OD_{600}. Data

was analyzed using one-way analysis of variance (ANOVA) and Bonferroni's multiple comparison test. Statistical significant values are represented as *** $p < 0.001$, ns, differences were not significant. (B) Top and orthogonal views of biofilms formed in flow cells by wild type, Δ*vxrB*, Δ*hcp1*Δ*hcp2*, and Δ*vxrB*Δ*hcp1*Δ*hcp2* after 72 hours. The scale bar represents 30 μm.

TABLE 2.3

COMSTAT analysis biofilms formed after 72h by wild type, *ΔvxrB*, *Δhcp12*, Δ*vxrBΔhcp12*

Strain	Biomass (μm3/μm2)	Thickness (μm)		Substrate coverage[b]	Roughness Coefficient
		Average	Maximum		
		Mean (SD) and Signficance[a]			
wt	20.41 (2.63)	22 (3.34)	33.74 (6.084)	1.00 (00)	0.11 (0.02)
ΔvxrB	11.68 (2.34)***	13.58 (2.12)***	23.48 (2.76)***	0.95 (0.05)*	0.21 (0.06)***
Δhcp1Δhcp2	21.77 (0.73)^{ns}	22.97 (0.88)^{ns}	36.1 (2.65)^{ns}	1.00 (00)^{ns}	0.11 (0.02)^{ns}
ΔvxrBΔhcp1Δhcp2	18.57 (2.82)^{ns}	17.26 (1.68)**	27.70 (2.832)*	0.99 (0.02)^{ns}	0.14 (0.01)^{ns}

[a]Total biomass, average and maximum thickness, substrate coverage, and roughness coefficient were calculated using COMSTAT. The values are the means (standard deviations) of data from at least six z-series image stacks. Significance was determined by ANOVA. Bonferroni's multiple comparison test identified samples that differ significantly from biofilms formed by the wild-type strain. ns, not significant, *, p≤0.05, **, p≤0.001, ***, p≤0.0001.

[b]A value of 0 indicates no coverage (equivalent to 0%), while a value of 1 indicates full coverage (equivalent to 100%).

Discussion

V. cholerae biofilms enhance survival in the aquatic environment and facilitate transmission to a human host. This study serves to evaluate the role of TCSs, typically utilized to regulate cellular processes in response to extracellular signals, in biofilm formation. We systematically analyzed the role of *V. cholerae* RRs in biofilm formation and identified several that play a role in biofilm regulation (Figure 2.8). Consistent with previous studies, we observed a decrease in *vpsL* expression in a Δ*vpsR* (VC0665) mutant, a Δ*luxO* (VC1021) mutant, and a Δ*vpsT* (VCA0952) mutant and an increase in *vpsL* expression in a Δ*carR* (VC1320) mutant (24, 27, 28, 30, 31). We did not observe a phenotype for Δ*phoB* (VC0719), which is only expected to act as repressor of biofilm under phosphate limiting conditions (25, 26). As expected for the El Tor biotype, a Δ*vieA* (VC1652) mutant did not alter *vpsL* levels. In the classical biotype of *V. cholerae,* VieA negatively regulates biofilm via an EAL domain, independently of its phosphorylation status and DNA-binding activity. The EAL domain functions as a phosphodiesterase (PDE) that degrades the secondary messenger c-di-GMP, an important positive regulator of biofilm formation (29). This phenotype is not observed in the El Tor biotype, as transcription of *vieSAB* is subject to H-NS silencing (49, 50). We also did not observe a phenotype for ΔVC1348 or ΔVCA0210, however, this was also consistent with previously published findings, which demonstrated a biofilm phenotype only when these proteins were overexpressed (33).

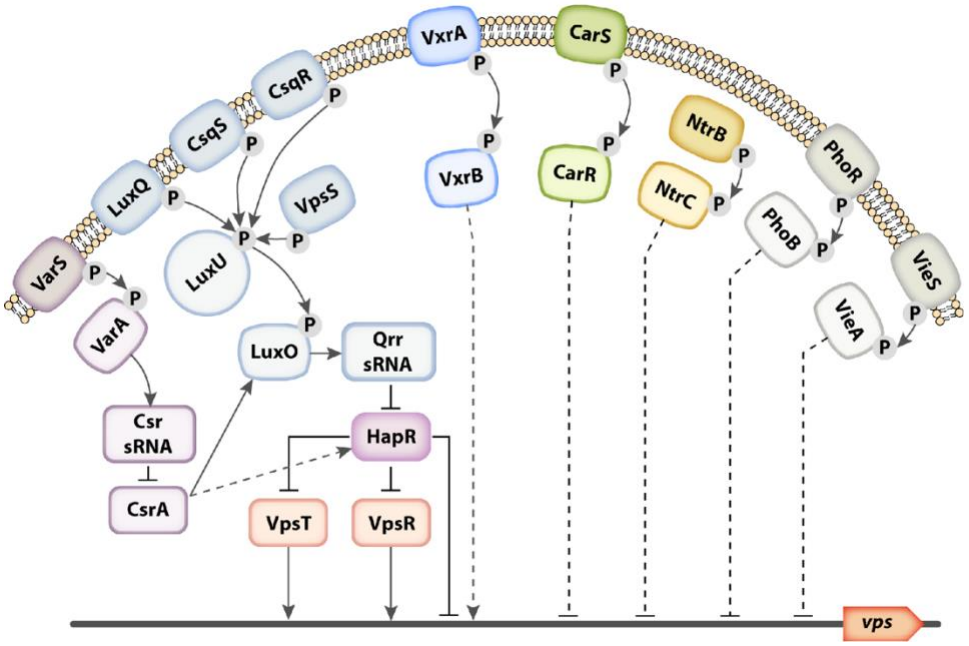

Figure 2.8. Model of all known TCS that regulate *V. cholerae* biofilm formation. The RRs VpsR (VC0665) and VpsT (VCA0952) are the major positive regulators of biofilm formation. Their cognate TCS partners have yet to be identified. The PhoRB (VC0719-20) TCS acts as a repressor of biofilm formation under phosphate limited conditions. LuxO (VC1021) acts as an activator of biofilm formation by positively regulating expression of small regulatory RNAs responsible for repressing translation of *hapR*, the master quorum sensing regulator and the major negative regulator of biofilm formation. VarSA (VC2453/VC1213) represses biofilm formation by interfering with the LuxO-mediated activation of Qrr sRNAs through its activation of the inhibitory regulatory small RNAs CsrBCD and their subsequent inhibition of the global regulator CsrA. Repression of CsrA reduces Qrr sRNA levels, leading to increased HapR levels and decreased *vps* gene expression. CarSR (VC1319-20) negatively regulates biofilm formation. VieA (VC1652)

represses biofilm formation independently of its cognate histidine kinase via an EAL domain responsible for degrading the secondary messenger c-di-GMP, an important positive regulator of biofilm formation. The NtrBC (VC2748-49) TCS was identified as a potential repressor of biofilm in this study. Though described in the text, VC1348 and VCA0210 are not pictured. These RRs contain HD-GYP domains responsible for degrading c-di-GMP. Though deletion of these genes does not impact biofilm formation, their overexpression leads to a significant decrease biofilm formation indicating that they may act as repressors of biofilm formation. Finally, we have included the newly identified VxrAB (VCA0565-66) TCS, which positively regulates of biofilm formation.

Interestingly, we observed a 47-fold decrease in *vpsL* expression in the absence of Δ*varA* (VC1213), which is contradictory to previously published work (32). The VarSA TCS is thought to impact biofilm formation through its control of CsrA levels, a small RNA binding protein that regulates a number of cellular processes. Specifically, VarA is predicted to repress biofilm formation by interfering with the LuxO-mediated activation of Qrr sRNAs through its positive regulation of the inhibitory regulatory small RNAs CsrBCD. These small RNAs sequester CsrA, which in turn reduces Qrr sRNA levels, leading to increased HapR levels and decreased *vps* gene expression (51–54). However, a recent study demonstrated that loss of VarA results in excessive levels of active CsrA, which negatively impacts cell growth and leads to single amino acid suppressor mutations in CsrA (55). These mutations were shown to alter the regulatory function of CsrA. Our sequence analysis of *csrA* in the Δ*varA vpsL*-lux strain revealed that this strain had amino acid substitution of T11P. It was speculated by Mey et al. that the amino acid substitutions clustered in the N-terminal half of CsrA (R6H, R6L, T11P, I14T, and T19P) result in accumulation of a "less active" form CsrA (55). Thus, our finding is consistent with the observation that loss of VarA results in suppressor mutations in *csrA* and that these mutations can alter CsrA activity, including its positive regulation of biofilm. Collectively, these observations explain why we did not observe the expected increase in *vpsL* expression in our Δ*varA* strain. Though *varA* mutant strains do not produce the CsrA-sequestering sRNAs and have increased levels of the positive biofilm regulator, CsrA, we hypothesize that CsrA's regulatory activity was altered due to the accumulation of a suppressor mutation.

Finally, we found an increase in *vpsL* expression a Δ*ntrC* (VC2749) mutant, indicating that this RR may be a repressor of biofilm formation.

We focused our studies mainly on a new positive regulator of *vps* and biofilm formation, VxrB. The observations reported here demonstrate that VxrAB TCS activates biofilm formation and *vpsL* expression and represses motility. We showed that VxrB positively regulates *vpsR* and *vpsT*, the two major regulators of *V. cholerae* biofilm and that VxrB regulates *vpsL* expression upstream of VpsR and VpsT. Finally, we demonstrated that VxrB positively regulates cellular levels of the second messenger signaling molecule, ci-di-GMP, which acts as a positive regulator of biofilm formation and a negative regulator of motility (41). While we demonstrated that VxrB may act through major biofilm regulators to exert its regulatory control on biofilm formation, further investigation of where VxrB is integrated into the *vps* regulatory network is necessary. It is possible that VxrB controls activity of *vps* genes through its modulation of cellular c-di-GMP levels, as increased c-di-GMP levels have been shown to lead to increased *vpsL*, *vpsR,* and *vpsT* expression (49, 56). Alternatively, VpsR and VpsT may be the direct regulatory targets of VxrB, as both regulators positively regulate diguanylate cyclases (DGC) genes, which are responsible for producing c-di-GMP (57). Given that a VxrA mutant did not demonstrate a decrease in c-di-GMP levels and that a VxrC mutant had a decrease in c-di-GMP levels despite positively regulating biofilm formation, further investigation into the regulatory role of the Vxr TCS on c-di-GMP levels is merited. Determining the direct regulatory targets of VxrB would

provide additional insight into our understanding of the role of TCS in the regulation and control of biofilm formation.

Our previous work demonstrated that *vxrABCDE* are co-transcribed and that *vxrCDE* have minor, but significant, roles in intestinal colonization (34). Here we demonstrated that only Δ*vxrA*, Δ*vxrB*, and Δ*vxrC* strains produced biofilms that were different from wild-type, though Δ*vxrD* and Δ*vxrE* strains did demonstrate decreased *vpsL* expression. It is possible that VxrD and VxrE play a minor role in the activation of *vpsL* expression, potentially through the VxrAB pathway, but that they do not significantly impact biofilm formation. VxrC was shown to act as a repressor of *vpsL* and biofilm formation and this phenotype was shown to be dependent on the presence of VxrB. This indicates that VxrC is in a pathway with the VxrAB TCS and that VxrC may interact with VxrA or VxrB to inhibit its regulation of biofilm formation. Further analysis of the Vxr operon members and their role in activating or repressing the VxrAB TCS will be essential for fully understanding the mechanism of action of this system.

C-di-GMP positively regulates biofilm formation and negatively regulates motility. Given the role of VxrAB in positively regulating biofilm formation and c-di-GMP levels, we investigated the impact of VxrB on motility. Our results demonstrated that deletion of *vxrB* did not impact motility, but that over expression of VxrB led to a decrease in motility. This is consistent with a previous study that demonstrated

that overexpression of wild-type VxrB or constitutively active VxrB resulted in a loss of motility (47).

We have previously shown that VxrB is a positive regulator of the T6SS, a protein delivery system that requires cell to cell contact to translocate toxic effector proteins into a diverse group of target cells, including other bacteria, phagocytic amoebas, and human macrophages (34, 48, 58–60). In a biofilm, where cells are already in close contact, the T6SS could contribute to localized death and biofilm remodeling. The role of the T6SS in *V. cholerae* biofilms is unknown and very few studies have been done in other species linking the T6SS to biofilm formation. In the *Pseudomonas aeruginosa* PAO1 the structural component that makes up the inner sheath of the T6SS, Hcp, was shown to take part in biofilm maturation stage (61). Additionally, a structural component of the outer sheath of the T6SS, *tssC1*, was demonstrated to promote antibiotic resistance in *P. aeruginosa* biofilms (62). In *Agrobacterium tumefaciens*, the ExoR regulator, an important regulator of biofilm formation, was shown to also regulate the T6SS and in *Burkholderia cencepacia* a novel hybrid HK was identified that controls biofilm formation and the T6SS (63, 64). Thus, we wanted to determine contribution of the T6SS on biofilm formation in *V. cholerae* and whether decreased biofilm formation phenotype of the *vxrB* mutant is due to decreased T6SS activity. Our initial results indicate that the T6SS does not impact *V. cholerae* biofilm formation under the conditions tested. However, it is possible that under alternative growth conditions the T6SS plays a structural or functional role within biofilms.

Determining the activating signals sensed by the VxrAB TCS will provide valuable insight into its mechanism of action. A recent study indicated that the VxrAB system may sense signals generated in response to beta-lactam exposure, potentially either directly sensing the antibiotics themselves or sensing cell wall stress or degradation products (47). A VxrA homolog in *V. parahaemolyticus*, VbrK, was shown to directly bind β-lactams to activate its cognate RR and stimulate expression of a β-lactamase and additional β-lactam antibiotics resistance genes (65). Given that *V. cholerae* does not encode for β-lactamase genes, it is interesting to consider the conditions under which VxrAB might encounter these potential signals and speculate about the role they might play in directing the activity of this TCS. Sub-inhibitory concentrations of aminoglycoside antibiotics have been demonstrated to induce biofilm formation in *P. aeruginosa* and *Escherichia coli* and it possible VxrAB mediates a similar response to beta lactam antibiotics in *V. cholerae* (66). Further investigation of the signals sensed by VxrAB is needed to fully elucidate the mechanism by which this TCS regulates diverse processes in *V. cholerae*.

It is evident that the VxrAB TCS plays an important regulatory role in *V. cholerae* and governs the T6SS, virulence, and cell wall homeostasis. This work identifies a new role for this system in biofilm formation and provides a better understanding of how VxrAB regulates important phases in the *V. cholerae* life cycle.

ACKNOWLEDGEMENTS

We thank Benjamin Abrams from the UCSC Life Sciences Microscopy Center for his technical support, Qiangli Zhang for help with the high-performance liquid chromatography-tandem mass spectrometry (HPLC MS/MS) experiments and analysis, and David Zamorano-Sánchez for his comments on the manuscript.

FUNDING SOURCES

This work was supported by the NIH grant R01AI055987 to F.H.Y.

References

1. **Kaper JB**, **Morris JG**, **Levine MM**. 1995. Cholera. Clin. Microbiol. Rev. **8**:48–86.
2. **Faruque SM**, **Albert MJ**, **Mekalanos JJ**. 1998. Epidemiology, genetics, and ecology of toxigenic *Vibrio cholerae*. Microbiol. Mol. Biol. Rev. **62**:1301–14.
3. **Charles RC**, **Ryan ET**. 2011. Cholera in the 21st century. Curr. Opin. Infect. Dis. **24**:472–7.
4. **Teschler JK**, **Zamorano-Sánchez D**, **Utada AS**, **Warner CJA**, **Wong GCL**, **Linington RG**, **Yildiz FH**. 2015. Living in the matrix: assembly and control of *Vibrio cholerae* biofilms. Nat. Rev. Microbiol. **13**:255–68.
5. **Islam MS**, **Jahid MIK**, **Rahman MM**, **Rahman MZ**, **Islam MS**, **Kabir MS**, **Sack DA**, **Schoolnik GK**. 2007. Biofilm acts as a microenvironment for plankton-associated *Vibrio cholerae* in the aquatic environment of Bangladesh. Microbiol. Immunol. **51**:369–79.
6. **Faruque SM**, **Biswas K**, **Udden SMN**, **Ahmad QS**, **Sack DA**, **Nair GB**, **Mekalanos JJ**. 2006. Transmissibility of cholera: *in vivo*-formed biofilms and their relationship to infectivity and persistence in the environment. Proc. Natl. Acad. Sci. U. S. A. **103**:6350–5.
7. **Alam M**, **Sultana M**, **Nair GB**, **Siddique AK**, **Hasan NA**, **Sack RB**, **Sack DA**, **Ahmed KU**, **Sadique A**, **Watanabe H**, **Grim CJ**, **Huq A**, **Colwell RR**. 2007. Viable but nonculturable *Vibrio cholerae* O1 in biofilms in the aquatic environment and their role in cholera transmission. Proc. Natl. Acad. Sci.

U. S. A. **104**:17801–6.

8. **Conner JG**, **Teschler JK**, **Jones CJ**, **Yildiz FH**. 2016. Staying alive: *Vibrio cholerae*'s cycle of environmental survival, transmission, and dissemination. Microbiol. Spectr. asm Pub2Web.
9. **Nielsen AT**, **Dolganov NA**, **Rasmussen T**, **Otto G**, **Miller MC**, **Felt SA**, **Torreilles S**, **Schoolnik GK**. 2010. A bistable switch and anatomical site control *Vibrio cholerae* virulence gene expression in the intestine. PLoS Pathog. **6**:e1001102.
10. **Berk V**, **Fong JCN**, **Dempsey GT**, **Develioglu ON**, **Zhuang X**, **Liphardt J**, **Yildiz FH**, **Chu S**. 2012. Molecular architecture and assembly principles of *Vibrio cholerae* biofilms. Science **337**:236–9.
11. **Absalon C**, **Van Dellen K**, **Watnick PI**. 2011. A communal bacterial adhesin anchors biofilm and bystander cells to surfaces. PLoS Pathog. **7**:e1002210.
12. **Fong JCN**, **Syed KA**, **Klose KE**, **Yildiz FH**. 2010. Role of *Vibrio* polysaccharide (*vps*) genes in VPS production, biofilm formation and *Vibrio cholerae* pathogenesis. Microbiology **156**:2757–69.
13. **Yildiz FH**, **Schoolnik GK**. 1999. *Vibrio cholerae* O1 El Tor: identification of a gene cluster required for the rugose colony type, exopolysaccharide production, chlorine resistance, and biofilm formation. Proc. Natl. Acad. Sci. U. S. A. **96**:4028–33.
14. **Fong JCN**, **Karplus K**, **Schoolnik GK**, **Yildiz FH**. 2006. Identification and characterization of RbmA, a novel protein required for the development of

rugose colony morphology and biofilm structure in *Vibrio cholerae*. J. Bacteriol. **188**:1049–59.

15. **Fong JCN**, **Yildiz FH**. 2007. The *rbmBCDEF* gene cluster modulates development of rugose colony morphology and biofilm formation in *Vibrio cholerae*. J. Bacteriol. **189**:2319–30.
16. **Moorthy S**, **Watnick PI**. 2005. Identification of novel stage-specific genetic requirements through whole genome transcription profiling of *Vibrio cholerae* biofilm development. Mol. Microbiol. **57**:1623–35.
17. **Yildiz FH**, **Visick KL**. 2009. *Vibrio* biofilms: so much the same yet so different. Trends Microbiol. **17**:109–18.
18. **Townsley L**, **Sison Mangus MP**, **Mehic S**, **Yildiz FH**. 2016. Response of *Vibrio cholerae* to low-temperature shift: CpsV regulates type VI secretion, biofilm formation, and association with zooplankton. Appl. Environ. Microbiol. **82**:AEM.00807-16.
19. **Shikuma NJ**, **Yildiz FH**. 2009. Identification and characterization of OscR, a transcriptional regulator involved in osmolarity adaptation in *Vibrio cholerae*. J. Bacteriol. **191**:4082–96.
20. **Beier D**, **Gross R**. 2006. Regulation of bacterial virulence by two-component systems. Curr. Opin. Microbiol. **9**:143–152.
21. **Calva E**, **Oropeza R**. 2006. Two-component signal transduction systems, environmental signals, and virulence. Microb. Ecol. **51**:166–76.
22. **Bilecen K**, **Yildiz FH**. 2010. Identification of a calcium-controlled negative regulatory system affecting *Vibrio cholerae* biofilm formation. Environ.

Microbiol. **11**:2015–2029.

23. **Shikuma NJ**, **Davis KR**, **Fong JNC**, **Yildiz FH**. 2013. The transcriptional regulator, CosR, controls compatible solute biosynthesis and transport, motility and biofilm formation in *Vibrio cholerae*. Environ. Microbiol. **15**:1387–99.
24. **Yildiz FH**, **Dolganov NA**, **Schoolnik GK**. 2001. VpsR, a Member of the response regulators of the two-component regulatory systems, is required for expression of *vps* biosynthesis genes and EPS(ETr)-associated phenotypes in *Vibrio cholerae* O1 El Tor. J. Bacteriol. **183**:1716–26.
25. **Pratt JT**, **McDonough E**, **Camilli A**. 2009. PhoB regulates motility, biofilms, and cyclic di-GMP in *Vibrio cholerae*. J. Bacteriol. **191**:6632–42.
26. **Sultan SZ**, **Silva AJ**, **Benitez JA**. 2010. The PhoB regulatory system modulates biofilm formation and stress response in El Tor biotype *Vibrio cholerae*. FEMS Microbiol. Lett. **302**:22–31.
27. **Casper-Lindley C**, **Yildiz FH**. 2004. VpsT Is a transcriptional regulator required for expression of *vps* biosynthesis genes and the development of rugose colonial morphology in *Vibrio cholerae* O1 El Tor. J. Bacteriol. **186**:1574–1578.
28. **Hammer BK**, **Bassler BL**. 2003. Quorum sensing controls biofilm formation in *Vibrio cholerae*. Mol. Microbiol. **50**:101–4.
29. **Tischler AD**, **Camilli A**. 2004. Cyclic diguanylate (c-di-GMP) regulates *Vibrio cholerae* biofilm formation. Mol. Microbiol. **53**:857–69.
30. **Bilecen K**, **Fong JCN**, **Cheng A**, **Jones CJ**, **Zamorano-Sánchez D**,

Yildiz FH. 2015. Polymyxin B resistance and biofilm formation in *Vibrio cholerae* is controlled by the response regulator CarR. Infect. Immun.

31. **Bilecen K**, **Yildiz FH**. 2009. Identification of a calcium-controlled negative regulatory system affecting *Vibrio cholerae* biofilm formation. Environ. Microbiol. **11**:2015–29.
32. **Lenz DH**, **Miller MB**, **Zhu J**, **Kulkarni R V**, **Bassler BL**. 2005. CsrA and three redundant small RNAs regulate quorum sensing in *Vibrio cholerae*. Mol. Microbiol. **58**:1186–202.
33. **McKee RW**, **Kariisa A**, **Mudrak B**, **Whitaker C**, **Tamayo R**. 2014. A systematic analysis of the *in vitro* and *in vivo* functions of the HD-GYP domain proteins of *Vibrio cholerae*. BMC Microbiol. **14**:272.
34. **Cheng AT**, **Ottemann KM**, **Yildiz FH**. 2015. *Vibrio cholerae* response regulator VxrB controls colonization and regulates the Type VI secretion system. PLoS Pathog. **11**:e1004933.
35. **Liu X**, **Beyhan S**, **Lim B**, **Linington RG**, **Yildiz FH**. 2010. Identification and characterization of a phosphodiesterase that inversely regulates motility and biofilm formation in *Vibrio cholerae*. J. Bacteriol. **192**:4541–52.
36. **Zamorano-Sánchez D**, **Fong JCN**, **Kilic S**, **Erill I**, **Yildiz FH**. 2015. Identification and characterization of VpsR and VpsT binding sites in *Vibrio cholerae*. J. Bacteriol. JB.02439-14-.
37. **Heydorn A**, **Nielsen AT**, **Hentzer M**, **Sternberg C**, **Givskov M**, **Ersbøll BK**, **Molin S**. 2000. Quantification of biofilm structures by the novel computer program COMSTAT. Microbiology **146 (Pt 1**:2395–407.

38. **Herrero M**, **de Lorenzo V**, **Timmis KN**. 1990. Transposon vectors containing non-antibiotic resistance selection markers for cloning and stable chromosomal insertion of foreign genes in gram-negative bacteria. J. Bacteriol. **172**:6557–67.

39. **de Lorenzo V**, **Timmis KN**. 1994. Analysis and construction of stable phenotypes in gram-negative bacteria with Tn5- and Tn10-derived minitransposons. Methods Enzymol. **235**:386–405.

40. **Yildiz FH**, **Schoolnik GK**. 1998. Role of *rpoS* in stress survival and virulence of *Vibrio cholerae*. J. Bacteriol. **180**:773–84.

41. **Beyhan S**, **Tischler AD**, **Camilli A**, **Yildiz FH**. 2006. Transcriptome and phenotypic responses of *Vibrio cholerae* to increased cyclic di-GMP level. J. Bacteriol. **188**:3600–13.

42. **Bao Y**, **Lies DP**, **Fu H**, **Roberts GP**. 1991. An improved Tn7-based system for the single-copy insertion of cloned genes into chromosomes of gram-negative bacteria. Gene **109**:167–8.

43. **Hammer BK**, **Bassler BL**. 2007. Regulatory small RNAs circumvent the conventional quorum sensing pathway in pandemic *Vibrio cholerae*. Proc. Natl. Acad. Sci. U. S. A. **104**:11145–9.

44. **Shikuma NJ**, **Fong JCN**, **Yildiz FH**. 2012. Cellular levels and binding of c-di-GMP control subcellular localization and activity of the *Vibrio cholerae* transcriptional regulator VpsT. PLoS Pathog. **8**:e1002719.

45. **Butler SM**, **Camilli A**. 2005. Going against the grain: chemotaxis and infection in *Vibrio cholerae*. Nat. Rev. Microbiol. **3**:611–20.

46. **Butler SM**, **Camilli A**. 2004. Both chemotaxis and net motility greatly influence the infectivity of *Vibrio cholerae*. Proc. Natl. Acad. Sci. **101**:5018–23.

47. **Dörr T**, **Alvarez L**, **Delgado F**, **Davis BM**, **Cava F**, **Waldor MK**. 2016. A cell wall damage response mediated by a sensor kinase/response regulator pair enables beta-lactam tolerance. Proc. Natl. Acad. Sci. U. S. A. **113**:404–9.

48. **Pukatzki S**, **Ma AT**, **Sturtevant D**, **Krastins B**, **Sarracino D**, **Nelson WC**, **Heidelberg JF**, **Mekalanos JJ**. 2006. Identification of a conserved bacterial protein secretion system in *Vibrio cholerae* using the *Dictyostelium* host model system. Proc. Natl. Acad. Sci. U. S. A. **103**:1528–33.

49. **Beyhan S**, **Tischler AD**, **Camilli A**, **Yildiz FH**. 2006. Differences in gene expression between the classical and El Tor biotypes of *Vibrio cholerae* O1. Infect. Immun. **74**:3633–42.

50. **Wang H**, **Ayala JC**, **Benitez JA**, **Silva AJ**. 2015. RNA-Seq analysis identifies new genes regulated by the histone-like nucleoid structuring protein (H-NS) affecting *Vibrio cholerae* virulence, stress response and chemotaxis. PLoS One **10**:e0118295.

51. **Lenz DH**, **Mok KC**, **Lilley BN**, **Kulkarni R V**, **Wingreen NS**, **Bassler BL**. 2004. The small RNA chaperone Hfq and multiple small RNAs control quorum sensing in *Vibrio harveyi* and *Vibrio cholerae*. Cell **118**:69–82.

52. **Tsou AM**, **Liu Z**, **Cai T**, **Zhu J**. 2011. The VarS/VarA two-component

system modulates the activity of the *Vibrio cholerae* quorum-sensing transcriptional regulator HapR. Microbiology **157**:1620–8.

53. **Jang J**, **Jung K-T**, **Yoo C-K**, **Rhie G-E**. 2010. Regulation of hemagglutinin/protease expression by the VarS/VarA-CsrA/B/C/D system in *Vibrio cholerae*. Microb. Pathog. **48**:245–50.

54. **Jang J**, **Jung K-T**, **Park J**, **Yoo C-K**, **Rhie G-E**. 2011. The *Vibrio cholerae* VarS/VarA two-component system controls the expression of virulence proteins through ToxT regulation. Microbiology **157**:1466–1473.

55. **Mey AR**, **Butz HA**, **Payne SM**. 2015. *Vibrio cholerae* CsrA regulates ToxR levels in response to amino acids and is essential for virulence. MBio **6**:e01064.

56. **Krasteva P V**, **Fong JCN**, **Shikuma NJ**, **Beyhan S**, **Navarro MVAS**, **Yildiz FH**, **Sondermann H**. 2010. *Vibrio cholerae* VpsT regulates matrix production and motility by directly sensing cyclic di-GMP. Science **327**:866–8.

57. **Beyhan S**, **Bilecen K**, **Salama SR**, **Casper-Lindley C**, **Yildiz FH**. 2007. Regulation of rugosity and biofilm formation in *Vibrio cholerae*: comparison of VpsT and VpsR regulons and epistasis analysis of *vpsT*, *vpsR*, and *hapR*. J. Bacteriol. **189**:388–402.

58. **Zheng J**, **Ho B**, **Mekalanos JJ**. 2011. Genetic analysis of anti-amoebae and anti-bacterial activities of the type VI secretion system in *Vibrio cholerae*. PLoS One **6**:e23876.

59. **Pukatzki S**, **Ma AT**, **Revel AT**, **Sturtevant D**, **Mekalanos JJ**. 2007. Type

VI secretion system translocates a phage tail spike-like protein into target cells where it cross-links actin. Proc. Natl. Acad. Sci. U. S. A. **104**:15508–13.

60. **MacIntyre DL**, **Miyata ST**, **Kitaoka M**, **Pukatzki S**. 2010. The *Vibrio cholerae* type VI secretion system displays antimicrobial properties. Proc. Natl. Acad. Sci. U. S. A. **107**:19520–4.

61. **Southey-Pillig CJ**, **Davies DG**, **Sauer K**. 2005. Characterization of temporal protein production in *Pseudomonas aeruginosa* biofilms. J. Bacteriol. **187**:8114–26.

62. **Zhang L**, **Hinz AJ**, **Nadeau J-P**, **Mah T-F**. 2011. *Pseudomonas aeruginosa tssC1* links type VI secretion and biofilm-specific antibiotic resistance. J. Bacteriol. **193**:5510–3.

63. **Heckel BC**, **Tomlinson AD**, **Morton ER**, **Choi J-H**, **Fuqua C**. 2014. *Agrobacterium tumefaciens exoR* controls acid response genes and impacts exopolysaccharide synthesis, horizontal gene transfer, and virulence gene expression. J. Bacteriol. **196**:3221–33.

64. **Aubert DF**, **Flannagan RS**, **Valvano MA**. 2008. A novel sensor kinase-response regulator hybrid controls biofilm formation and type VI secretion system activity in *Burkholderia cenocepacia*. Infect. Immun. **76**:1979–91.

65. **Li L**, **Wang Q**, **Zhang H**, **Yang M**, **Khan MI**, **Zhou X**. 2016. Sensor histidine kinase is a β-lactam receptor and induces resistance to β-lactam antibiotics. Proc. Natl. Acad. Sci. U. S. A. **113**:1648–1653.

66. **Hoffman LR**, **D'Argenio DA**, **MacCoss MJ**, **Zhang Z**, **Jones RA**, **Miller**

SI. 2005. Aminoglycoside antibiotics induce bacterial biofilm formation. Nature **436**:1171–1175.

CHAPTER 3: *Vibrio cholerae* T6SS activity during biofilm formation

Jennifer K Teschler and Fitnat H. Yildiz

ABSTRACT

Biofilms are surface-associated microbial communities composed of cell aggregates encased by a self-produced or acquired extracellular matrix. Biofilms contribute to the environmental persistence of *V. cholerae* and provide protection from a number of environmental stresses, including nutrient limitation and predation by protozoa and bacteriophages. The type six secretion system (T6SS) is a protein delivery system that translocates toxic effector proteins into a diverse group of target cells, including other bacteria, phagocytic amoebas, and human macrophages. RNA-seq analysis demonstrated that T6SS genes are more highly regulated in biofilm cells compared to planktonic cells and that the response regulator (RR), VxrB, co-regulates T6SS and biofilm genes. To assess if the T6SS is active in biofilm formation I first tested the ability of biofilm-grown cells to kill prey in a T6SS-dependent manner and determined that biofilm-grown cells can kill as well or better than planktonic-grown cells. Next, I visualized T6SS firing and killing of neighboring cells during biofilm formation, establishing that the T6SS is actively fired and capable of killing susceptible prey during biofilm formation. Finally, I assessed overall biofilm formation in mixed strain biofilms and showed that *V. cholerae* strains with an active T6SS are better able to compete during mixed-strain biofilm formation than a strain lacking the T6SS. This is the first evidence that the *V. cholerae* T6SS can actively kill prey strains within the biofilm and that this killing contributes to its ability to compete for space and resources within the biofilm.

Introduction

The social interactions among intra- and inter- species biofilms are an area of recent exploration, and the phenomena of cooperation and competition among the species that inhabit these unique environments is only beginning to be examined (1, 2). Antagonistic behavior, such as killing via the T6SS, is predicted to favor a competitive hierarchy that enriches for one strain over susceptible strains (1, 3, 4). Additionally, this behavior is expected to be tightly regulated, as once the antagonistic strain has established a dominant niche the necessity for toxin secretion is drastically reduced (1). In fact, the T6SS is a highly regulated process in *V. cholerae* (Figure 1.4). The VxrB response regulator is known to co-regulate the T6SS and biofilm formation, indicating that it may mediate this antagonistic behavior within the biofilm.

As discussed in Chapter 1, the T6SS is a well-characterized toxin delivery system that can be utilized to compete with neighboring bacteria and maintain clonal populations by attacking susceptible competitors. Work in two microbes has suggested that the T6SS plays an important role in mixed-species biofilms. *Burkholderia thailandensis* requires one of its five T6SS to compete with *Pseudomonas putida* during mixed species biofilm formation (5). In this case, a wild type *B. thailandensis* was able to persist and outcompete *P. putida* in mixed species biofilms, while a T6SS-1 *B. thailandensis* mutant was rapidly displaced by *P. putida* (5). The gut symbiont *Bacteroides fragilis* utilizes the T6SS to maintain its niche in the microbiota, a complex microbial biofilm, killing non-kin neighbors in

a spatial-dependent manner (6). While the role of the *V. cholerae* T6SS in biofilm formation is not known, it has been shown that the T6SS plays an important role in invading and displacing the microbiota to colonize the small intestine (7–10). Additionally, *V. cholerae* exopolysaccharide protects itself against exogenous T6SS attack from other species without preventing *V. cholerae* from utilizing its own T6SS (11).

More work is needed to understand the role of the T6SS in biofilm formation and community dynamics. Though cell death and DNA release is known to be an important feature of biofilm formation and structure, the contribution of T6SS killing is unknown (12). Additionally, in a heterogenous environment such as a biofilm, it has not been shown if the T6SS is active and if activity is localized to certain regions of the biofilm. In *Pseudomonas aeruginosa,* cells respond to kin lysis as a danger signal to activate T6SS activity, indicating that T6SS-mediated cell lysis in mixed species biofilms may play a complex role, potentially serving structural and signaling roles (13). Given that VxrB co-regulates biofilm formation, the T6SS, and cell envelope homeostasis, it is interesting to speculate that this system may also respond to a danger signal to activate protective responses, similar to *P. aeruoginosa*.

Here we explore the role of the T6SS in competitive mixed *V. cholerae* strain biofilms. We hypothesize that the T6SS contributes to competition with other

bacterial species during biofilm expansion, the exclusion of invaders once biofilms are established, and alters biofilm structure via cell lysis and DNA release.

Materials and methods

Strains and growth conditions. Strains used in this study are listed in Table 3.1. *V. cholerae, Pseudomonas aeruginosa,* and *Escherichia coli* strains were grown aerobically in Luria-Bertani (LB) broth (1% tryptone, 0.5% Yeast Extract, 1% NaCl), pH 7.5, at 30°C, 37°C, and 37°C, respectively. LB agar contained granulated agar (Difco) at 1.5% (w/v). Media additives were used when necessary at the following concentrations: rifampicin (100 µg/mL) and ampicillin (100 µg/mL).

Strain and plasmid construction. Plasmids were constructed using standard cloning methods or the Gibson Assembly recombinant DNA technique (New England Biolabs, Ipswich, MA). Gene deletions were carried out using allelic exchange of the native ORF with the truncated ORF, as previously described (14). Generation of Tn7 complementations and insertions were carried out using a Tn7-based system, as previously described (7). Briefly, triparental matings with donor *E. coli* S17λpir carrying pGP704-Tn7 with gene of interest, helper *E. coli* S17λpir harboring pUX-BF13, and *V. cholerae* deletion strains were carried out by mixing all three strains, and incubating mating mixtures on LB agar plates for 18 hours at 30°C. Transconjugants were selected on thiosulfate-citrate-bile salts-sucrose (TCBS) (BD Difco, Franklin Lakes, NJ) agar medium containing gentamicin 15µg/µL) at 30˚C. Insertion of the construct to the Tn7 site was verified by PCR.

Table 3.1. Bacterial strains and plasmids used in this study.

Strain or plasmid	Relevant genotype	Source
E. coli strains		
CC118λ*pir*	Δ(*ara-leu*) *araD* Δ*lacX74 galE galK phoA20 thi-1 rpsE rpoB argE*(*Am*) *recA1* λ*pir*	(15)
S17-1λ*pir*	Tp^r Sm^r *recA thi pro* r_K^- m_K^+ RP4::2-Tc::MuKm Tn7 λ*pir*	(16)
V. cholerae strains		
FY_VC_0001	*Vibrio cholerae* O1 El Tor A1552, wild type, Rif^r	(17)
FY_VC_8758	ΔVCA0566 (*vxrB*)	(7)
FY_VC_9469	Δ*vxrB*-Tn7::*vxrB*	(7)
FY_VC_13604	A1552 *vipA*::sfGFP A	This study
FY_VC_13617	A1552 *vipA*::sfGFP Δ*vasK*	This study
FY_VC_13690	A1552 *vipA*::sfGFP Δ*vxrB*	This study
FY_VC_13654	A1552 *vipA*::sfGFP Δ*vxrB* Δ*vasK*	This study
FY_VC_13664	A1552 *vipA*::_sfGFP tn7::RFP	This study
FY_VC_13665	A1552 *vipA*::_sfGFP Δ*vasK* tn7::RFP	This study
FY_VC_13686	A1552 *vipA*::_sfGFP Δ*vasH*	This study
FY_VC_13688	A1552 *vipA*::_sfGFP Δ*vasH* Δ*vasK*	This study
FY_VC_13956	A1552 *vipA*::sfGFP ∆*vxrB*-Tn7::*vxrB*	This study
FY_VC_13958	A1552 *vipA*::sfGFP ∆*vasK* ∆*vxrB*-Tn7::*vxrB*	This study
FY_VC_13960	A1552 *vipA*::sfGFP Δ*tfoY*	This study
FY_VC_13994	A1552 *vipA*::sfGFP Δ*tfoY* Δ*vasK*	This study
FY_VC_14066	A1552 *vipA*::sfGFP Tn7::pTAC-*vxrB*	This study
FY_VC_14065	A1552 *vipA*::sfGFP Tn7::pTAC-*tfoY*	This study
FY_VC_14180	A1552 *vipA*::sfGFP Δ*vpsI-II*	This study
FY_VC_14182	A1552 *vipA*::sfGFP Δ*rbmA* Δ*lacZ*	This study
FY_VC_13868	Rugose A1552 S *vipA*::sfGFP A	This study
FY_VC_13950	Rugose A1552 *vipA*::_sfGFP Δ*vasK*	This study
FY_VC_13948	Rugose A1552 *vipA*::_sfGFP Δ*vxrB*	This study
FY_VC_13973	Rugose A1552 *vipA*::_sfGFP Δ*vxrB* Δ*vasK*	This study
FY_VC_13870	Haiti (2010EL-1786) *vipA*::sfGFP	This study
FY_VC_13954	Haiti (2010EL-1786) *vipA*::sfGFP Δ*vasK*	This study
FY_VC_13952	Haiti (2010EL-1786) *vipA*::sfGFP Δ*vxrB*	This study
FY_VC_13975	Haiti (2010EL-1786) *vipA*::sfGFP Δ*vxrB* Δ*vasK*	This study
FY_VC_13334	V52 *vipA*::sfGFP	(18)
FY_VC_13977	V52 *vipA*::sfGFP Δ*vasK*	This study
FY_VC_13674	V52 *vipA*::sfGFP Δ*vxrB*	This study
FY_VC_13418	V52 Smooth *vipA*::_sfGFP Tn7::rfp	This study
FY_VC_13414	V52 Smooth *vipA*::_mcherry Tn7::gfp	This study
FY_VC_13358	C6706 Δ*tsiV1-3*	(19)
FY_VC_14340	C6706 Δ*tsiV1-3* Tn7::CFP	This study
FY_VC_13360	AM19226	(20)
FY_VC_13358	AM19226 Δ*vasK*	(19)

P. aeruginosa strains		
FY_YE_87	PAO1 Δ*retS*	(21)
FY_YE_88	PAO1 Δ*tssM1*	(22)
Plasmids		
pGP704*sacB*28	pGP704 derivative, *mob*/*oriT sacB*, Ap^r	(23)
pUX-BF13	oriR6K helper plasmid, mob/oriT, provides the Tn7 transposition function in trans, Ap^r	(24)
pMCM11	pGP704::mTn*7*-*cfp*, Gm^r Ap^r	M. Miller and G. Schoolnik
pFY-5676	pGP704SacB-*vipA*-sfGFP	This study

T6SS killing assays

Killing assays were performed as described previously (25). Briefly, bacterial strains were grown overnight on LB plates and resuspended in LB broth containing 340 mM NaCl, as *V*. *cholerae* strain A1552 displayed enhanced interbacterial virulence towards *E*. *coli* under high osmolarity (26). *V*. *cholerae* and prey strains were mixed at a 10:1 ratio and 25 µl was spotted onto LB agar plates containing 340 mM NaCl and incubated at 37°C for 4 hours. Spots were harvested, serially diluted, and plated onto LB plates containing 50 µg/ml of streptomycin or chloramphenicol to enumerate surviving prey cells. Statistical analyses were performed using Prism 8 software (GraphPad Software, Inc., San Diego, CA) using a one-way analysis of variance (ANOVA) and Dunnett's multiple-comparison test. P values of <0.05 were determined to be statistically significant.

Biofilm assays. Flow cells were inoculated by diluting overnight-grown cultures of gfp-tagged *V. cholerae* strains 1:200 (OD_{600} of 0.02) and injecting cells into an Ibidi m-Slide VI0.4 (Ibidi 80601 ; Ibidi LLC, Verona, WI). After inoculation the bacteria were allowed to adhere at room temperature for 1 h with no flow. Then, flow of 2% (vol/vol) LB (0.2 g/liter tryptone, 0.1 g/liter yeast extract, 1% NaCl) was initiated at a rate of 7.5 ml/h and continued for up to 24 h. Confocal laser scanning microscopy (CLSM) images of the biofilms were captured with an 880 Zeiss confocal using an excitation wavelength of 488 nm and an emission wavelength of 543 nm (GFP) and an excitation wavelength of 434 nm and an emission wavelength of 477 nm (CFP). Three-dimensional images of the biofilms were reconstructed using Imaris

software (Bitplane). For tube-biofilms, cells were grown in 15 cm silicon tubes (ID 0.125/OD 0.250) with 2% LB medium (0.02% tryptone, 0.01% yeast extract, 1% NaCl [pH 7.5]), and incubated at room temperature for 48 hr using a peristaltic pump to deliver constant flow at a rate of 4.4 ml per hr. Biofilm-grown cells were prepared by scraping into 1X phosphate-buffered saline (PBS) and vortexing with beads.

Results

T6SS genes are upregulated in biofilms. Our first goal was to determine whether the T6SS was expressed in *V. cholerae* biofilms. Analysis of RNA-seq results comparing biofilm-grown and planktonic-grown cells revealed that 15 T6SS genes found across all known T6SS gene clusters are upregulated in biofilm-grown cells (Figure 3.1A) (27). Additionally, our previous RNA-seq analysis of WT and a Δ*vxrB* strain showed that VxrB co-regulated biofilm genes and T6SS genes (Figure 3.1B-C).

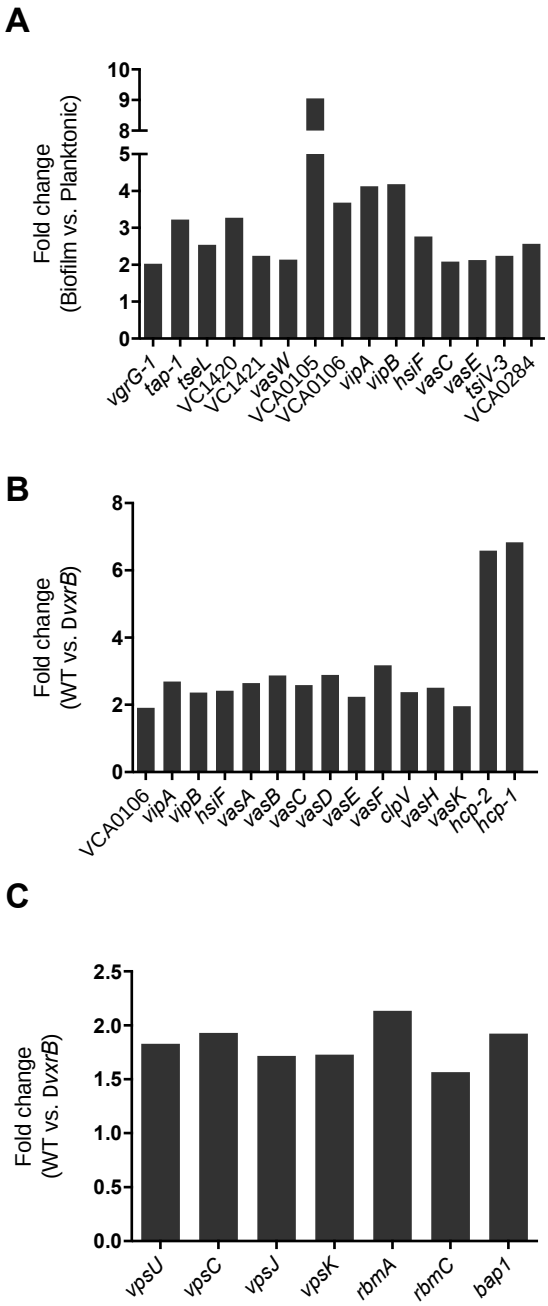

Figure 3.1. Differentially regulated genes in biofilm-grown cells compared to planktonic-grown cells and wild-type strain compared to *vxrB* mutant strains.

A) T6SS genes upregulated in biofilm-grown cells compared to planktonic cells. Cutoff values: 2-fold difference in gene expression, a 1% false-discovery rate (FDR), p-value<0.0001. RNA-seq data will be published in a currently in

preparation publication (27). B) T6SS genes upregulated by VxrB. RNA-seq data was published as a part of a prior lab member's thesis (28). C) Biofilm genes upregulated by VxrB. Cutoff values: 1.5-fold difference in gene expression, a 1% false-discovery rate (FDR), p-value<0.0001. RNA-seq data was published as a part of a prior lab member's thesis (28).

Biofilm-grown cells kill susceptible prey in a T6SS-dependent manner. To determine if the T6SS is actively assembled and fired in biofilms, I assessed the ability of biofilm-grown cells to kill *E. coli* in a T6SS killing assay. Planktonic-grown cells were grown under conditions that induce the T6SS and biofilm-grown cells were grown for 48 hours in tube biofilms before being removed for killing assays. The total number of surviving *E. coli* was greatly reduced when incubated with wild type planktonic-grown or wild type biofilm-grown cells. Killing was dependent on the presence of an active T6SS system, as deletion of either *vxrB* or the T6SS *hcp* structural genes greatly reduced killing (Figure 3.2). This indicates that biofilm-grown cells can kill using their T6SS.

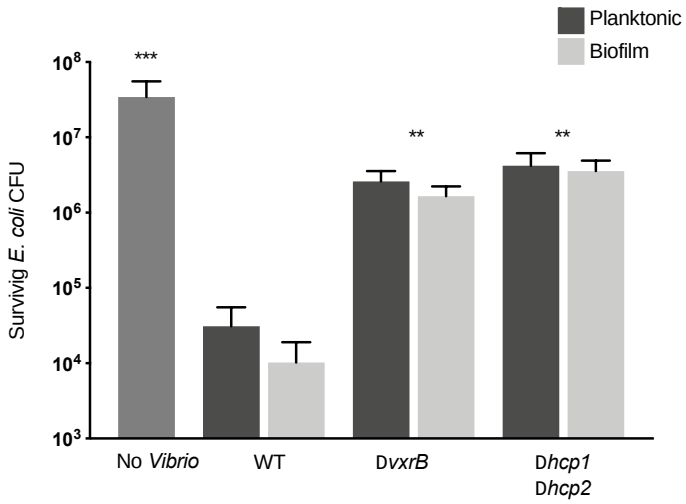

Figure 3.2. T6SS-killing by planktonic- and biofilm-grown cells.

Planktonic- and biofilm-grown wild-type *V*. *cholerae* kills prey strain *E*. *coli* strain MC4100. Killing is ablated in the absence of *hcp1* and *hcp2*, which are required for T6SS firing. Statistical analysis was carried out using a one-way analysis of variance (ANOVA) and Kruskal-Wallis test. (**, $p<0.05$, ***, $p<0.005$).

T6SS assembly and killing can be observed in mixed strain biofilms. I next determined if T6SS killing could be observed during biofilm formation. I utilized a *vipA*-sfGFP fusion strain to visualize T6SS assembly in the *V. cholerae* predator strain and a CFP-tagged *V. cholerae* prey strain, C6706 Δ*tsiV1-V3*, which lacks the immunity proteins required for T6SS resistance. Though C6706 does encode for an active T6SS, previous work has shown that it is T6SS-silent and does not produce T6SS components or effectors and in the absence of immunity proteins becomes susceptible to T6SS killing (25). I first confirmed the ability of the tagged predator strain to kill the prey strain using a T6SS killing assay to confirm that C6706 Δ*tsiV1-V3* is killed by A1552 *vipA*-sfGFP (Figure 3.3A). I then analyzed strain interactions in the biofilm using fluorescent microscopy. A one-hour time lapse video was collected from growing biofilms formed under flow conditions on a plastic surface. During this time course, C6706 Δ*tsiV1-V3* killing was observed, as indicated by cell rounding, in response to T6SS firing (Figure 3.3B-C).

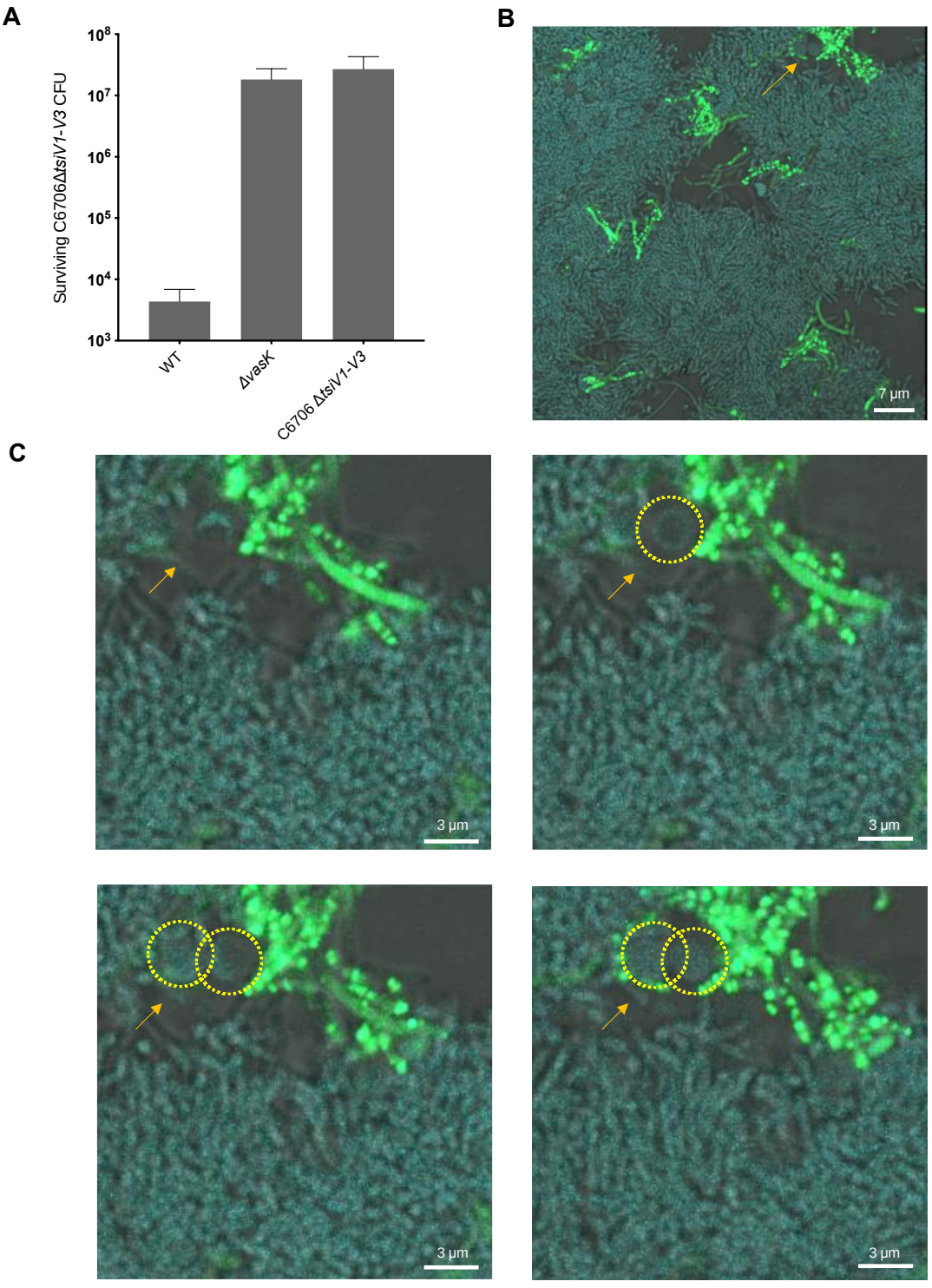

Figure 3.3. T6SS-killing in mixed strain biofilms.

A) A1552 *vipA*-sfGFP kills prey strain C6706 Δ*tsiV1-V3* during an interbacterial killing assay. Killing is ablated in the absence of *vasK*, which is required for T6SS

firing. B) T6SS firing is shown in green using a *vipA*-sfGFP fusion and prey strains are shown in blue using CFP tagged C6706 Δ*tsiV1-V3*. The arrow shows area enlarged in part C to show cell rounding in response to T6SS firing. C) Enlarged time lapse images from top left to right showing cell rounding in response to T6SS firing.

The T6SS confers a competitive advantage within the biofilm. To assess the impact of T6SS killing within the biofilm I compared 24-hour biofilm formation in mixed strains biofilms containing either A1552 *vipA*-sfGFP or A1552 *ΔvasK vipA*-sfGFP (T6SS- strain) with prey strain C6706 Δ*tsiV1-V3* Tn7::CFP. C6706 forms robust biofilms and outcompetes A1552 in the absence of an active T6SS (Figure 3.4). However, when A1552 has an active T6SS it is better able to maintain its foothold in the biofilm and makes up a larger proportion of the mixed strain biofilm (Figure 3.4). Additionally, *vps* has been shown to protect from T6SS killing so it may be interesting to examine how C6706 Δ*tsiV1-V3* or non-*Vibrio* species killing is impacted in in the absence of *vps* within biofilms, as more drastic differences may be observed.

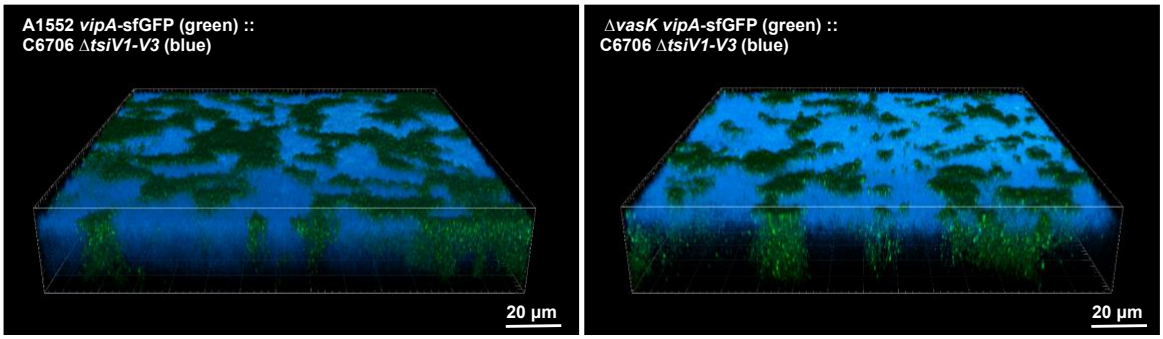

Figure 3.4. T6SS-killing in mixed strain biofilms.

A1552 *vipA*-sfGFP (green) competes with susceptible prey strain C6706 Δ*tsiV1-V3* (blue) and occupies a greater proportion of the biofilm (left), while a T6SS null strain does not compete as well and occupies less of the overall biofilm.

VxrB regulates the T6SS in various *V. cholerae* strains. VxrB is a positive regulator of the *V. cholerae* T6SS and has been shown to be required for T6SS mediated killing (7). These initial studies were done in a toxigenic A1552 strain of *V. cholerae*, which is known to regulate its T6SS in response to various environmental signals (26, 29). In contrast, other toxigenic strains of *V. cholerae,* including V52, have been shown to constitutively express the T6SS (30). It is not known if VxrB also regulates the T6SS in other strains of *V. cholerae*. To determine the contribution of VxrB to T6SS killing in various *V. cholerae* strains, I examined the impact of VxrB on interbacterial killing in 4 different *V. cholerae* strains (Figure 3.5). Again using *E. coli* as a prey strain, I performed T6SS assays with a rugose variant of A1552, the V52 strain, and the Haiti outbreak type isolate 2010EL-1786. Wild type versions of the rugose variant of A1552, a high biofilm forming strain, and V52, a T6SS constitutively active strain, efficiently killed *E. coli* prey, however, removal of *vxrB* in either of these backgrounds significantly reduced killing (Fig. 3.5). This indicates that VxrB regulates the T6SS in various *V. cholerae* strains. No T6SS killing was observed for Haiti outbreak type isolate 2010EL-1786, indicating that this strain may be T6SS-silent or that the T6SS is not regulated in this strain under these lab conditions. Future directions include characterizing the role of VxrB in modulating T6SS-killing within biofilms among different strains with varying biofilm capabilities or lacking key biofilm components. Additionally, it will be useful to assess the impact of T6SS killing on other susceptible prey species and evaluate the consequences of T6SS killing on biofilm community dynamics, structure, and stability.

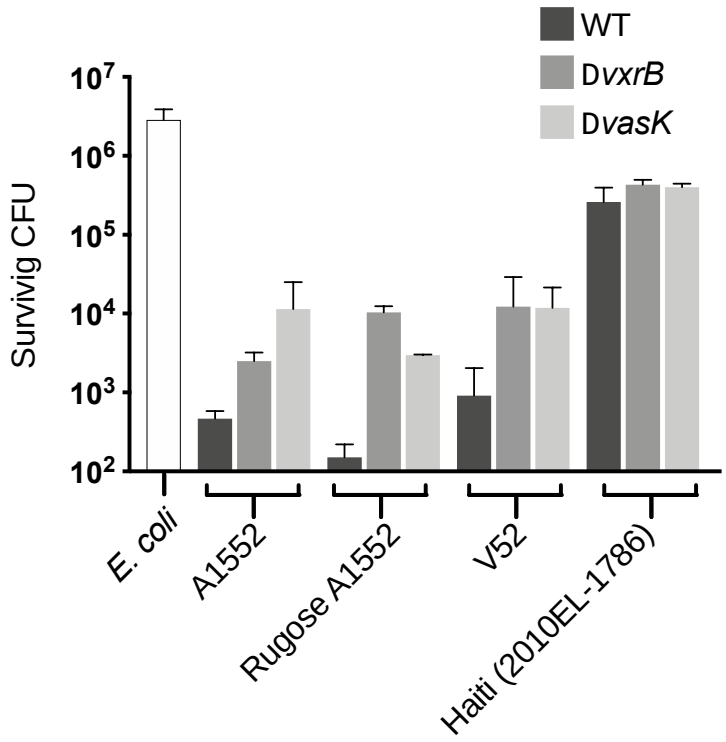

Figure 3.5. Impact of VxrB on T6SS-killing in various *V. cholerae* strains.

VxrB regulates T6SS killing in A1552, a rugose variant of A1552, and the T6SS constitutively active V52 strain. Under the conditions tested, Haiti outbreak type isolate 2010EL-1786 did not show T6SS-mediated killing.

Discussion

This study lays the groundwork for further study of the impact of *V. cholerae* T6SS activity within the biofilm and the role of VxrB in regulating T6SS activity within the biofilm. We show that the T6SS is upregulated in biofilms and that biofilm-grown cells are capable of killing susceptible prey. We additionally visualize T6SS killing within a biofilm and demonstrate that the absence of a T6SS diminishes the ability of *V. cholerae* to maintain a niche within mixed species biofilms. Finally, we show that VxrB mediates T6SS activity in both planktonic-grown and biofilm-grown cells and can modulate T6SS in various strain backgrounds.

In the previous chapter, I assessed the contribution of the T6SS to biofilm formation in mono-strain biofilms and determined that the T6SS did not significantly contribute to biofilm formation or structure under the conditions tested (31). However, immunity proteins confer resistance to self-killing when the T6SS is fired into sister cells (19, 32, 33). The contribution of the T6SS to biofilm structure and organization may be masked when killing is prevented, as cell death within the biofilm can contribute to biofilm structure and nutrient availability. For example, *Bacillus subtilis* can ‘cannibalize’ lysed cells, utilizing the debris as nutrients, and *Pseudomonas aeruginosa* produces extracellular DNases in order to utilize extracellular DNA from lysed cells as a nutrient source (34–36). Localized cell death has been shown to alter the structures of biofilms and extracellular DNA is an important structural component of biofilms (37–40).

Here, we establish that the T6SS is actively fired and able to kill susceptible competitors within a biofilm. This confers a competitive advantage during biofilm formation, allowing strains with an active T6SS to better maintain their foothold within the biofilm. However, additional consequences of T6SS killing in biofilms, such as DNA release or localized regions of cell death, still need to be assessed to better understand the contribution of the T6SS to biofilm development and structure.

ACKNOWLEDGEMENTS

We thank Benjamin Abrams from the UCSC Life Sciences Microscopy Center for his technical support.

References

1. **Nadell CD**, **Drescher K**, **Foster KR**. 2016. Spatial structure, cooperation and competition in biofilms. Nat. Rev. Microbiol. **14**:589–600.
2. **Flemming H-C**, **Wingender J**, **Szewzyk U**, **Steinberg P**, **Rice SA**, **Kjelleberg S**. 2016. Biofilms: an emergent form of bacterial life. Nat. Rev. Microbiol. **14**:563–575.
3. **Kerr B**, **Riley MA**, **Feldman MW**, **Bohannan BJM**. 2002. Local dispersal promotes biodiversity in a real-life game of rock–paper–scissors. Nature **418**:171–174.
4. **Bucci V**, **Nadell CD**, **Xavier JB**. 2011. The evolution of bacteriocin production in bacterial biofilms. Am. Nat. **178**:E162-73.
5. **Schwarz S**, **West TE**, **Boyer F**, **Chiang W-C**, **Carl MA**, **Hood RD**, **Rohmer L**, **Tolker-Nielsen T**, **Skerrett SJ**, **Mougous JD**. 2010. *Burkholderia* Type VI secretion systems have distinct roles in eukaryotic and bacterial cell interactions. PLoS Pathog. **6**:e1001068.
6. **Wexler AG**, **Bao Y**, **Whitney JC**, **Bobay L-M**, **Xavier JB**, **Schofield WB**, **Barry NA**, **Russell AB**, **Tran BQ**, **Goo YA**, **Goodlett DR**, **Ochman H**, **Mougous JD**, **Goodman AL**. 2016. Human symbionts inject and neutralize antibacterial toxins to persist in the gut. Proc. Natl. Acad. Sci. U. S. A. **113**:3639–44.
7. **Cheng AT**, **Ottemann KM**, **Yildiz FH**. 2015. *Vibrio cholerae* response regulator VxrB controls colonization and regulates the Type VI Secretion System. PLoS Pathog. **11**:e1004933.

8. **Fu Y**, **Ho BT**, **Mekalanos JJ**. 2018. Tracking *Vibrio cholerae* cell-cell interactions during infection reveals bacterial population dynamics within intestinal microenvironments. Cell Host Microbe **23**:274-281.e2.

9. **Zhao W**, **Caro F**, **Robins W**, **Mekalanos JJ**. 2018. Antagonism toward the intestinal microbiota and its effect on *Vibrio cholerae* virulence. Science **359**:210–213.

10. **Logan SL**, **Thomas J**, **Yan J**, **Baker RP**, **Shields DS**, **Xavier JB**, **Hammer BK**, **Parthasarathy R**. 2018. The *Vibrio cholerae* type VI secretion system can modulate host intestinal mechanics to displace gut bacterial symbionts. Proc. Natl. Acad. Sci. U. S. A. **115**:E3779–E3787.

11. **Toska J**, **Ho BT**, **Mekalanos JJ**. 2018. Exopolysaccharide protects *Vibrio cholerae* from exogenous attacks by the type VI secretion system. Proc. Natl. Acad. Sci. U. S. A. **115**:7997–8002.

12. **Bayles KW**. 2007. The biological role of death and lysis in biofilm development. Nat. Rev. Microbiol. **5**:721–726.

13. **LeRoux M**, **Kirkpatrick RL**, **Montauti EI**, **Tran BQ**, **Peterson SB**, **Harding BN**, **Whitney JC**, **Russell AB**, **Traxler B**, **Goo YA**, **Goodlett DR**, **Wiggins PA**, **Mougous JD**. 2015. Kin cell lysis is a danger signal that activates antibacterial pathways of *Pseudomonas aeruginosa*. Elife **4**:e05701.

14. **Liu X**, **Beyhan S**, **Lim B**, **Linington RG**, **Yildiz FH**. 2010. Identification and characterization of a phosphodiesterase that inversely regulates motility and biofilm formation in *Vibrio cholerae*. J. Bacteriol. **192**:4541–52.

15. **Herrero M**, **de Lorenzo V**, **Timmis KN**. 1990. Transposon vectors containing non-antibiotic resistance selection markers for cloning and stable chromosomal insertion of foreign genes in gram-negative bacteria. J. Bacteriol. **172**:6557–67.

16. **de Lorenzo V**, **Timmis KN**. 1994. Analysis and construction of stable phenotypes in gram-negative bacteria with Tn5- and Tn10-derived minitransposons. Methods Enzymol. **235**:386–405.

17. **Yildiz FH**, **Schoolnik GK**. 1998. Role of *rpoS* in stress survival and virulence of *Vibrio cholerae*. J. Bacteriol. **180**:773–84.

18. **Bachmann V**, **Kostiuk B**, **Unterweger D**, **Diaz-Satizabal L**, **Ogg S**, **Pukatzki S**. 2015. Bile salts modulate the mucin-activated type VI secretion system of pandemic *Vibrio cholerae*. PLoS Negl. Trop. Dis. **9**:e0004031.

19. **Unterweger D**, **Miyata ST**, **Bachmann V**, **Brooks TM**, **Mullins T**, **Kostiuk B**, **Provenzano D**, **Pukatzki S**. 2014. The *Vibrio cholerae* type VI secretion system employs diverse effector modules for intraspecific competition. Nat. Commun. **5**:3549.

20. **Tam VC**, **Serruto D**, **Dziejman M**, **Brieher W**, **Mekalanos JJ**. 2007. A type III secretion system in *Vibrio cholerae* translocates a formin/spire hybrid-like actin nucleator to promote intestinal colonization. Cell Host Microbe **1**:95–107.

21. **Mougous JD**, **Cuff ME**, **Raunser S**, **Shen A**, **Zhou M**, **Gifford CA**, **Goodman AL**, **Joachimiak G**, **Ordoñez CL**, **Lory S**, **Walz T**, **Joachimiak**

A, **Mekalanos JJ**. 2006. A virulence locus of *Pseudomonas aeruginosa* encodes a protein secretion apparatus. Science **312**:1526–30.

22. **Silverman JM**, **Austin LS**, **Hsu F**, **Hicks KG**, **Hood RD**, **Mougous JD**. 2011. Separate inputs modulate phosphorylation-dependent and -independent type VI secretion activation. Mol. Microbiol. **82**:1277–90.
23. **Casper-Lindley C**, **Yildiz FH**. 2004. VpsT Is a transcriptional regulator required for expression of *vps* biosynthesis genes and the development of rugose colonial morphology in *Vibrio cholerae* O1 El Tor. J. Bacteriol. **186**:1574–1578.
24. **Bao Y**, **Lies DP**, **Fu H**, **Roberts GP**. 1991. An improved Tn7-based system for the single-copy insertion of cloned genes into chromosomes of gram-negative bacteria. Gene **109**:167–8.
25. **Miyata ST**, **Unterweger D**, **Rudko SP**, **Pukatzki S**. 2013. Dual expression profile of type VI secretion system immunity genes protects pandemic *Vibrio cholerae*. PLoS Pathog. **9**:e1003752.
26. **Ishikawa T**, **Sabharwal D**, **Bröms J**, **Milton DL**, **Sjöstedt A**, **Uhlin BE**, **Wai SN**. 2012. Pathoadaptive conditional regulation of the type VI secretion system in *Vibrio cholerae* O1 strains. Infect. Immun. **80**:575–84.
27. **Gallego-Hernandez, A.L.**, **DePas WH**, **J.H. P**, **Teschler JK**, **Hartmann R**, **Jeckel H**, **Drescher K**, **Beyhan S**, **Newman DK**, **Yildiz FH**. 2019. Mechanism of *Vibrio cholerae* biofilm hyperinfectivity. Prep.
28. **Tak A**, **Cheng T**. 2015. Systematic analysis of two-component signal transduction systems in *Vibrio cholerae* biofilm formation and virulence. A

dissertation submitted in partial satisfaction of the requirements for the degree of Doctor of Philosophy in Microbiology and Environmental Toxicology.

29. **Ishikawa T**, **Rompikuntal PK**, **Lindmark B**, **Milton DL**, **Wai SN**. 2009. Quorum sensing regulation of the two *hcp* alleles in *Vibrio cholerae* O1 strains. PLoS One **4**:e6734.

30. **Unterweger D**, **Kitaoka M**, **Miyata ST**, **Bachmann V**, **Brooks TM**, **Moloney J**, **Sosa O**, **Silva D**, **Duran-Gonzalez J**, **Provenzano D**, **Pukatzki S**. 2012. Constitutive type VI secretion system expression gives *Vibrio cholerae* intra- and interspecific competitive advantages. PLoS One **7**:e48320.

31. **Teschler JK**, **Cheng AT**, **Yildiz FH**. 2017. The two-component signal transduction system VxrAB positively regulates *Vibrio cholerae* biofilm formation. J. Bacteriol. **199**:e00139-17.

32. **Dong TG**, **Ho BT**, **Yoder-Himes DR**, **Mekalanos JJ**. 2013. Identification of T6SS-dependent effector and immunity proteins by Tn-seq in *Vibrio cholerae*. Proc. Natl. Acad. Sci. U. S. A. **110**:2623–8.

33. **Brooks TM**, **Unterweger D**, **Bachmann V**, **Kostiuk B**, **Pukatzki S**. 2013. Lytic activity of the *Vibrio cholerae* type VI secretion toxin VgrG-3 is inhibited by the antitoxin TsaB. J. Biol. Chem. **288**:7618–25.

34. **López D**, **Vlamakis H**, **Losick R**, **Kolter R**. 2009. Cannibalism enhances biofilm development in *Bacillus subtilis*. Mol. Microbiol. **74**:609–618.

35. **Mulcahy H**, **Charron-Mazenod L**, **Lewenza S**. 2010. *Pseudomonas*

aeruginosa produces an extracellular deoxyribonuclease that is required for utilization of DNA as a nutrient source. Environ. Microbiol. **12**:1621–9.

36. **Webb JS**, **Thompson LS**, **James S**, **Charlton T**, **Tolker-Nielsen T**, **Koch B**, **Givskov M**, **Kjelleberg S**. 2003. Cell death in *Pseudomonas aeruginosa* biofilm development. J. Bacteriol. **185**:4585–92.

37. **Asally M**, **Kittisopikul M**, **Rué P**, **Du Y**, **Hu Z**, **Çağatay T**, **Robinson AB**, **Lu H**, **Garcia-Ojalvo J**, **Süel GM**. 2012. Localized cell death focuses mechanical forces during 3D patterning in a biofilm. Proc. Natl. Acad. Sci. U. S. A. **109**:18891–6.

38. **Novotny LA**, **Amer AO**, **Brockson ME**, **Goodman SD**, **Bakaletz LO**. 2013. Structural stability of *Burkholderia cenocepacia* biofilms is reliant on eDNA structure and presence of a bacterial nucleic acid binding protein. PLoS One **8**:e67629.

39. **Gloag ES**, **Turnbull L**, **Huang A**, **Vallotton P**, **Wang H**, **Nolan LM**, **Mililli L**, **Hunt C**, **Lu J**, **Osvath SR**, **Monahan LG**, **Cavaliere R**, **Charles IG**, **Wand MP**, **Gee ML**, **Prabhakar R**, **Whitchurch CB**. 2013. Self-organization of bacterial biofilms is facilitated by extracellular DNA. Proc. Natl. Acad. Sci. U. S. A. **110**:11541–6.

40. **Seper A**, **Fengler VHI**, **Roier S**, **Wolinski H**, **Kohlwein SD**, **Bishop AL**, **Camilli A**, **Reidl J**, **Schild S**. 2011. Extracellular nucleases and extracellular DNA play important roles in *Vibrio cholerae* biofilm formation. Mol. Microbiol. **82**:1015–37.

CHAPTER 4: Contribution of the VxrB regulon members to virulence and cell wall homoeostasis

Jennifer K. Teschler and Fitnat H. Yildiz

Abstract

Two-component signal transduction systems (TCSs) play an important role in the ability of pathogenic bacteria to sense fluctuating environmental conditions and elicit the appropriate biological responses. The facultative human pathogen *Vibrio cholerae* utilizes TCSs to sense and activate responses to the variety of environmental factors inside and outside of the host. The *V. cholerae* TCS VxrAB was recently characterized to be a positive regulator of virulence, the Type Six Secretion System, and cell wall homeostasis. The mechanisms by which this TCS regulates this array of cellular responses are still being deciphered, however, RNA-seq data revealed that a number of genes regulated by VxrB are annotated as hypothetical. We thus investigated the contribution of the top VxrB-regulated genes of unknown function to virulence, the T6SS, and cell wall homoeostasis, identifying new players involved in these important *V. cholerae* phenotypes. Bioinformatics analyses, homology searches, and structural modeling provided insights into the function of these genes, as did the use of phenotypic microarrays. Our analysis identified two new operons with roles in virulence and one operon that plays a role in cell wall homeostasis. TCSs are important systems that allow bacteria to sense and respond to their environment and our further characterization of VxrAB provides additional insight into our understanding of TCSs and the function of hypothetical proteins.

Introduction

Bacteria frequently alter their physiology in response to fluctuating environmental conditions, including changes in temperature, pH, host defenses, osmolarity, nutrient availability, and antimicrobials (1–5). The cell envelope of gram-negative bacteria, comprised of a cytoplasmic membrane, a thin layer of peptidoglycan, and an outer membrane, acts as a protective barrier for the cell and is the first line of defense against environmental stress. The cell envelope must be maintained, repaired, and modified in response to perturbations and damage caused by environmental stressors (6).

Two component signal transduction systems (TCSs) are one way that bacteria can sense and respond to environmental assaults, allowing for cellular adaptation and envelope remodeling to better withstand threats to cell viability (2, 3, 7). TCSs systems are composed of a sensor histidine kinase (HK), responsible for recognizing a cognate signal, and a response regulator (RR), which is activated by the HK in the presence of the cognate signal (2). *Vibrio cholerae*, the causative agent of the disease cholera, is an important environmental pathogen. During its life cycle in the aquatic environment and human host *V. cholerae* must sense and respond to a number of shifting extracellular signals and encodes for a high number of TCSs that contribute to its ability to adapt and survive its ever-changing milieu.

In *V. cholerae,* several TCS have been shown to be activated in response to extracytoplasmic stress, including CarRS, CpxAR, and VC1638-39 (4, 8–11). CarRS responds to extracellular calcium levels, antimicrobial peptides, bile, and low pH. When activated, it stimulates lipid A modification, leading to increased resistance to the cationic antimicrobial peptide, Polymyxin B. The CarRS system also represses biofilm formation and enhances colonization (4, 12, 13). The CpxAR TCS has been shown to respond to envelope stress cues, including extracellular iron chelation, chloride ions, toxic compounds, and altered or interrupted Resistance-nodulation-division (RND) mediated efflux (9, 14–16). CpxAR activates a number membrane localized and transport proteins, as well as iron-regulated proteins, and enhances antibiotic resistance and represses virulence (8–10, 17). VC1638-39 responds to Polymyxin B to activate expression of the Stress-inducible protein A (SipA/VCA0732), which binds antimicrobial peptides and provides enhanced protection to antimicrobial peptides in the *V. cholerae* O1 classical strain (11, 18).

Recently, the VxrAB (also called WigKR) TCS was shown to respond to extracellular stressors such as beta lactam antibiotics (19). Though the exact signal that activates the VxrAB TCS is still unknown, its *V. parahaemolyticus* homolog, VbrKR, was shown to directly sense β-lactams to enhance β-lactamase production (20). VxrAB, positively regulates virulence, the Type Six Secretion System (T6SS), biofilm formation, and cell wall homeostasis (19, 21, 22).

While some members of the VxrB regulon have been identified that contribute to these phenotypes, a large number of the genes regulated by VxrB are predicted to encode for hypothetical proteins and their role in creating the VxrB response is unknown. Characterizing the function of hypothetical genes can enhance our understanding of *V. cholerae* biology but doing so can be extremely challenging. The published N16961 annotation predicts that 42% and 59% of genes on the large and small chromosomes respectively are hypothetical, indicating that there is a large portion of the *V. cholerae* genome that remains poorly understood (23). Since the key phenotypes governed by the TCS VxrAB have been identified, we chose to investigate the contribution of the top VxrB-regulated genes of unknown function to virulence, the T6SS, and cell wall homoeostasis.

Notably, we identified two operons that contribute to virulence, both of which encode for components that localize to the cell envelope, and another operon that encodes for a membrane phospholipid trafficking system and contributes to β-lactam resistance. These findings support a model in which VxrAB is able to respond to cell envelope stress and activate components in the cell envelope that contribute to VxrB-mediated phenotypes, including enhanced survival in the human host and in the presence of environmental insults such as antibiotic treatment.

Methods

Ethics statement

All animal procedures used were in strict accordance with the NIH *Guide for the Care and Use of Laboratory Animals* and were approved by the UC Santa Cruz Institutional Animal Care and Use Committee (Yildf1806).

Strains and growth conditions. Strains used in this study are listed in Table 4.1. *V. cholerae* and *Escherichia coli* strains were grown aerobically in Luria-Bertani (LB) broth (1% tryptone, 0.5% Yeast Extract, 1% NaCl), pH 7.5, at 30°C and 37°C, respectively. LB agar contained granulated agar (Difco) at 1.5% (w/v). Media additives were used when necessary at the following concentrations: rifampicin (100 µg/mL), ampicillin (100 µg/mL), and chloramphenicol (20 µg/mL for *E. coli* and 5 µg/mL or 2.5 µg/mL for *V. cholerae*).

Strain and plasmid construction. Plasmids were constructed using standard cloning methods or the Gibson Assembly recombinant DNA technique (New England Biolabs, Ipswich, MA). Gene deletions were carried out using allelic exchange of the native ORF with the truncated ORF, as previously described, or via the previously described TransFLP method (24–26). Complementation of Δ*vxrB* was carried out using a Tn7-based system, as previously described (21). Briefly, triparental matings with donor *E. coli* S17λpir carrying pGP704-Tn7 with gene of interest, helper *E. coli* S17λpir harboring pUX-BF13, and *V. cholerae* deletion strains were carried out by mixing all three strains, and incubating mating

mixtures on LB agar plates for 18 hours at 30°C. Transconjugants were selected on thiosulfate-citrate-bile salts-sucrose (TCBS) (BD Difco, Franklin Lakes, NJ) agar medium containing gentamicin 15µg/mL) at 30°C. Insertion of the complementation construct to the Tn7 site was verified by PCR. *V. cholerae* wild-type and mutant strains were tagged with the green fluorescent protein gene *(gfp*) according to a previously described procedure (27). The *gfp* tagged *V. cholerae* strains were verified by PCR and used in biofilm analysis. Transcriptional fusions were constructed by cloning the upstream regulatory regions of selected genes into the pBBR-*lux* plasmid, as previously described (28).

Intestinal colonization assay. An *in vivo* competition assay for intestinal colonization was performed as described previously (29). Briefly, each of the *V. cholerae* mutant strains (*lacZ*$^{+}$) and the fully virulent reference strain (*lacZ*$^{-}$ otherwise wild-type)) were grown to stationary phase at 30°C with aeration in LB broth. Mutant strains and wild-type were mixed at 1:1 ratios in 1x Phosphate Buffered Saline (PBS). The inoculum was plated on LB agar plates containing 5-bromo-4-chloro-3-indoyl-β-D-galactopyranoside (X-gal) to differentiate wild-type and mutant colonies and to determine the input ratios. Approximately, 10^{6}–10^{7} cfu were intragastrically administered to groups of 5–7 anesthetized 5-day old CD-1 mice (Charles River Laboratories, Hollister, CA). After 20 hours of incubation, the small intestine was removed, weighed, homogenized, and plated on appropriate selective and differential media to enumerate mutant and wild-type cells recovered and to obtain the output ratios. *In vivo* competitive indices were calculated by

dividing the small intestine output ratio by the inoculum input ratio of mutant to wild-type strains. Statistical analyses were performed using Prism 8 software (GraphPad Software, Inc., San Diego, CA) using a one-way analysis of variance (ANOVA) and Dunnett's multiple-comparison test. P values of <0.05 were determined to be statistically significant.

Luminescence assays. Overnight cultures *of V. cholerae* cells were diluted 1:500 in appropriate medium containing chloramphenicol (5 µg/ml). Cells were then grown aerobically at 30°C to OD_{600} of 0.3-0.4 and then luminescence of cells was measured using a Perkin Elmer Victor3 Multi-label Counter (PerkinElmer, Waltham, MA). Lux expression is reported as counts min^{-1} ml^{-1}/OD_{600}, shown as relative light units (RLU). Assays were repeated with three biological replicates. Three technical replicates were measured for all assays. Statistical analyses were performed using Prism 8 software (GraphPad Software, Inc., San Diego, CA) using two-tailed Student's t tests. P values of <0.05 were determined to be statistically significant.

Pencillin G resistance assays. Cells were grown with shaking at 30°C to exponential phase in 10 mL LB broth in 50-mL flasks, followed by addition of antibiotic. At designated time points, cfu/mL were enumerated by serial dilution and spot-plating. Statistical analyses were performed using Prism 8 software (GraphPad Software, Inc., San Diego, CA) using a one-way analysis of variance

(ANOVA) and Dunnett's multiple-comparison test. P values of <0.05 were determined to be statistically significant.

T6SS killing assays. Killing assays were performed as described previously (30). Briefly, bacterial strains were grown overnight on LB plates and resuspended in LB broth containing 340 mM NaCl, as *V*. *cholerae* strain A1552 displayed enhanced interbacterial virulence towards *E*. *coli* under high osmolarity (31). *V*. *cholerae* and *E*. *coli* MC4100 were mixed at a 10:1 ratio and 25 µl was spotted onto LB agar plates containing 340 mM NaCl and incubated at 37°C for 4 hours. Spots were harvested, serially diluted, and plated onto LB plates containing 50 µg/ml of streptomycin to enumerate surviving *E*. *coli* prey cells. Statistical analyses were performed using Prism 8 software (GraphPad Software, Inc., San Diego, CA) using a one-way analysis of variance (ANOVA) and Dunnett's multiple-comparison test. P values of <0.05 were determined to be statistically significant.

Biolog plate assays. BIOLOG-GN MicroPlates (BIOLOG) were used to evaluate substrate utilization patterns of VC1162-60 deletion mutant and wild type strains. The cells were streaked on LB and incubated for 16 h at 30°C. Wells of a plate were inoculated with 150 ul of bacterial suspensions adjusted to the appropriate density in PBS. The inoculated microplates were incubated at 30°C for 48 h and analyzed using a BIOLOG Microstation reader. Statistical analyses were performed using Prism 8 software (GraphPad Software, Inc., San Diego, CA) using a multiple t tests to create a volcano plot. Each dot represents three replicates of

one growth condition (one well in the PM plate). The X axis plots the difference between means and the dotted grid line is shown at X=0, no difference. The Y value is minus one times the logarithm of the P value. A dotted grid line is shown where the P value is 0.01, so the logarithm (base 10) is -2, and the value plotted on the Y axis is 2.0.

Table 4.1. Bacterial strains and plasmids used in this study.

Strain or plasmid	Relevant genotype	Source
E. coli strains		
CC118λ*pir*	Δ(*ara-leu*) *araD* Δ*lacX74 galE galK phoA20 thi-1 rpsE rpoB argE*(*Am*) *recA1* λ*pir*	(32)
S17-1λ*pir*	Tp^r Sm^r *recA thi pro* r_K^- m_K^+ RP4::2-Tc::MuKm Tn*7* λ*pir*	(33)
V. cholerae strains		
FY_VC_0001	*Vibrio cholerae* O1 El Tor A1552, wild type, Rif^r	(34)
FY_VC_8758	ΔVCA0566 (*vxrB*)	(21)
FY_VC_9469	Δ*vxrB*-Tn7::*vxrB*	(21)
FY_VC_12436	ΔVC2662	This study
FY_VC_9874	ΔVC0483	This study (21)(21)(21)(20)(20)
FY_VC_11363	ΔVC1160	This study
FY_VC_11353	ΔVC1161	This study
FY_VC_11383	ΔVC1162	This study
FY_VC_11409	ΔVC1162-60	This study
FY_VC_12435	ΔVC1162-60-Tn7::VC1162-60	This study
FY_VC_12621	ΔVCA0271	This study (21)(21)(21)(20)(20)
FY_VC_15029	ΔVCA0484	This study
FY_VC_11379	ΔVCA0026	This study
FY_VC_15030	ΔVC2612	This study
FY_VC_15031	ΔVCA0845	This study
FY_VC_15032	ΔVC2518	This study
FY_VC_15033	ΔVC2518-Tn7::pTAC-VC2520-16	This study
FY_VC_15034	ΔVCA0846	This study
FY_VC_15035	ΔVCA0365	This study
FY_VC_15036	ΔVC2076	This study
FY_VC_15037	ΔVCA0426	This study
FY_VC_15038	ΔVC2548	This study
FY_VC_15039	ΔVC2548-Tn7::VC2548	This study
FY_VC_15040	ΔVC2547	This study
FY_VC_15041	ΔVC2547-Tn7::VC2547	This study
FY_VC_15042	ΔVC1207	This study
FY_VC_12625	ΔVC2516	This study
FY_VC_15043	ΔVC2516-Tn7::pTAC-VC2520-16	This study
FY_VC_14449	ΔVC2517	This study
FY_VC_15044	ΔVC2517-Tn7::pTAC-VC2520-16	This study
FY_VC_15045	WT pBBR-VC1162-60-lux	This study
FY_VC_15046	Δ*vxrB* pBBR-VC1162-60-lux	This study
FY_VC_15047	WT pBBR-VC2548-47-lux	This study
FY_VC_15048	Δ*vxrB* pBBR-VC2548-47-lux	This study
FY_VC_15049	WT pBBR-VC2520-16-lux	This study

FY_VC_15050	Δ*vxrB* pBBR-VC2520-16-lux	This study
FY_VC_9569	ΔVC1415ΔVCA0017 (Δ*hcp1*Δ*hcp2*)	(21)
Plasmids		
pGP704*sacB*28	pGP704 derivative, *mob*/*oriT sacB*, Ap^r	(35)
pUX-BF13	oriR6K helper plasmid, mob/oriT, provides the Tn7 transposition function in trans, Ap^r	(36)
pMCM11	pGP704::mTn*7*-*gfp*, Gm^r Ap^r	M. Miller and G. Schoolnik
pFY-4835	pGP704::mTn*7*-VC1162-60	This study
pFY-6104	pGP704::mTn*7*-VC2548	This study
pFY-6105	pGP704::mTn*7*-VC2547	This study
pFY-6101	pGP704::mTn*7*-pTAC-VC2520-16	This study
pBBR*lux*	*luxCDABE*-based promoter fusion vector, Cm^r	(37)
pFY-6106	pBBR*lux* VC1162-60 promoter, Cm^r	This study
pFY-6107	pBBR*lux* VC2548-47 promoter, Cm^r	This study
pFY-6108	pBBR*lux* VC2520-16 promoter, Cm^r	This study

Results

VxrB regulates a number of hypothetical genes. In our previous work, RNA-seq analysis was used to identify genes regulated by VxrB under virulence inducing conditions (AKI) and LB growth conditions (21, 38). We reanalyzed these results and found that a number of genes regulated by VxrB under both AKI and LB growth conditions are predicted to be hypothetical. (Figure 4.1, Table 4.2).

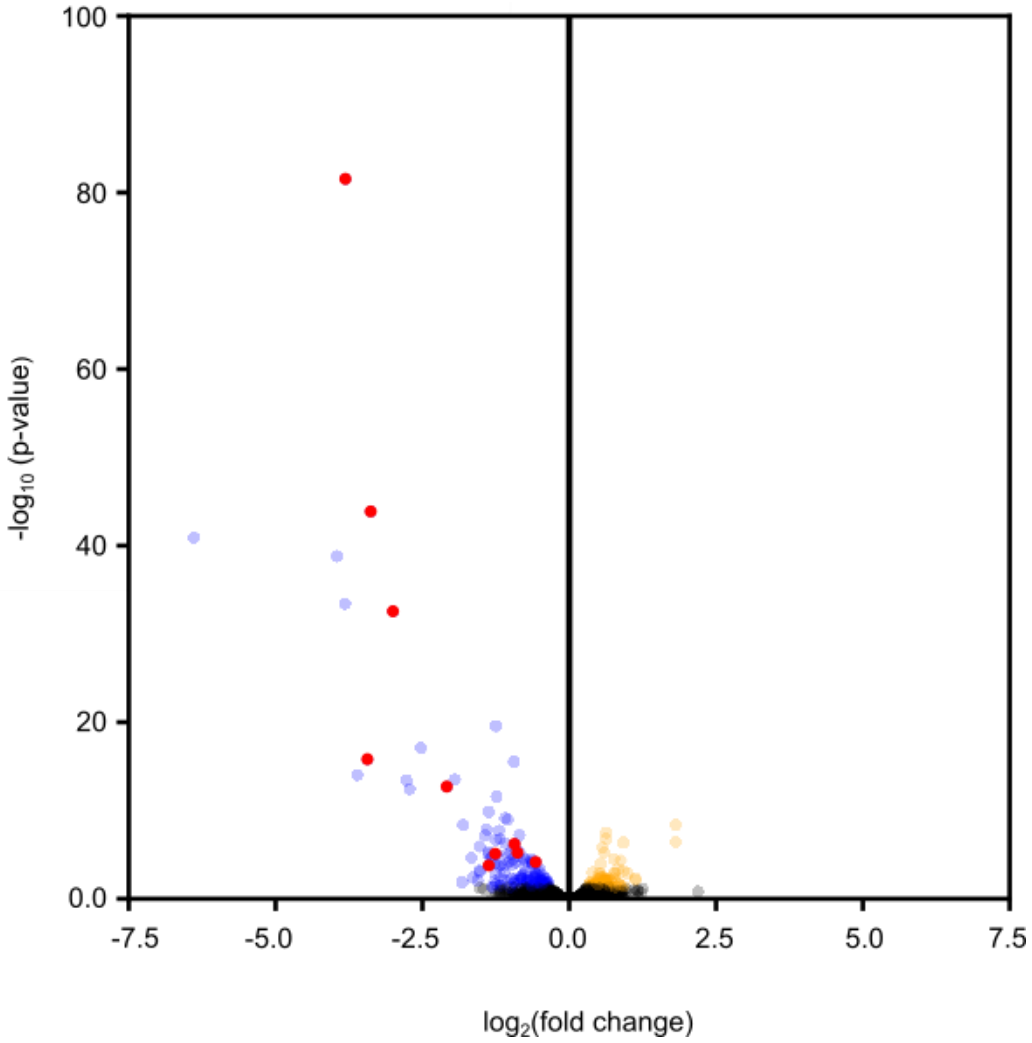

Figure 4.1. Volcano plot of total genes found to be differentially regulated under LB growth conditions in the Δ*vxrB* mutant relative to wild type. Blue dots show genes significantly downregulated in the mutant, orange dots show genes significantly upregulated in the mutant, and red dots highlight the hypothetical genes analyzed in this study.

Table 4.2. Hypothetical genes differentially regulated under AKI and LB growth conditions in the Δ*vxrB* mutant relative to wild type.

Gene	AKI	LB
VC2662 conserved hypothetical protein	-6.69	-12.5
VC0483 conserved hypothetical protein	-3.83	-3.46
VC1160 hypothetical protein	-3.26	-9.29
VCA0271 hypothetical protein	-3.19	-2.74
VCA0484 hypothetical protein	-3.18	--
VCA0026 conserved hypothetical protein	-2.73	-2.27
VC2612 conserved hypothetical protein	-2.31	--
VC1162 hypothetical protein	-2.34	-8.27
VC1161 gonadoliberin III-related protein	-2.28	-7.09
VCA0845 hypothetical protein	-2.24	-2.13
VC2518 conserved hypothetical protein	-2.17	--
VCA0846 conserved hypothetical protein	-2.16	--
VCA0365 hypothetical protein	-2.14	--
VC2076 hypothetical protein	-1.81	--
VCA0426 conserved hypothetical protein	-1.76	+1.69
VC2548 conserved hypothetical protein	-1.75	-2.07
VC2547 conserved hypothetical protein	-1.73	-1.53
VC1207 hypothetical protein	-1.63	-1.56
VC2516 anti-sigma B factor antagonist, putative	-1.62	--
VC2517 conserved hypothetical protein	-1.62	--

Fold change in mutant compared to WT.
Cutoff values: 1.5-fold difference in gene expression, 1% false-discovery rate (FDR), p-value<0.0001.

Two operons regulated by VxrB encode for hypothetical genes that contribute to *V. cholerae* virulence. To better understand how hypothetical genes regulated by VxrB contribute to virulence, we generated in-frame deletions of the 20 genes of unknown function that are most highly regulated by VxrB (Table 4.2). We then performed intestinal colonization experiments in a 5-day-old infant mouse model to determine the contribution of these genes to virulence. We identified two operons that positively contribute to virulence, VC1160-62 and VC2547-48 (Figure 4.2A-B). The virulence phenotypes of these genes could be complemented, as shown in Figure 4.2B. Using structural and localization analyses we found that VC1160-62 may encode for a potential protein modification system, as VC1160 encodes a predicted peptide ligase, VC1161 encodes for an inner membrane bound 7 transmembrane (7-TM) protein containing a potential ligand binding site, and VC1162 encodes for a predicted aspartic peptidase. Our analyses additionally showed that VC2547-48 encodes for the TamAB transport system. These operons represent previously unidentified virulence factors.

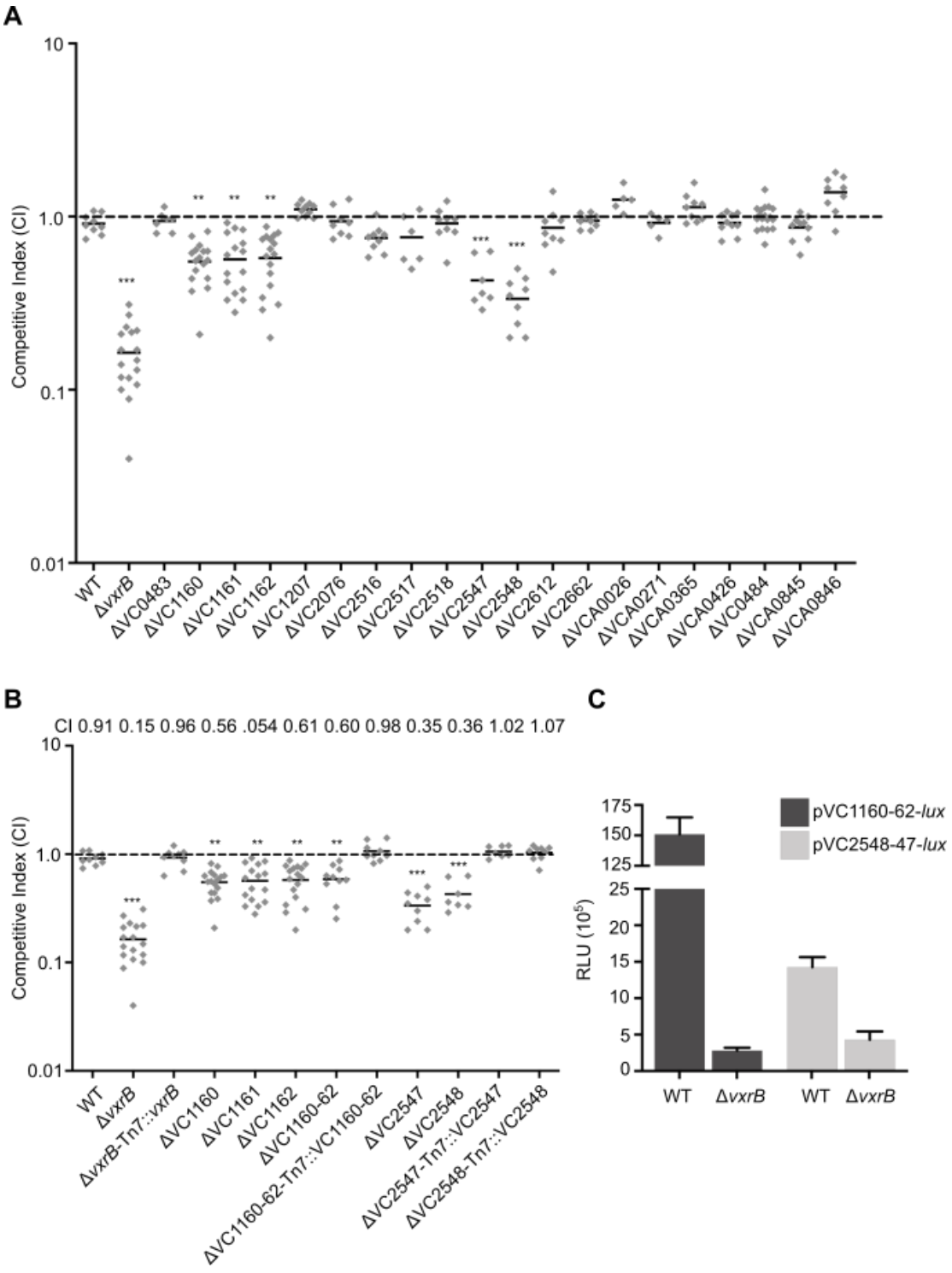

Figure 4.2 Identification of VxrB-regulated hypothetical genes impacting colonization in the infant mouse infection model.

A) 20 hypothetical genes were analyzed for their role in intestinal colonization. Data were analyzed using a one-way analysis of variance (ANOVA) and Dunnett's multiple-comparison test. ***, $P < 0.0001$, **, $P < 0.0005$. B) 5 genes organized into 2 operons were shown to impact intestinal colonization and this defect could be complemented. Data were analyzed using a one-way analysis of variance (ANOVA) and Dunnett's multiple-comparison test. ***, $P < 0.0001$, **, $P < 0.0005$. C) Expression of VC1160-62 and VC2548 in the Δ*vxrB* mutant relative to wild type. The graph represents the averages and standard deviations of RLU obtained from three technical replicates from three biological replicates. RLU are reported in luminescence counts $\cdot$ min^{-1} $\cdot$ ml^{-1} $\cdot$ $OD_{600}{}^{-1}$. Data were analyzed using two-tailed Student's t tests. ***, $P < 0.0001$.

VxrB-regulated hypothetical genes do not contribute to T6SS killing. Given that our previous work demonstrated that VxrB's regulation of the T6SS contributes to its virulence phenotype, we next wanted to determine if any of the hypothetical genes could contribute to virulence via the T6SS or might be uncharacterized components of this system. Our analysis determined that the hypothetical genes analyzed do not contributed to T6SS killing (Figure 4.3).

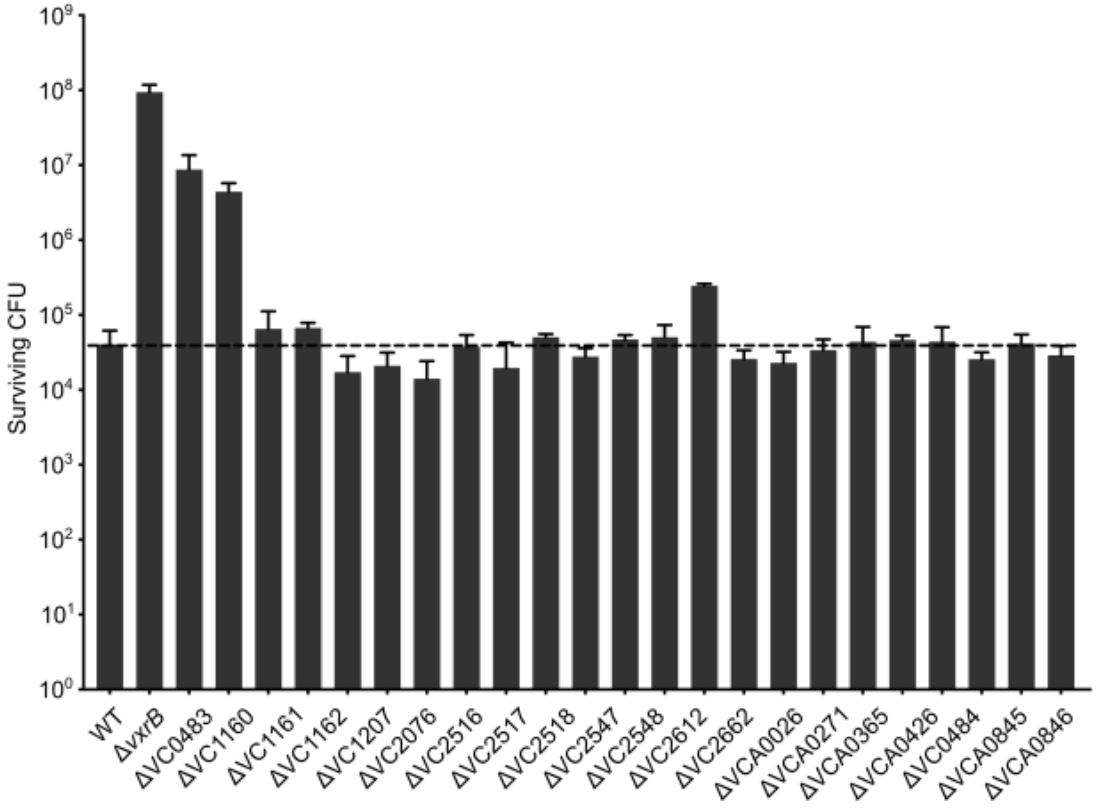

Figure 4.3 Analysis of T6SS-killing in hypothetical genes deletions.

Interbacterial killing was analyzed by mixing *V. cholerae* strains and prey *E. coli* strain MC4100 in a 10:1 ratio, followed by incubation on LB agar plates for 4 hours at 30°C and determination of surviving *E. coli* MC4100.

One operon regulated by VxrB encodes for hypothetical genes that contribute to *V. cholerae* cell wall homeostasis We next performed cell wall homeostasis assays using β-lactam stress survival assays, given that VxrB has a known defect in β-lactam stress survival. We identified 3 genes annotated as hypothetical encoded in an operon that contributed to β-lactam survival, VC2516-18 (Figure 4.4). Using structural predictions and domain analysis we identified these genes as encoding for components of the *mla* pathway, a six-component system that mediates retrograde transport of misplaced phospholipids from the outer leaflet of the OM to the cytoplasmic membrane (39). VC2516 encodes for *mlaB*, a predicted NTP binding protein with a STAS domain. VC2517 encodes for *mlaC*, a phospholipid-binding protein. VC2518 encodes for *mlaD*, a phospholipid abc transporter-binding protein (39). We hypothesize that the deletion of these genes decreased the effectiveness of the *mla* system and increased cell membrane permeability to β-lactam, thus contributing to the cell wall homeostasis phenotype we observed.

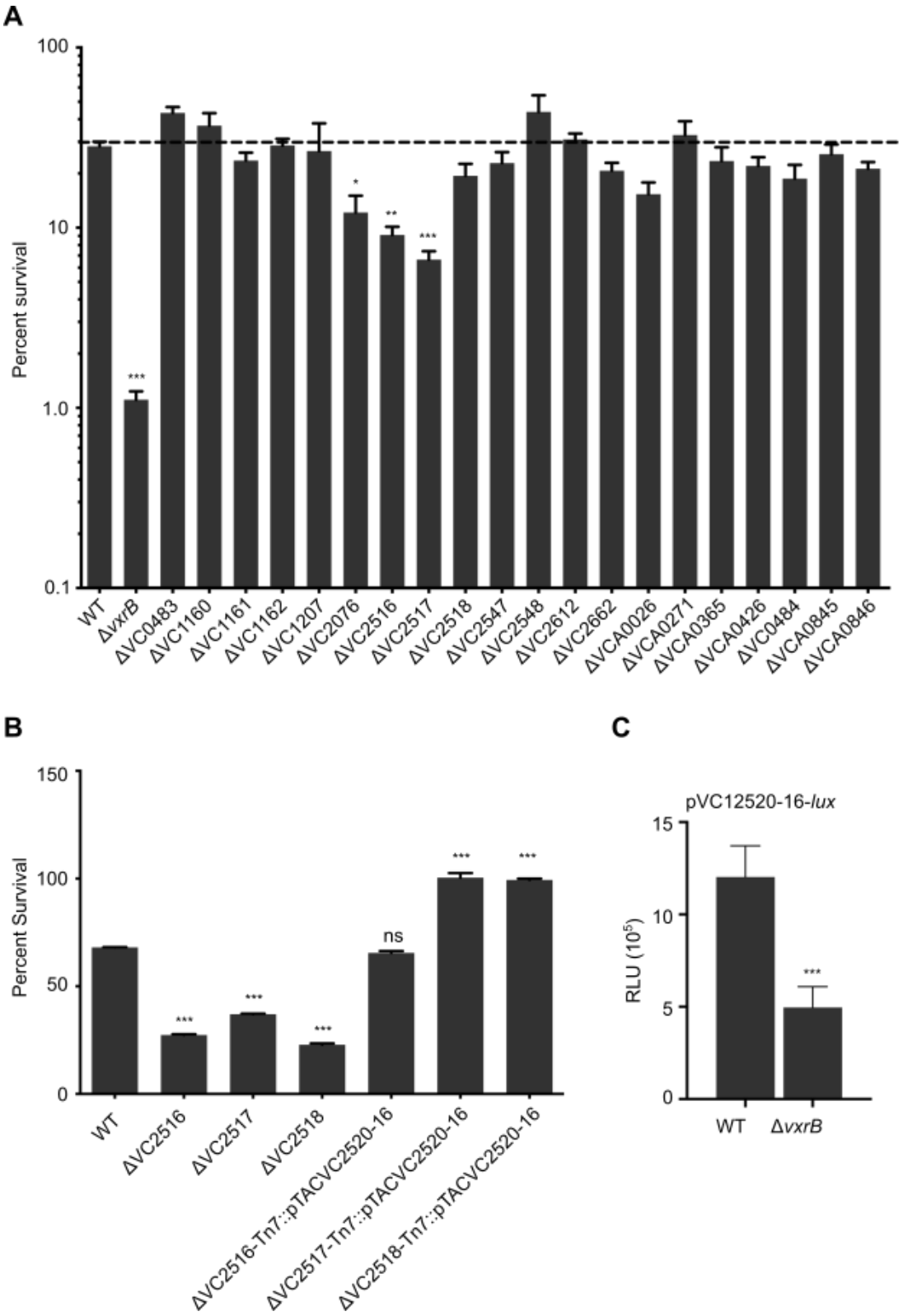

Figure 4.4. Identification of VxrB-regulated hypothetical genes impacting Pencillin G survival.

A) 20 hypothetical genes were analyzed for their role in surviving β-lactam stress. Data were analyzed using a one-way analysis of variance (ANOVA) and Dunnett's multiple-comparison test. ***, $P < 0.0001$, **, $P < 0.0005$, *, $P<0.001$. B) 3 genes organized into 1 operon were shown to impact β-lactam stress survival. Data were analyzed using a one-way analysis of variance (ANOVA) and Dunnett's multiple-comparison test. ***, $P < 0.0001$, **, $P < 0.0005$, *, $P<0.001$. C) Expression of VC2520-16 in the Δ*vxrB* mutant relative to wild type. Cultures of wild-type and Δ*vxrB* strains containing PVC2520-16-lux were grown to exponential phase (OD_{600} of~0.3) and luminescence was measured. The graph represents the averages and standard deviations of RLU obtained from three technical replicates from three biological replicates. RLU are reported in luminescence counts $\cdot$ min^{-1} $\cdot$ ml^{-1} $\cdot$ OD_{600}^{-1}. Data were analyzed using two-tailed Student's t tests. ***, $P < 0.0001$.

Phenotypic microarrays demonstrate altered stress responses of *vxrB* and VC1160-62 operon mutants. Bioinformatic analysis of VC2547-48 and VC2516-18 revealed that these genes encode for a transport system and phospholipid trafficking system, respectively, and have been characterized in other species. However, though the VC1160-62 genes are also highly conserved in other species, their function has not yet been characterized. Therefore, we sought to further understand the function of this system using a phenotypic microarray.

We analyzed growth of the VC1160-62 mutant, the *vxrB* mutant, and the wild-type strain on various carbon and nitrogen sources, and in the presence of several stressors, including osmolytes, pH, and antibiotics. Growth was measured using the Biolog system, which utilizes 96 well plates containing different classes of chemical compounds. A tetrazolium dye is used to measure active respiration, as actively respiring cells will reduce the dye and form a strong color. This analysis allows for a large-scale screening of specific cellular phenotypes in the presence of these compounds. We selected 9 phenotypic microarray plates (PM) for analysis, however, we did not observe any differences in growth on various carbon and nitrogen plates. Several conditions in the stressor plates yielded differences in growth (Figure 4.5A-F). For the VC1160-62 mutant, it showed enhanced growth on 5% urea and decreased growth on 3% sodium lactate on PM Plate 9 (osmolytes), as well as decreased growth on pH 4.5 + D-lysine, pH 4.5 +5-hydroxy-L-lysine, pH 9.5 + Agmatine on PM plate 10 (pH) (Fig. 4.5 B and C). The *vxrB* mutant showed decreased growth on 6% Potassium chloride, 6% sodium chloride

+ trigonelline, and 7% sodium chloride on PM Plate 9 (osmolytes) and decreased growth on pH 9.5 + cadaverine, pH 4.5 + D-lysine, and pH 4.5 +L-cysteic acid on PM plate 10 (pH) (Fig. 4.5A and C). These results were reproducible for three replicates under the PM conditions tested and indicate that VxrB and VC1160-62 may play a role in mediated *V. cholerae* response and growth under various stressors, including osmotic and pH stress.

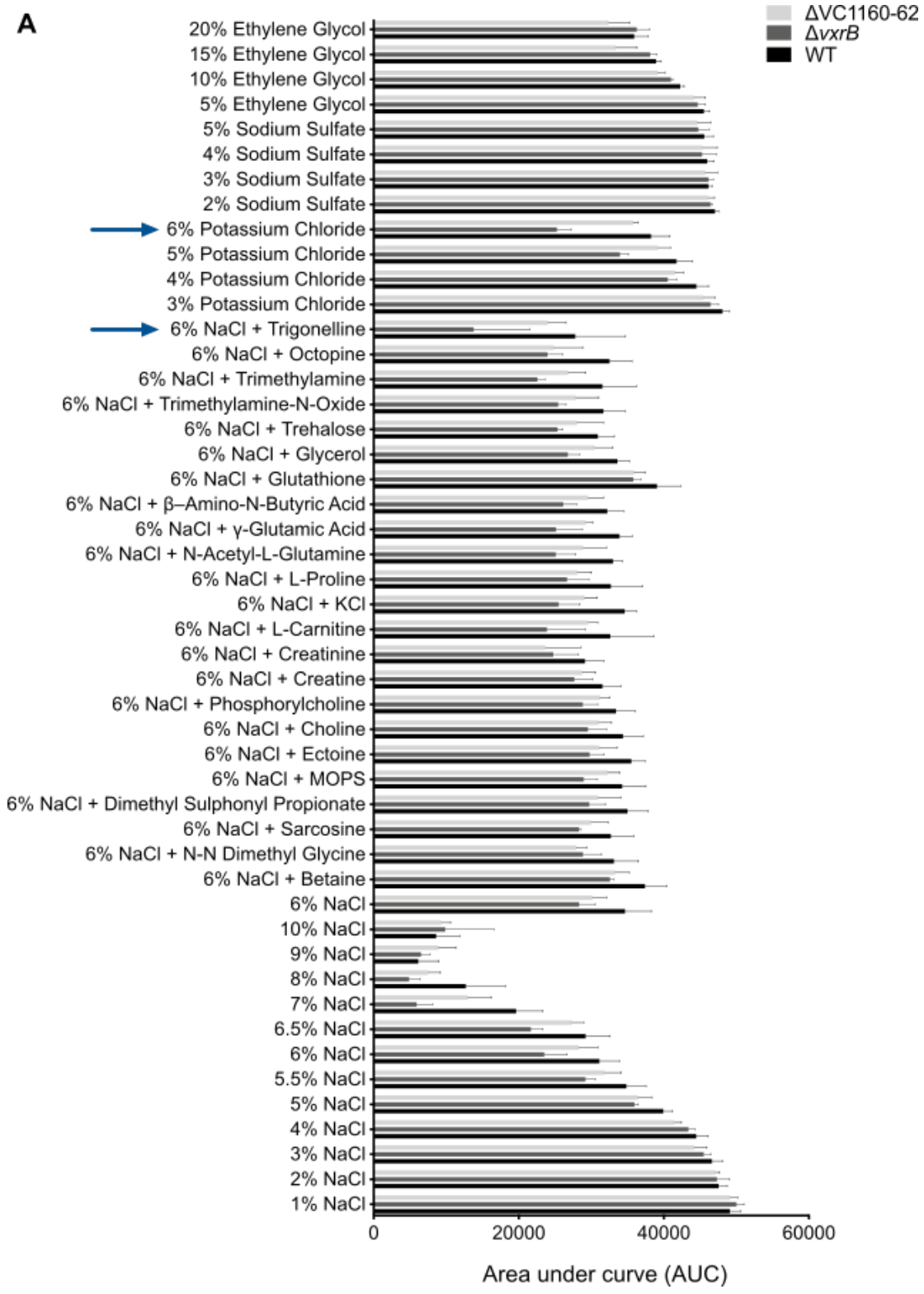
A
ΔVC1160-62
ΔvxrB
WT
20% Ethylene Glycol
15% Ethylene Glycol
10% Ethylene Glycol
5% Ethylene Glycol
5% Sodium Sulfate
4% Sodium Sulfate
3% Sodium Sulfate
2% Sodium Sulfate
6% Potassium Chloride
5% Potassium Chloride
4% Potassium Chloride
3% Potassium Chloride
6% NaCl + Trigonelline
6% NaCl + Octopine
6% NaCl + Trimethylamine
6% NaCl + Trimethylamine-N-Oxide
6% NaCl + Trehalose
6% NaCl + Glycerol
6% NaCl + Glutathione
6% NaCl + β–Amino-N-Butyric Acid
6% NaCl + γ-Glutamic Acid
6% NaCl + N-Acetyl-L-Glutamine
6% NaCl + L-Proline
6% NaCl + KCl
6% NaCl + L-Carnitine
6% NaCl + Creatinine
6% NaCl + Creatine
6% NaCl + Phosphorylcholine
6% NaCl + Choline
6% NaCl + Ectoine
6% NaCl + MOPS
6% NaCl + Dimethyl Sulphonyl Propionate
6% NaCl + Sarcosine
6% NaCl + N-N Dimethyl Glycine
6% NaCl + Betaine
6% NaCl
10% NaCl
9% NaCl
8% NaCl
7% NaCl
6.5% NaCl
6% NaCl
5.5% NaCl
5% NaCl
4% NaCl
3% NaCl
2% NaCl
1% NaCl
0
20000
40000
60000
Area under curve (AUC)

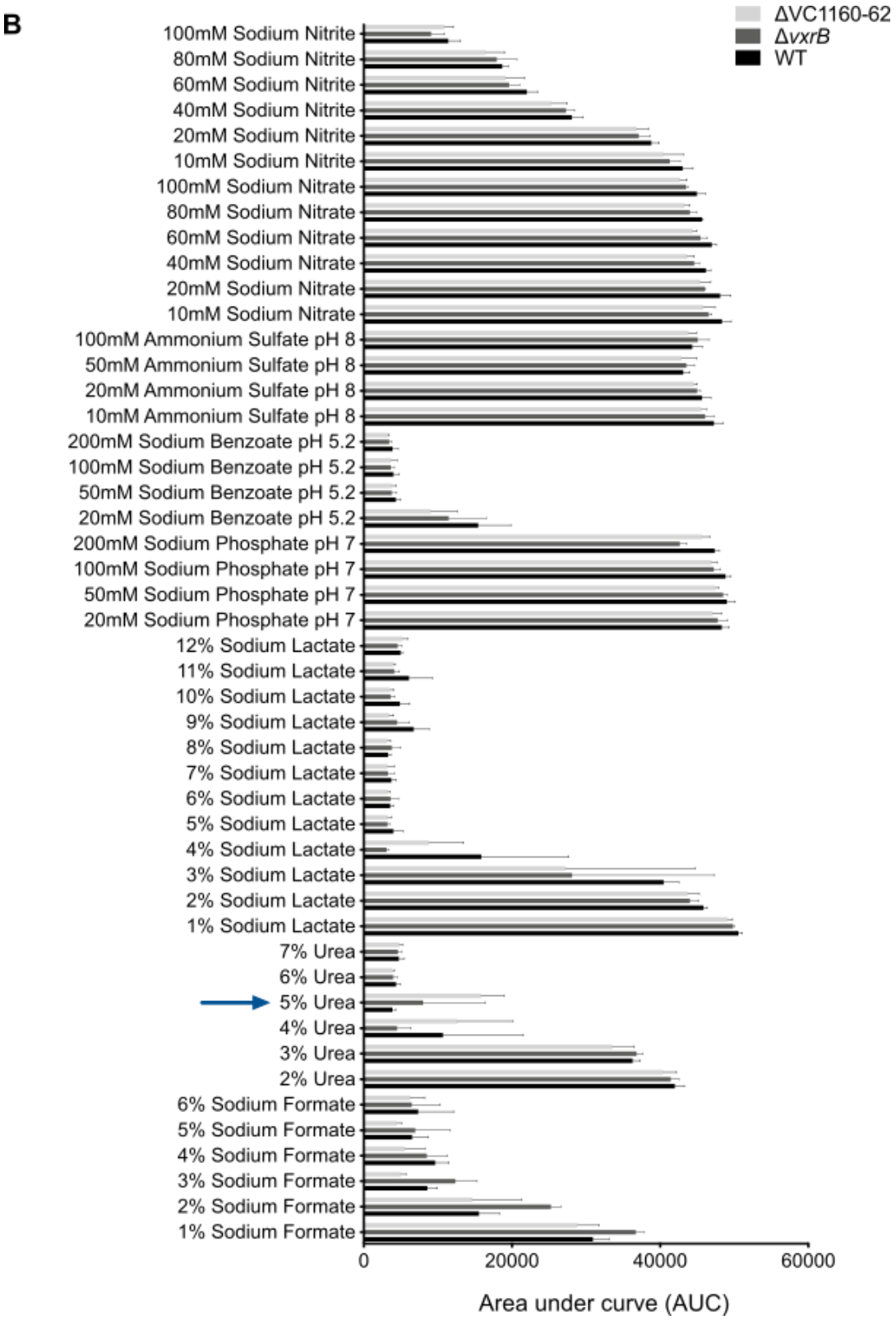
B
ΔVC1160-62
ΔvxrB
WT
100mM Sodium Nitrite
80mM Sodium Nitrite
60mM Sodium Nitrite
40mM Sodium Nitrite
20mM Sodium Nitrite
10mM Sodium Nitrite
100mM Sodium Nitrate
80mM Sodium Nitrate
60mM Sodium Nitrate
40mM Sodium Nitrate
20mM Sodium Nitrate
10mM Sodium Nitrate
100mM Ammonium Sulfate pH 8
50mM Ammonium Sulfate pH 8
20mM Ammonium Sulfate pH 8
10mM Ammonium Sulfate pH 8
200mM Sodium Benzoate pH 5.2
100mM Sodium Benzoate pH 5.2
50mM Sodium Benzoate pH 5.2
20mM Sodium Benzoate pH 5.2
200mM Sodium Phosphate pH 7
100mM Sodium Phosphate pH 7
50mM Sodium Phosphate pH 7
20mM Sodium Phosphate pH 7
12% Sodium Lactate
11% Sodium Lactate
10% Sodium Lactate
9% Sodium Lactate
8% Sodium Lactate
7% Sodium Lactate
6% Sodium Lactate
5% Sodium Lactate
4% Sodium Lactate
3% Sodium Lactate
2% Sodium Lactate
1% Sodium Lactate
7% Urea
6% Urea
5% Urea
4% Urea
3% Urea
2% Urea
6% Sodium Formate
5% Sodium Formate
4% Sodium Formate
3% Sodium Formate
2% Sodium Formate
1% Sodium Formate
0
20000
40000
60000
Area under curve (AUC)

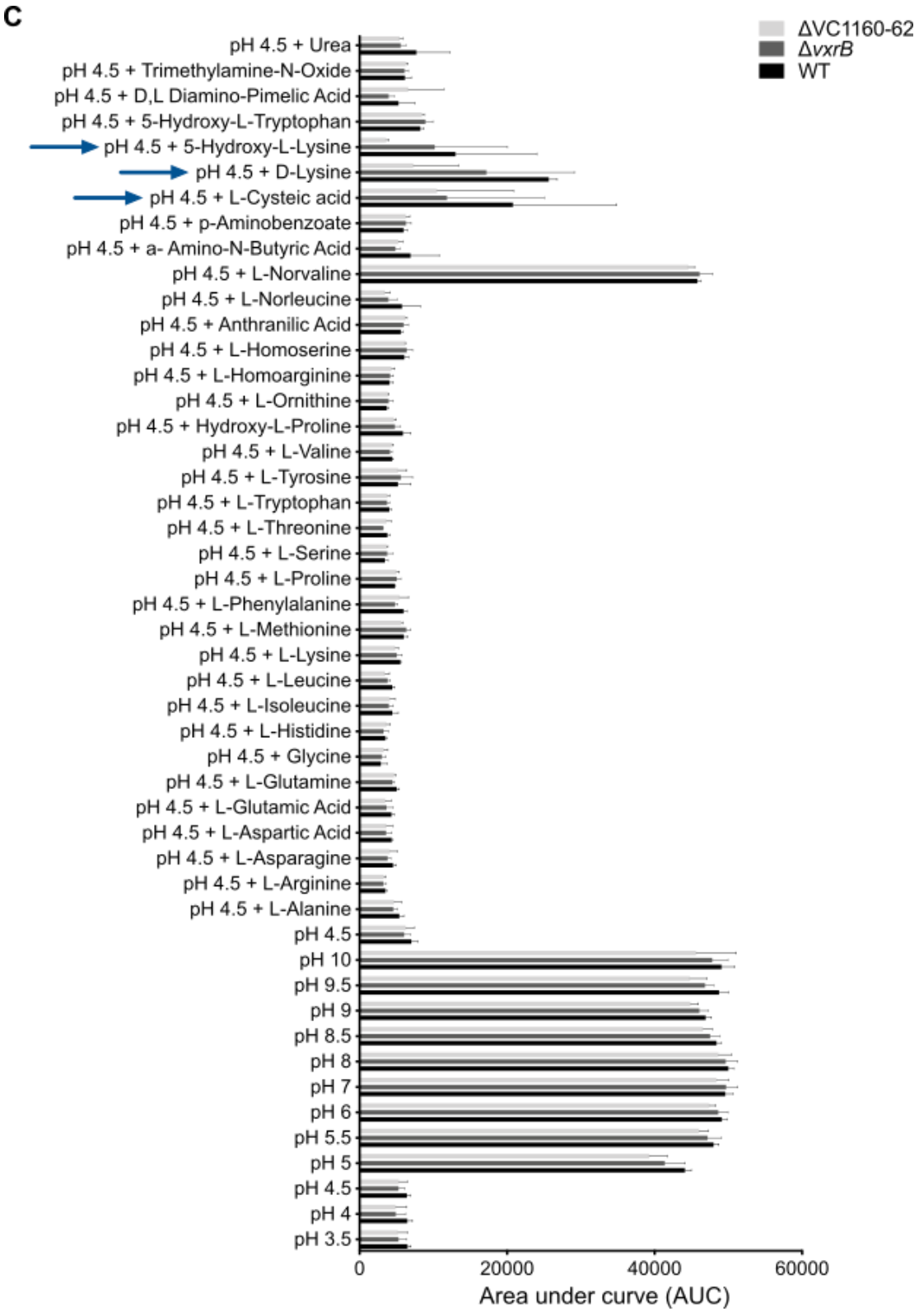
C
ΔVC1160-62
ΔvxrB
WT
pH 4.5 + Urea
pH 4.5 + Trimethylamine-N-Oxide
pH 4.5 + D,L Diamino-Pimelic Acid
pH 4.5 + 5-Hydroxy-L-Tryptophan
pH 4.5 + 5-Hydroxy-L-Lysine
pH 4.5 + D-Lysine
pH 4.5 + L-Cysteic acid
pH 4.5 + p-Aminobenzoate
pH 4.5 + a- Amino-N-Butyric Acid
pH 4.5 + L-Norvaline
pH 4.5 + L-Norleucine
pH 4.5 + Anthranilic Acid
pH 4.5 + L-Homoserine
pH 4.5 + L-Homoarginine
pH 4.5 + L-Ornithine
pH 4.5 + Hydroxy-L-Proline
pH 4.5 + L-Valine
pH 4.5 + L-Tyrosine
pH 4.5 + L-Tryptophan
pH 4.5 + L-Threonine
pH 4.5 + L-Serine
pH 4.5 + L-Proline
pH 4.5 + L-Phenylalanine
pH 4.5 + L-Methionine
pH 4.5 + L-Lysine
pH 4.5 + L-Leucine
pH 4.5 + L-Isoleucine
pH 4.5 + L-Histidine
pH 4.5 + Glycine
pH 4.5 + L-Glutamine
pH 4.5 + L-Glutamic Acid
pH 4.5 + L-Aspartic Acid
pH 4.5 + L-Asparagine
pH 4.5 + L-Arginine
pH 4.5 + L-Alanine
pH 4.5
pH 10
pH 9.5
pH 9
pH 8.5
pH 8
pH 7
pH 6
pH 5.5
pH 5
pH 4.5
pH 4
pH 3.5
0
20000
40000
60000
Area under curve (AUC)

D

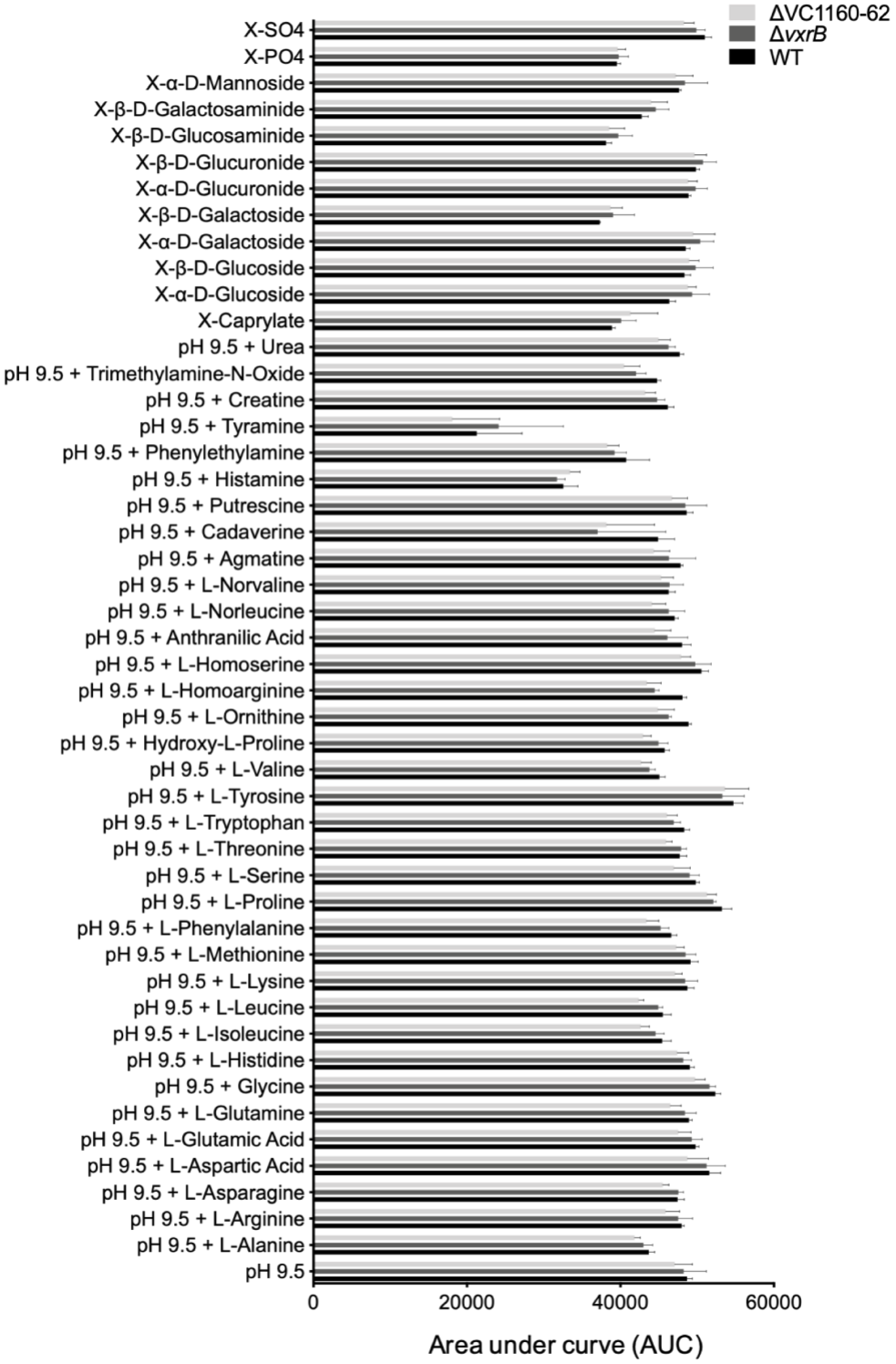
ΔVC1160-62
ΔvxrB
WT
X-SO4
X-PO4
X-α-D-Mannoside
X-β-D-Galactosaminide
X-β-D-Glucosaminide
X-β-D-Glucuronide
X-α-D-Glucuronide
X-β-D-Galactoside
X-α-D-Galactoside
X-β-D-Glucoside
X-α-D-Glucoside
X-Caprylate
pH 9.5 + Urea
pH 9.5 + Trimethylamine-N-Oxide
pH 9.5 + Creatine
pH 9.5 + Tyramine
pH 9.5 + Phenylethylamine
pH 9.5 + Histamine
pH 9.5 + Putrescine
pH 9.5 + Cadaverine
pH 9.5 + Agmatine
pH 9.5 + L-Norvaline
pH 9.5 + L-Norleucine
pH 9.5 + Anthranilic Acid
pH 9.5 + L-Homoserine
pH 9.5 + L-Homoarginine
pH 9.5 + L-Ornithine
pH 9.5 + Hydroxy-L-Proline
pH 9.5 + L-Valine
pH 9.5 + L-Tyrosine
pH 9.5 + L-Tryptophan
pH 9.5 + L-Threonine
pH 9.5 + L-Serine
pH 9.5 + L-Proline
pH 9.5 + L-Phenylalanine
pH 9.5 + L-Methionine
pH 9.5 + L-Lysine
pH 9.5 + L-Leucine
pH 9.5 + L-Isoleucine
pH 9.5 + L-Histidine
pH 9.5 + Glycine
pH 9.5 + L-Glutamine
pH 9.5 + L-Glutamic Acid
pH 9.5 + L-Aspartic Acid
pH 9.5 + L-Asparagine
pH 9.5 + L-Arginine
pH 9.5 + L-Alanine
pH 9.5
0
20000
40000
60000
Area under curve (AUC)

E

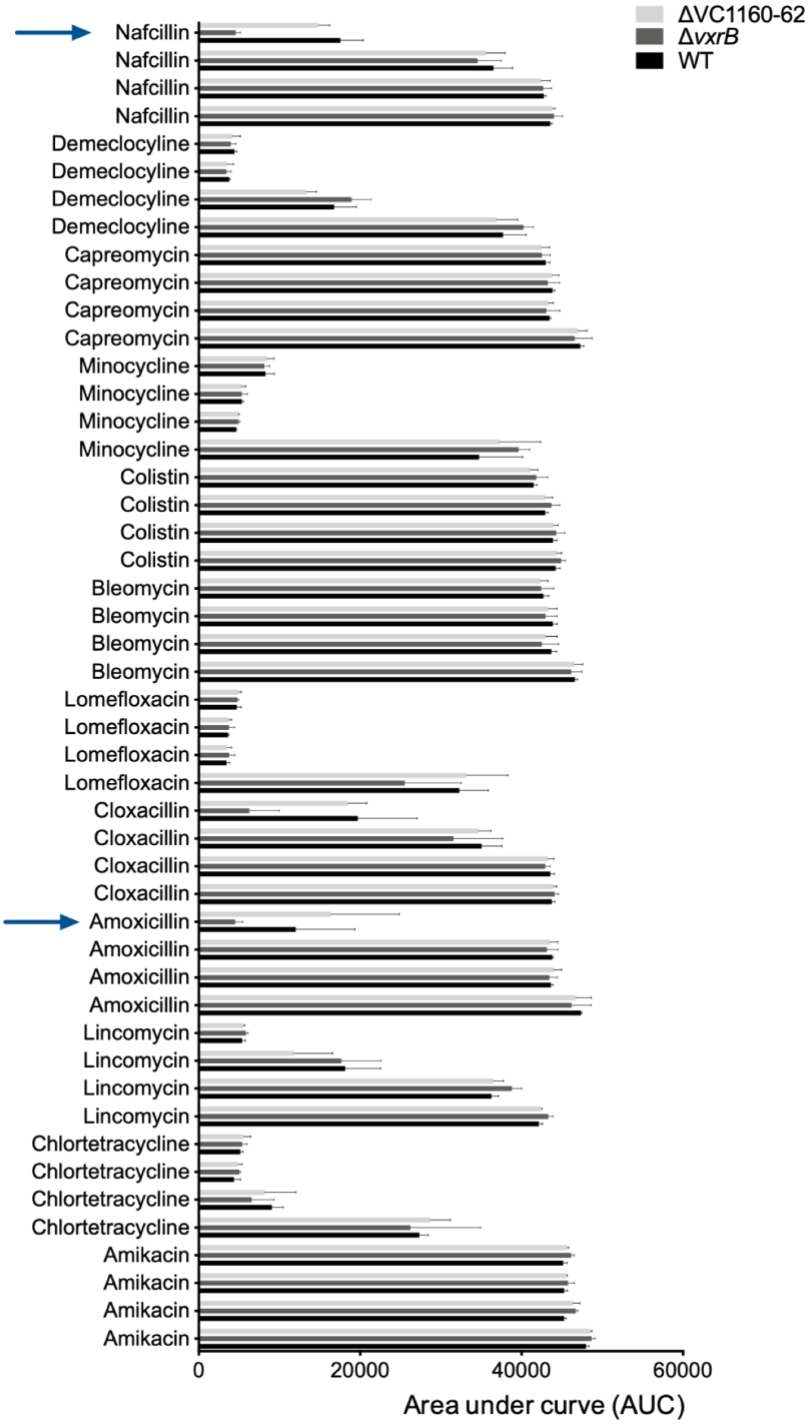
ΔVC1160-62
ΔvxrB
WT
Nafcillin
Nafcillin
Nafcillin
Nafcillin
Demeclocyline
Demeclocyline
Demeclocyline
Demeclocyline
Capreomycin
Capreomycin
Capreomycin
Capreomycin
Minocycline
Minocycline
Minocycline
Minocycline
Colistin
Colistin
Colistin
Colistin
Bleomycin
Bleomycin
Bleomycin
Bleomycin
Lomefloxacin
Lomefloxacin
Lomefloxacin
Lomefloxacin
Cloxacillin
Cloxacillin
Cloxacillin
Cloxacillin
Amoxicillin
Amoxicillin
Amoxicillin
Amoxicillin
Lincomycin
Lincomycin
Lincomycin
Lincomycin
Chlortetracycline
Chlortetracycline
Chlortetracycline
Chlortetracycline
Amikacin
Amikacin
Amikacin
Amikacin
0
20000
40000
60000
Area under curve (AUC)

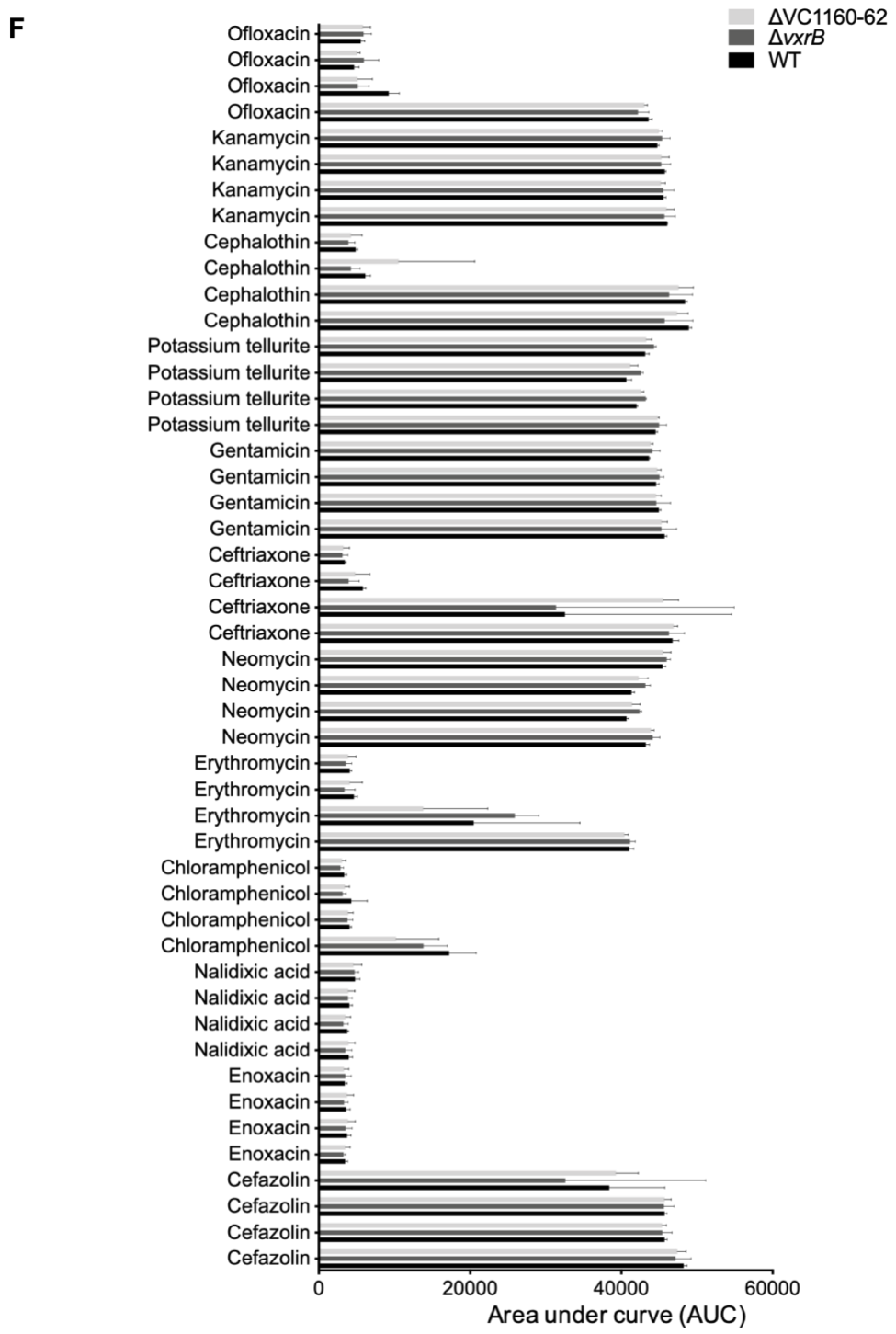

Figure 4.5. Phenotypic microarray analysis of in the ΔVC1162-60 and *ΔvxrB* mutant relative to wild type.

Biolog plates were used to perform a high-throughput screen of the ability of *V. cholerae* WT, ΔVC1162-60 and *ΔvxrB* to grow in the presence of various stressors. The area under the curve (AUC) was determined for each condition tested. Data represent the averages of results of three biological replicates for each strain for each of the PM plates. A) Growth of WT, ΔVC1162-60 and *ΔvxrB* on 48 osmolytes found in PM9 plate. B) Growth of WT, ΔVC1162-60 and *ΔvxrB* on additional 48 osmolytes found in PM9 plate. C) Growth of WT, ΔVC1162-60 and *ΔvxrB* on 48 pH conditions found in PM10 plate. D) Growth of WT, ΔVC1162-60 and *ΔvxrB* on additional 48 pH conditions found in PM10 plate. E) Growth of WT, ΔVC1162-60 and *ΔvxrB* on 48 antimicrobial conditions found in PM11 plate. F) Growth of WT, ΔVC1162-60 and *ΔvxrB* on additional 48 antimicrobial conditions found in PM11 plate.

Discussion

In our analysis of VxrB-regulated hypothetical genes we identified three operons that contribute to VxrB-mediated phenotypes. Each of these operons are highly conserved in *Vibrios* and other bacterial species and further investigation using homology searches, structural modeling, and phenotypic microarrays provided deeper insights into the function of these genes.

We demonstrated that the VC1160-62 operon contributes to *V. cholerae* intestinal colonization. Homologs of the VC1160-62 operon are found in numerous bacterial species but its function has yet to be characterized. VC1160 encodes a predicted RimK-like ATP-grasp peptide ligase, VC1161 encodes for an inactive transglutaminase 7 transmembrane (7-TM) protein, and VC1162 encodes for a predicted aspartic peptidase. A homolog to this operon exists in *Pseudomonas aeruginosa,* and it has been proposed in this system that the RimK-like ATP-grasp ligase carries out a peptide ligase activity in connection with the 7-TM protein, either modifying the intracellular regions of the 7-TM protein or a small molecule that interacts with the 7-TM protein in response to an external stress signal (40). The peptidase in this system is predicted to reverse the modification (40).

A signature-tagged mutagenesis screen previously identified VC1162 as a colonization factor (41), but a role for the operon had not been shown. In *P. aeruginosa* (PA1768-1766) the homolog for this operon has also been shown to be important for infection (42). Additionally, PA1766 expression was increased

during anaerobic growth (43), PA1768-1766 was shown to contribute to polymyxin/antimicrobial peptide resistance (44), with loss of PA1766 and PA1767 leading to reduced antibiotic susceptibility. We analyzed a *V. cholerae* ΔVC1160-62 mutant but did not observe any defects in antimicrobial or antibiotic resistance (in preparation as part of a collaboration with the Sondermann lab) (45). In our analysis we demonstrate that this operon contributes to infection and use phenotypic microarrays to begin to explore the other phenotypes that this operon influences. Given that this system is predicted to bridge the inner membrane it is possible that it plays a role in maintaining membrane integrity or modification during infection, however, further analysis of these genes is required to reveal their function and better understand their contribution to pathogenesis.

Deletion of *tamA* (VC2548) or *tamB* (VC2547) results in a colonization defect. Though annotated as hypothetical, bioinformatic-based structural analysis using Protein Homology/analogY Recognition Engine V 2.0 (Phyre) show that the VC2548-47 operon encodes for the TamAB transport system (46). The TamAB system is conserved across a diverse range of bacteria (47). The translocation and assembly module (TAM) was first identified and characterized in *Citrobacter rodentium, Salmonella enterica* and *Escherichia coli* and was initially thought to be involved in assisting the transport of so called ‘autotransporters,’ which are surface-localized proteins that were initially thought to cross the outer membrane (OM) autonomously (47). The complex consists of an Omp85 superfamily outer membrane protein, TamA and a large anchored inner membrane protein, TamB,

which together form an oligomeric protein complex that spans the periplasm. *V. cholerae* is not predicted to encode for any autotransporters and we do not know the target of this system in *V. cholerae.* TamAB has been shown to be important for colonization in *V. fischeri* and has been identified as a virulence factor in a number of other species, including *V. parahaemolyticus, Escherichia coli, Citrobacter rodentium, Salmonella enterica, Proteus mirabilis* and *Klebsiella pneumonia* (47–51).

In *E. coli*, deletion of the TAM system abolishes cell to cell aggregation and reduces biofilm formation by preventing the secretion of the autotransporter adhesions Ag43 and EhaA (47). The *E. coli* TAM system has been shown to work with the beta barrel assembly machinery (BAM) complex to mediate efficient assembly of the fimbriae usher protein, facilitating rapid deployment of fimbrial extensions. In the absence of TAM, the usher protein can still assemble, but more slowly. Less efficient assembly of the usher results in diminished adherence during early fimbriae induction and is expected to impact host colonization, resulting in a virulence defect (52). Deletion of TamB in *E. coli* has also been shown to result in increased susceptibility to vancomycin (53) through an unknown mechanism.

Deletion of TamB (MorC) in *Aggregatibacter actinomycetemcomitans* leads to altered membrane morphology and alterations in levels of several membrane proteins, including proteins involved in quality control systems, oxidative stress responses and toxin secretion (54, 55). The extremophile *Deinococcus*

radiodurans encodes for TamB homolog though it does not encode for TamA. In this bacterium, TamB was shown to contribute to cell growth, cell envelope integrity, and stress resistance, potentially by facilitating the assembly of the surface layer (S-layer) (56). *Borrelia burgdorferi* also encodes for a TamB homolog, though it does not encode for a TamA homolog. In *B. burgdorferi*, TamB was observed to interact with BamA and a *tamB* mutant demonstrated altered cell morphology and antibiotic sensitivity (57).

We demonstrate that the TamAB system contributes to *V. cholerae* pathogenesis. Based on its functions in other bacterial species it is interesting to speculate if this system contributes to cell envelope integrity in the face of host defenses, however, further characterization of this system and its substrates will enhance our understanding of how this system contributes to virulence.

We demonstrated that the VC2516-18 genes contribute to cell wall homeostasis. Further analysis of these genes revealed that they are part of the Mla (*m*aintenance of OM *l*ipid *a*symmetry) pathway. This system was originally characterized in *E. coli* and is a six-component system that mediates retrograde transport of misplaced phospholipids (PL) from the outer leaflet of the outer membrane (OM) to the cytoplasmic membrane, thus contributing to outer membrane stability and resistance to perturbations (39). In contrast to our findings and previous work done in *E. coli*, work in *Acinetobacter baumannii* demonstrated that disruption of *mla* genes and phospholipid retention in the absence of an

asymmetrical outer membrane could contribute to enhanced resistance to last resort antibiotics (58). This suggests tight regulation of this system in crucial in the face of various environmental assaults.

A recent study demonstrated that deletion or repression of other components of this system, *mlaA* (also called *vacJ*) or *mlaE* (also called *yrbE*) increases outer membrane vesicles (OMVs) in *Haemophilus influenzae* and *V. cholerae*. OMVs from MlaA/MlaE-defective mutants in *H. influenzae* are enriched in phospholipids and certain fatty acids. The authors also demonstrate that OMV production and regulation of the MlaA/MlaE transport system respond to iron starvation. Though in other species *mla* mutants have shown increased sensitivity to SDS/EDTA, in this study the authors did not observe increased sensitivity of the mutant strains to cell lysis, SDS, and polymyxin B treatment compared to the wild-type (59).

P. aeruginosa Tn5 transposon mutants in genes from the Mla pathway showed increased susceptibility to killing by the antimicrobial peptide, LL-37, when compared to the wild-type parent strain. The *P. aeruginosa mlaA* mutant demonstrated increased sensitivity to SDS and EDTA and increased membrane permeability upon damage. When exposed to human whole blood and serum complement, the *mlaA* mutant was killed more rapidly when compared to the wild-type parent strain and complemented mutant. Finally, in an *in vivo* mouse lung infection model, infection with the *mlaA* mutant resulted in reduced mortality, lower bacterial burden, and reduced lung damage when compared to the wild-type strain

(60). In *Shigella flexneri* mutations in *mlaA* (*vacJ*) or *mlaD* (*vpsC*) resulted in increased SDS sensitivity and a *mlaD* mutant has a slightly altered phospholipid (PL) profile compared to wild type and was unable to form plaques on cultured epithelial cells. Because expression of *pldA* restored resistance to SDS, but did not restore the PL profile or the ability to form plaques the author propose that system has a dual role in maintaining outer membrane asymmetry and intercellular spread of bacteria between adjacent cells (61).

The *V. cholerae mla* genes contribute to β-lactam survival but did not impact virulence in an infant mouse model or resistance to other cell wall stresses tested, including Polymyxin B treatment, EDTA/SDS, and osmotic stress (unpublished). We speculate that they likely contribute to cell envelope stability under additional conditions that have not been tested. Furthermore, a recent study presents evidence that the *mla* system may act as an anterograde phospholipid trafficking system rather than a retrograde tracking system in *A. baumannii*, suggesting that further characterization of the function and action of this system is required to fully understand its contribution to envelope maintenance and stability (62).

This study allowed us to identify new players involved in these important *V. cholerae* phenotypes. Our analysis identified two new operons with roles in virulence and one operon with a role in cell envelope stability, all of which encode for proteins that converge around the cell envelope. This further suggests that many of the VxrB-mediated phenotypes may be either responding to or mediating

cell envelope stress encountered during its dynamic life cycle that requires survival in the face of various aquatic and host stressors. TCSs are important systems that allow bacteria to sense and respond to their environment and our further characterization of VxrAB provides additional insight into our understanding of TCSs and the function of hypothetical proteins.

Conclusion

In this study, we identify new players in VxrB-mediated phenotypes, all of which converge around the cell envelope (Figure 4.6). Our analysis of the role of VxrB-regulated hypothetical genes in infection revealed a previously unknown role for the VC1162-60 genes and VC2548-47 genes in intestinal colonization. We additionally identified three genes, VC2516-18, encoded in the *mla* operon that contribute to resistance to antibiotic stress.

All three systems that we identified appear to impact the cell envelope in either *V. cholerae* or other species, affecting cell envelope integrity, transport of proteins into or across the inner membrane, or outer membrane lipid composition. This is especially interesting in the context of what we know about the T6SS secretion system. *V. cholerae* can attack other bacteria with its T6SS but it can also be attacked by other bacterial species that also encode for T6SS. In fact, *V. cholerae* T6SS firing into *P. aeruginosa* is known to illicit a counterattack from the neighboring cell (63). The toxic effectors utilized by the T6SS all target cell envelope processes, and include lipases, peptidoglycan degrading toxins, and

pore forming toxins (Fig. 4.6B). We hypothesize that VxrB's coregulation of T6SS genes and genes that can fortify the cell envelope may preemptively protect the cell from T6SS counterattacks. This is an idea we plan to explore in future studies by looking at T6SS firing in each of these mutants, as well whether or not these mutants are more susceptible to killing by foreign T6SS systems.

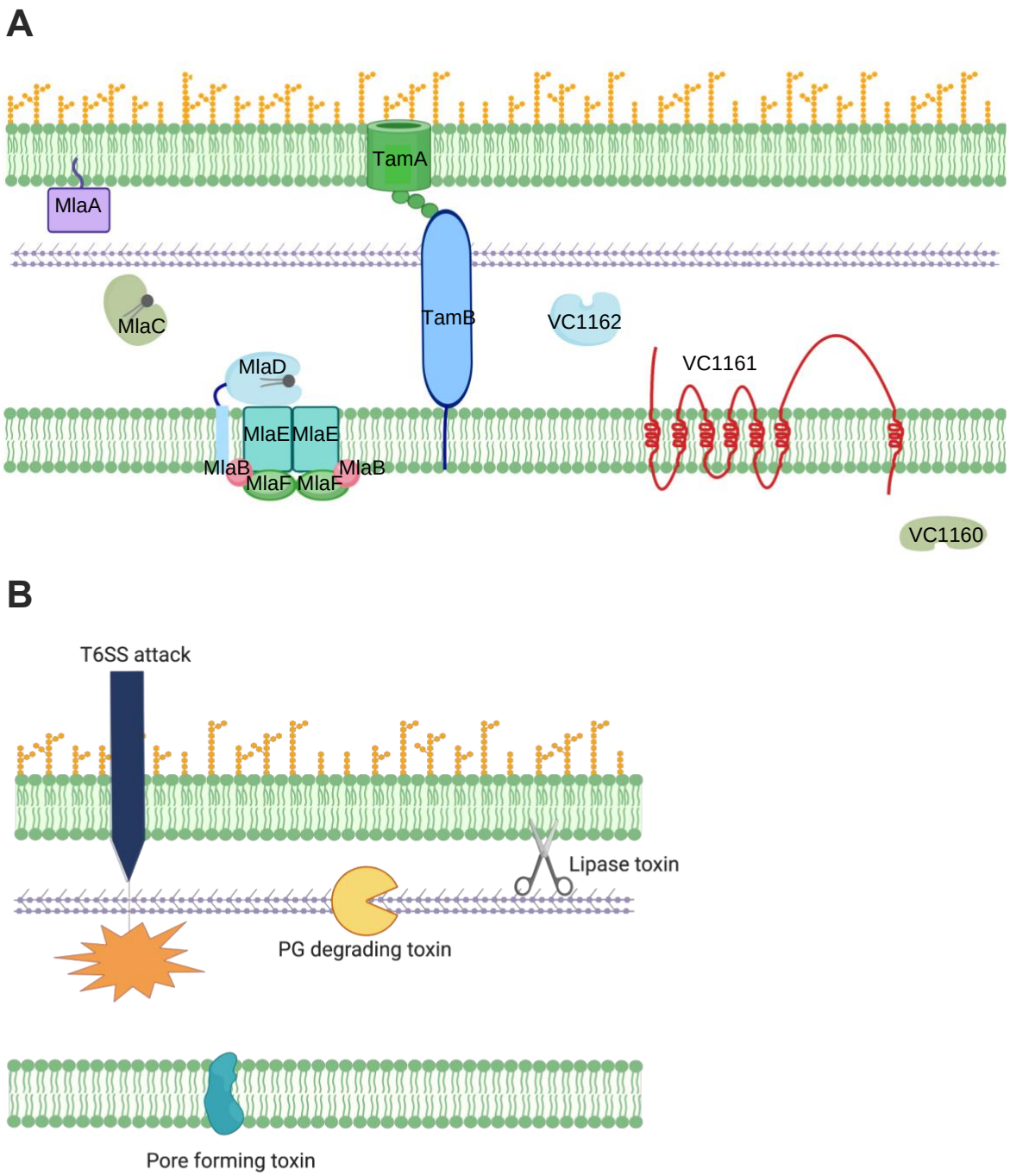

Figure 4.6. Newly identified systems contributing to VxrB-mediated phenotypes. A) VC1160 encodes for a cytoplasmic RimK-like glutathione synthase/Ribosomal protein S6 modification enzyme, VC1161 encodes for an inner membrane inactive

transglutaminase fused to 7 transmembrane helices, and VC1162 encodes for periplasmic aspartic peptidase. Analysis of structural predictions show that the VC2548-47 operon encodes for the TamAB transport system, located in the outer membrane and periplasm, respectively. Structural analysis identified VC2516-18 is part the Mla (*m*aintenance of OM *l*ipid *a*symmetry) pathway. VC2516 encodes for *mlaB*, a predicted NTP binding protein with a STAS domain. VC2517 encodes for *mlaC*, a phospholipid-binding protein. VC2518 encodes for *mlaD*, a phospholipid ABC transporter-binding protein. All of these systems converge at the cell envelope and we hypothesize that VxrB may be co-regulated these systems as a mechanism to fortify the cell envelope in preparation for T6SS attack. B) The toxic effectors utilized by the T6SS target various aspects of the cell envelope, including both inner and outer membranes and peptidoglycan.

References

1. **Shikuma NJ**, **Yildiz FH**. 2009. Identification and characterization of OscR, a transcriptional regulator involved in osmolarity adaptation in *Vibrio cholerae*. J. Bacteriol. **191**:4082–96.
2. **Beier D**, **Gross R**. 2006. Regulation of bacterial virulence by two-component systems. Curr. Opin. Microbiol. **9**:143–152.
3. **Calva E**, **Oropeza R**. 2006. Two-component signal transduction systems, environmental signals, and virulence. Microb. Ecol. **51**:166–76.
4. **Bilecen K**, **Yildiz FH**. 2009. Identification of a calcium-controlled negative regulatory system affecting *Vibrio cholerae* biofilm formation. Environ. Microbiol. **11**:2015–29.
5. **Shikuma NJ**, **Davis KR**, **Fong JNC**, **Yildiz FH**. 2013. The transcriptional regulator, CosR, controls compatible solute biosynthesis and transport, motility and biofilm formation in *Vibrio cholerae*. Environ. Microbiol. **15**:1387–99.
6. **Grabowicz M**, **Silhavy TJ**. 2017. Envelope stress responses: an interconnected safety net. Trends Biochem. Sci. **42**:232–242.
7. **MacRitchie DM**, **Buelow DR**, **Price NL**, **Raivio TL**. 2008. Two-component signaling and gram negative envelope stress response systems, p. 80–110. *In* Bacterial Signal Transduction: Networks and Drug Targets. Springer New York, New York, NY.
8. **Acosta N**, **Pukatzki S**, **Raivio TL**. 2015. The *Vibrio cholerae* Cpx envelope stress response senses and mediates adaptation to low iron. J.

Bacteriol. **197**:262–276.

9. **Taylor DL**, **Bina XR**, **Slamti L**, **Waldor MK**, **Bina JE**. 2014. Reciprocal regulation of resistance-nodulation-division efflux systems and the Cpx two-component system in *Vibrio cholerae*. Infect. Immun. **82**:2980–91.
10. **Slamti L**, **Waldor MK**. 2009. Genetic analysis of activation of the *Vibrio cholerae* Cpx pathway. J. Bacteriol. **191**:5044–56.
11. **Matson JS**, **Livny J**, **DiRita VJ**. 2017. A putative *Vibrio cholerae* two-component system controls a conserved periplasmic protein in response to the antimicrobial peptide polymyxin B. PLoS One **12**:e0186199.
12. **Bilecen K**, **Fong JCN**, **Cheng A**, **Jones CJ**, **Zamorano-Sánchez D**, **Yildiz FH**. 2015. Polymyxin B resistance and biofilm formation in *Vibrio cholerae* is controlled by the response regulator CarR. Infect. Immun.
13. **Herrera CM**, **Crofts AA**, **Henderson JC**, **Pingali SC**, **Davies BW**, **Trent MS**. 2014. The *Vibrio cholerae* VprA-VprB two-component system controls virulence through endotoxin modification. MBio **5**:e02283-14.
14. **Bina XR**, **Howard MF**, **Taylor-Mulneix DL**, **Ante VM**, **Kunkle DE**, **Bina JE**. 2018. The *Vibrio cholerae* RND efflux systems impact virulence factor production and adaptive responses via periplasmic sensor proteins. PLOS Pathog. **14**:e1006804.
15. **Kunkle DE**, **Bina XR**, **Bina JE**. 2017. The *Vibrio cholerae* VexGH RND efflux system maintains cellular homeostasis by effluxing *Vibrio*bactin. MBio **8**:e00126-17.
16. **Taylor DL**, **Ante VM**, **Bina XR**, **Howard MF**, **Bina JE**. 2015. Substrate-

Dependent Activation of the *Vibrio cholerae vexAB* RND Efflux System Requires vexR. PLoS One **10**:e0117890.

17. **Acosta N**, **Pukatzki S**, **Raivio TL**. 2015. The Cpx system regulates virulence gene expression in *Vibrio cholerae*. Infect. Immun. **83**:2396–408.
18. **Saul-McBeth J**, **Matson JS**. 2019. A Periplasmic antimicrobial peptide-binding protein is required for stress survival in *Vibrio cholerae*. Front. Microbiol. **10**:161.
19. **Dörr T**, **Alvarez L**, **Delgado F**, **Davis BM**, **Cava F**, **Waldor MK**. 2016. A cell wall damage response mediated by a sensor kinase/response regulator pair enables beta-lactam tolerance. Proc. Natl. Acad. Sci. U. S. A. **113**:404–9.
20. **Li L**, **Wang Q**, **Zhang H**, **Yang M**, **Khan MI**, **Zhou X**. 2016. Sensor histidine kinase is a β-lactam receptor and induces resistance to β-lactam antibiotics. Proc. Natl. Acad. Sci. U. S. A. **113**:1648–1653.
21. **Cheng AT**, **Ottemann KM**, **Yildiz FH**. 2015. *Vibrio cholerae* response regulator VxrB controls colonization and regulates the Type VI Secretion System. PLoS Pathog. **11**:e1004933.
22. **Teschler JK**, **Cheng AT**, **Yildiz FH**. 2017. The two-component signal transduction system VxrAB positively regulates *Vibrio cholerae* biofilm formation. J. Bacteriol. **199**:e00139-17.
23. **Heidelberg JF**, **Eisen JA**, **Nelson WC**, **Clayton RA**, **Gwinn ML**, **Dodson RJ**, **Haft DH**, **Hickey EK**, **Peterson JD**, **Umayam L**, **Gill SR**, **Nelson KE**, **Read TD**, **Tettelin H**, **Richardson D**, **Ermolaeva MD**, **Vamathevan J**,

Bass S, **Qin H**, **Dragoi I**, **Sellers P**, **McDonald L**, **Utterback T**, **Fleishmann RD**, **Nierman WC**, **White O**, **Salzberg SL**, **Smith HO**, **Colwell RR**, **Mekalanos JJ**, **Venter JC**, **Fraser CM**. 2000. DNA sequence of both chromosomes of the cholera pathogen *Vibrio cholerae*. Nature **406**:477–83.

24. **Liu X**, **Beyhan S**, **Lim B**, **Linington RG**, **Yildiz FH**. 2010. Identification and characterization of a phosphodiesterase that inversely regulates motility and biofilm formation in *Vibrio cholerae*. J. Bacteriol. **192**:4541–52.
25. **Marvig RL**, **Blokesch M**. 2010. Natural transformation of *Vibrio cholerae* as a tool - Optimizing the procedure. BMC Microbiol. **10**:155.
26. **Silva ODS**, **Blokesch M**. 2010. Genetic manipulation of *Vibrio cholerae* by combining natural transformation with FLP recombination. Plasmid **64**:186–195.
27. **Fong JCN**, **Karplus K**, **Schoolnik GK**, **Yildiz FH**. 2006. Identification and characterization of RbmA, a novel protein required for the development of rugose colony morphology and biofilm structure in *Vibrio cholerae*. J. Bacteriol. **188**:1049–59.
28. **Zamorano-Sánchez D**, **Fong JCN**, **Kilic S**, **Erill I**, **Yildiz FH**. 2015. Identification and characterization of VpsR and VpsT binding sites in *Vibrio cholerae*. J. Bacteriol. **Accepted**.
29. **Taylor RK**, **Miller VL**, **Furlong DB**, **Mekalanos JJ**. 1987. Use of *phoA* gene fusions to identify a pilus colonization factor coordinately regulated with cholera toxin. Proc. Natl. Acad. Sci. U. S. A. **84**:2833–7.

30. **Miyata ST**, **Unterweger D**, **Rudko SP**, **Pukatzki S**. 2013. Dual expression profile of type VI secretion system immunity genes protects pandemic *Vibrio cholerae*. PLoS Pathog. **9**:e1003752.

31. **Ishikawa T**, **Sabharwal D**, **Bröms J**, **Milton DL**, **Sjöstedt A**, **Uhlin BE**, **Wai SN**. 2012. Pathoadaptive conditional regulation of the type VI secretion system in *Vibrio cholerae* O1 strains. Infect. Immun. **80**:575–84.

32. **Herrero M**, **de Lorenzo V**, **Timmis KN**. 1990. Transposon vectors containing non-antibiotic resistance selection markers for cloning and stable chromosomal insertion of foreign genes in gram-negative bacteria. J. Bacteriol. **172**:6557–67.

33. **de Lorenzo V**, **Timmis KN**. 1994. Analysis and construction of stable phenotypes in gram-negative bacteria with Tn5- and Tn10-derived minitransposons. Methods Enzymol. **235**:386–405.

34. **Yildiz FH**, **Schoolnik GK**. 1998. Role of rpoS in stress survival and virulence of *Vibrio cholerae*. J. Bacteriol. **180**:773–84.

35. **Casper-Lindley C**, **Yildiz FH**. 2004. VpsT Is a transcriptional regulator required for expression of *vps* biosynthesis genes and the development of rugose colonial morphology in *Vibrio cholerae* O1 El Tor. J. Bacteriol. **186**:1574–1578.

36. **Bao Y**, **Lies DP**, **Fu H**, **Roberts GP**. 1991. An improved Tn7-based system for the single-copy insertion of cloned genes into chromosomes of gram-negative bacteria. Gene **109**:167–8.

37. **Hammer BK**, **Bassler BL**. 2007. Regulatory small RNAs circumvent the

conventional quorum sensing pathway in pandemic *Vibrio cholerae*. Proc. Natl. Acad. Sci. U. S. A. **104**:11145–9.

38. **Tak A**, **Cheng T**. 2015. Systematic analysis of two-component signal transduction systems in *Vibrio cholerae* biofilm formation and virulence. A dissertation submitted in partial satisfaction of the requirements for the degree of Doctor of Philosophy in Microbiology and Environmental Toxicology.

39. **Malinverni JC**, **Silhavy TJ**. 2009. An ABC transport system that maintains lipid asymmetry in the gram-negative outer membrane. Proc. Natl. Acad. Sci. U. S. A. **106**:8009–14.

40. **Iyer LM**, **Abhiman S**, **Maxwell Burroughs A**, **Aravind L**. 2009. Amidoligases with ATP-grasp, glutamine synthetase-like and acetyltransferase-like domains: synthesis of novel metabolites and peptide modifications of proteins. Mol. Biosyst. **5**:1636–60.

41. **Merrell DS**, **Hava DL**, **Camilli A**. 2002. Identification of novel factors involved in colonization and acid tolerance of *Vibrio cholerae*. Mol. Microbiol. **43**:1471–1491.

42. **Feinbaum RL**, **Urbach JM**, **Liberati NT**, **Djonovic S**, **Adonizio A**, **Carvunis A-R**, **Ausubel FM**. 2012. Genome-wide identification of *Pseudomonas aeruginosa* virulence-related genes using a *Caenorhabditis elegans* infection model. PLoS Pathog. **8**:e1002813.

43. **Wu M**, **Guina T**, **Brittnacher M**, **Nguyen H**, **Eng J**, **Miller SI**. 2005. The *Pseudomonas aeruginosa* proteome during anaerobic growth. J. Bacteriol.

187:8185–90.

44. **Gutu AD**, **Sgambati N**, **Strasbourger P**, **Brannon MK**, **Jacobs MA**, **Haugen E**, **Kaul RK**, **Johansen HK**, **Høiby N**, **Moskowitz SM**. 2013. Polymyxin resistance of *Pseudomonas aeruginosa phoQ* mutants is dependent on additional two-component regulatory systems. Antimicrob. Agents Chemother. **57**:2204–15.

45. **Wiegand I**, **Marr AK**, **Breidenstein EBM**, **Schurek KN**, **Taylor P**, **Hancock REW**. 2008. Mutator genes giving rise to decreased antibiotic susceptibility in *Pseudomonas aeruginosa*. Antimicrob. Agents Chemother. **52**:3810–3.

46. **Kelley LA**, **Mezulis S**, **Yates CM**, **Wass MN**, **Sternberg MJE**. 2015. The Phyre2 web portal for protein modeling, prediction and analysis. Nat. Protoc. **10**:845–858.

47. **Selkrig J**, **Mosbahi K**, **Webb CT**, **Belousoff MJ**, **Perry AJ**, **Wells TJ**, **Morris F**, **Leyton DL**, **Totsika M**, **Phan M-D**, **Celik N**, **Kelly M**, **Oates C**, **Hartland EL**, **Robins-Browne RM**, **Ramarathinam SH**, **Purcell AW**, **Schembri MA**, **Strugnell RA**, **Henderson IR**, **Walker D**, **Lithgow T**. 2012. Discovery of an archetypal protein transport system in bacterial outer membranes. Nat. Struct. Mol. Biol. **19**:506–510.

48. **Burall LS**, **Harro JM**, **Li X**, **Lockatell CV**, **Himpsl SD**, **Hebel JR**, **Johnson DE**, **Mobley HLT**. 2004. *Proteus mirabilis* genes that contribute to pathogenesis of urinary tract infection: identification of 25 signature-tagged mutants attenuated at least 100-fold. Infect. Immun. **72**:2922–38.

49. **Struve C**, **Forestier C**, **Krogfelt KA**. 2003. Application of a novel multi-screening signature-tagged mutagenesis assay for identification of *Klebsiella pneumoniae* genes essential in colonization and infection. Microbiology **149**:167–176.

50. **Brooks JF**, **Gyllborg MC**, **Cronin DC**, **Quillin SJ**, **Mallama CA**, **Foxall R**, **Whistler C**, **Goodman AL**, **Mandel MJ**. 2014. Global discovery of colonization determinants in the squid symbiont *Vibrio fischeri.* Proc. Natl. Acad. Sci. U. S. A. **111**:17284–9.

51. **Hubbard TP**, **Chao MC**, **Abel S**, **Blondel CJ**, **Abel Zur Wiesch P**, **Zhou X**, **Davis BM**, **Waldor MK**. 2016. Genetic analysis of *Vibrio parahaemolyticus* intestinal colonization. Proc. Natl. Acad. Sci. U. S. A. **113**:6283–8.

52. **Stubenrauch C**, **Belousoff MJ**, **Hay ID**, **Shen H-H**, **Lillington J**, **Tuck KL**, **Peters KM**, **Phan M-D**, **Lo AW**, **Schembri MA**, **Strugnell RA**, **Waksman G**, **Lithgow T**. 2016. Effective assembly of fimbriae in *Escherichia coli* depends on the translocation assembly module nanomachine. Nat. Microbiol. **1**:16064.

53. **Babu M**, **Díaz-Mejía JJ**, **Vlasblom J**, **Gagarinova A**, **Phanse S**, **Graham C**, **Yousif F**, **Ding H**, **Xiong X**, **Nazarians-Armavil A**, **Alamgir M**, **Ali M**, **Pogoutse O**, **Pe'er A**, **Arnold R**, **Michaut M**, **Parkinson J**, **Golshani A**, **Whitfield C**, **Wodak SJ**, **Moreno-Hagelsieb G**, **Greenblatt JF**, **Emili A**. 2011. Genetic interaction maps in *Escherichia coli* reveal functional crosstalk among cell envelope biogenesis pathways. PLoS Genet.

7:e1002377.

54. **Azari F**, **Nyland L**, **Yu C**, **Radermacher M**, **Mintz KP**, **Ruiz T**. 2013. Ultrastructural analysis of the rugose cell envelope of a member of the *Pasteurellaceae* family. J. Bacteriol. **195**:1680–8.

55. **Smith KP**, **Fields JG**, **Voogt RD**, **Deng B**, **Lam Y-W**, **Mintz KP**. 2015. Alteration in abundance of specific membrane proteins of *Aggregatibacter actinomycetemcomitans* is attributed to deletion of the inner membrane protein MorC. Proteomics **15**:1859–67.

56. **Yu J**, **Li T**, **Dai S**, **Weng Y**, **Li J**, **Li Q**, **Xu H**, **Hua Y**, **Tian B**. 2017. A *tamB* homolog is involved in maintenance of cell envelope integrity and stress resistance of *Deinococcus radiodurans*. Sci. Rep. **7**:45929.

57. **Iqbal H**, **Kenedy MR**, **Lybecker M**, **Akins DR**. 2016. The TamB ortholog of *Borrelia burgdorferi* interacts with the β-barrel assembly machine (BAM) complex protein BamA. Mol. Microbiol. **102**:757–774.

58. **Powers MJ**, **Trent MS**. 2018. Phospholipid retention in the absence of asymmetry strengthens the outer membrane permeability barrier to last-resort antibiotics. Proc. Natl. Acad. Sci. U. S. A. **115**:E8518–E8527.

59. **Roier S**, **Zingl FG**, **Cakar F**, **Durakovic S**, **Kohl P**, **Eichmann TO**, **Klug L**, **Gadermaier B**, **Weinzerl K**, **Prassl R**, **Lass A**, **Daum G**, **Reidl J**, **Feldman MF**, **Schild S**. 2016. A novel mechanism for the biogenesis of outer membrane vesicles in Gram-negative bacteria. Nat. Commun. **7**:10515.

60. **Munguia J**, **LaRock DL**, **Tsunemoto H**, **Olson J**, **Cornax I**, **Pogliano J**,

Nizet V. 2017. The Mla pathway is critical for *Pseudomonas aeruginosa* resistance to outer membrane permeabilization and host innate immune clearance. J. Mol. Med. **95**:1127–1136.

61. **Carpenter CD**, **Cooley BJ**, **Needham BD**, **Fisher CR**, **Trent MS**, **Gordon V**, **Payne SM**. 2014. The Vps/VacJ ABC transporter is required for intercellular spread of *Shigella flexneri*. Infect. Immun. **82**:660–9.

62. **Kamischke C**, **Fan J**, **Bergeron J**, **Kulasekara HD**, **Dalebroux ZD**, **Burrell A**, **Kollman JM**, **Miller SI**. 2019. The *Acinetobacter baumannii* Mla system and glycerophospholipid transport to the outer membrane. Elife **8**.

63. **Basler M**, **Ho BT**, **Mekalanos JJ**. 2013. Tit-for-tat: type VI secretion system counterattack during bacterial cell-cell interactions. Cell **152**:884–94.

PERSPECTIVES

Vibrio cholerae remains a significant global threat to human health (1). The onset of climate change threatens to escalate this risk, as flooding and infrastructure breakdowns become more frequent and suitable areas for *V. cholerae* blooms increase (2–4). Understanding the mechanisms by which this pathogen survives in the aquatic environment and causes disease in the human host is essential to our development of adequate prevention and treatment.

Biofilms play an important role in the *Vibrio cholerae*'s life cycle, providing protection from environmental stresses and contributing to the transmission of *V. cholerae* to the human host. *V. cholerae* can utilize two-component systems (TCS), composed of a histidine kinase (HK) and a response regulator (RR), to regulate biofilm formation in response to external cues. We performed a systematic analysis of *V. cholerae* RRs and identified a new regulator of biofilm formation, VxrB. We demonstrated that the VxrAB TCS is essential for robust biofilm formation and that this system may regulate biofilm formation via its regulation of key biofilm regulators and c-di-GMP levels. Additionally, we begin to explore the role of the co-regulation of biofilm and T6SS genes by VxrB through the investigation of T6SS activity within biofilms. Finally, we identify new players involved in VxrB-mediated phenotypes and open up new areas of investigation around cell envelope regulation and evolutionary differences and similarities between species. This research furthers our understanding of the role that TCSs play in regulation of *V. cholerae* biofilm formation, the role of T6SS activation within the biofilm, and the

contribution of hypothetical proteins to VxrB-mediated phenotypes and identifies the Vxr system as a potential target for antimicrobials (5).

There is still more to be discovered about the Vxr system, including what signals it responds to and the mechanisms by which it is regulated. In collaboration with the Satchell lab (Northwestern University) we now have a crystal structure of the sensor domain of VxrA and have identified residues for mutation that have the potential to disrupt binding. The TCS VxrAB is also encoded in a 5 gene operon and that includes 3 genes of unknown function; these genes also appear to influence Vxr-mediated phenotypes (6, 7). In particular, in Chapter 2 we demonstrate that VxrC has a repressive effect on VxrB's ability to positively regulate biofilm formation. VxrC is predicted to be a periplasmic protein and we plan to explore the potential for VxrC to interact with the VxrA sensor domain using structural studies. Given VxrB's ability to activate the T6SS and protective cell envelope responses we plan to the ability of so-called 'danger signals' to act as activating signals of the system, including cell lysate and membrane disrupting compounds.

Uncovering the phenotypes governed by the VxrAB TCS is only one component of understanding how this system contributes to *V. cholerae* biology. The next steps in characterizing this important system include identifying activating signals and establishing how this system is regulated, as well as better describing the mechanism of action and regulation by VxrAB. This can be done with further

structural and mutational analyses, phosphorelay studies, as well as DNA binding studies to parse out the direct regulatory targets of this system. These studies could lead to the identification potential antimicrobials that could inhibit Vxr-action and thus inhibit biofilm formation and virulence (5). The development of new and specific antimicrobials may be an important tool to combat cholera, as the potential for outbreaks become more common and severe (4).

References

1. 2017. WHO | Cholera. WHO.
2. **Escobar LE**, **Ryan SJ**, **Stewart-Ibarra AM**, **Finkelstein JL**, **King CA**, **Qiao H**, **Polhemus ME**. 2015. A global map of suitability for coastal *Vibrio cholerae* under current and future climate conditions. Acta Trop. **149**:202–211.
3. **Nasr-Azadani F**, **Khan R**, **Rahimikollu J**, **Unnikrishnan A**, **Akanda A**, **Alam M**, **Huq A**, **Jutla A**, **Colwell R**. 2017. Hydroclimatic sustainability assessment of changing climate on cholera in the Ganges-Brahmaputra basin. Adv. Water Resour. **108**:332–344.
4. **Wu X**, **Lu Y**, **Zhou S**, **Chen L**, **Xu B**. 2016. Impact of climate change on human infectious diseases: Empirical evidence and human adaptation. Environ. Int. **86**:14–23.
5. **Tiwari S**, **Jamal SB**, **Hassan SS**, **Carvalho PVSD**, **Almeida S**, **Barh D**, **Ghosh P**, **Silva A**, **Castro TLP**, **Azevedo V**. 2017. Two-component signal transduction systems of pathogenic bacteria as targets for antimicrobial

therapy: An Overview. Front. Microbiol. **8**:1878.

6. **Teschler JK**, **Cheng AT**, **Yildiz FH**. 2017. The two-component signal transduction system VxrAB positively regulates *Vibrio cholerae* biofilm formation. J. Bacteriol. **199**:e00139-17.

7. **Cheng AT**, **Ottemann KM**, **Yildiz FH**. 2015. *Vibrio cholerae* response regulator VxrB controls colonization and regulates the type VI secretion system. PLoS Pathog. **11**:e1004933.